Dissertation

# ELECTROCHEMICAL BIOMARKER DETECTION IN COMMON METABOLIC DISORDERS

submitted by

**Christoph Walter Haudum, MSc.**

for the Academic Degree of

**Doctor of Philosophy (PhD)**

at the

Medical University of Graz
Department of Internal Medicine
Division of Endocrinology and Diabetology

under the Supervision of

Univ.-Prof.in Dr. in Barbara Obermayer-Pietsch

2021

## Statutory Declaration

I hereby declare that this thesis is my own original work and that I have fully acknowledged by name all of those individuals and organizations that have contributed to the research for this thesis. The acknowledgement has been made in the text to all other materials used. Throughout this thesis and in all related publications I followed the “Guidelines of the Medical University of Graz on Good Scientific Practice”.

Graz, 2nd February 2021
Christoph Walter Haudum

# Disclosures

This thesis served a basis for publications of original data. I by myself acted as first author. I did not include results or figures of these publications that were derived from other research groups without any contribution by myself; but I included the results in the discussion. Since I wrote large parts of the manuscript, I included these parts in this thesis. Corresponding chapters are marked with an asterisk (*) and information about the publication is provided in the foot notes. In order to give this thesis a clear structure, these chapters were revised. I informed all co-authors about the publication of this thesis. All co-authors have agreed to the inclusion of their published data in the thesis and permission to reproduce illustrations and figures from own publications has been granted.



***List of Publications and Affiliations***

# Impact of short-term isoflavone intervention in polycystic ovary syndrome (PCOS) patients on microbiota composition and metagenomics

**Christoph Haudum[1, 4, *], Lisa Lindheim[1], Angelo Ascani[1], Christian Trummer[1], Julia Münzker[1, 2], Angela Horvath[3] and Barbara Obermayer-Pietsch[1, 4]**

[1] Department of Internal Medicine, Division of Endocrinology and Diabetology, Medical University Graz, Graz, Austria;
[2] Department of Medicine, Integrated Research and Treatment Centre for Adiposity Diseases, University of Leipzig, Leipzig, Germany;
[3] Department of Internal Medicine, Division of Gastroenterology and Hepatology, Medical University Graz, Graz, Austria;
[4] Center for Biomarker Research in Medicine (CBmed), Graz, Austria.
***** Correspondence: Christoph.haudum@medunigraz.at

Nutrients. 2020 Jun 1;12(6):1622. doi: 10.3390/nu12061622. PMID: 32492805; PMCID: PMC7656308.

# Acknowledgements

Welcome to the most important part of this thesis – the acknowledgments. Although it is my name written in capital letters on the first page, it is the cooperation and help from many people who made this project and therefore this thesis possible. I wish to express my deepest gratitude to Univ.-Prof.in Dr. in Barbara Obermayer-Pietsch. The professional as well as the personal development I went through the last four years was only possible because of her help and superior support. I could expect an answer within 5 minutes around the clock. Whatever the question, whatever the problem she helped or knew someone who could. Besides of a tight supervision I also got the freedom to develop the professional skills I was interested in. I cannot express how much her support means to me and how happy I am to have the privilege to be her PhD student. I also want to thank Mag.a Dr.in Julia Münzker and Univ.-Prof. Dr. Rudolf Zechner whose input throughout the project shaped my path to this thesis. The PhD Program AMBRA (Advanced Medical Biomarker Research) funded by CBmed supported me throughout the project.

But a project is nothing without a team. Therefore, I thank the whole team of the endocrinology unit (a.k.a BRUT). I especially want to point out Dr. Lisa Lindheim, PhD whose support vastly improved this project. Her knowledge and expertise in the field on PCOS and microbiome analysis helped me to start in that field.

Outside your own research group you also need help to finish a project that size. This help was kindly given to me by the amazing people of Prof. Ciara O´Sullivan´s research group at the Department of Chemical Engineering, Universitat Rovira I Virgili, Tarragona in Spain. Their patients and dedication to this project and their willingness to help was outstanding.

Scientific and personal progress can seldomly happen without discussion and constructive criticism. Dr.in Petra Kotzbeck and the PhD group were there for me whenever I had to blow off steam or when part of a project did not work out as planned. Thank you, Angelo, Ines and Vito, for the fun congresses and trips we had and for the good friendship we have developed. Going through a rough time not alone but with the help of friends who are in the same boat. This makes the unbearable a challenge solved together. Therefore, thank you to the "Biochemie" group for being there for me!

Having professional support is one thing, but to stay mentally healthy throughout the long PhD years you need encouragement and support in your private life. Although I think of myself of being a very happy person and do every project with the concept of *"Do. Or do not. There is no try"*(1) it is sometimes important being pushed into the right direction but also hugged when needed. Without my family and the mental support and calm relaxing environment they provide I would not have been able to endure these four challenging years. My last line of thank you is given to my love Patrizia showing me every single day that work is not the most important part of life.

*“It's still magic even if you know how it's done.”*

-Terry Pratchett (2)

# Table of Content

# Zusammenfassung in Deutsch

Diese Thesis stellt die wissenschaftliche Arbeit dar, die zwischen August 2016 und November 2020 im Rahmen des PhD-Programms AMBRA durchgeführt wurde. Ihr Hauptaugenmerk liegt auf dem Nachweis von Biomarkern bei häufigen Stoffwechselstörungen wie Diabetes mellitus (DM), Polyzystischem Ovarialsyndrom (PCOS) und Koronaren Herzerkrankungen (KHK) sowie deren komplexen Wechselwirkungen. Ein besseres interdisziplinäres Verständnis und die Entwicklung neuer diagnostischer Ansätze in Bezug auf diese Erkrankungen waren ein zusätzlicher Zweck dieser Arbeit. Kapitel I, Biomarker-Detektion mit neuen elektrochemischen Sensorsystemen, ist daher als Entwicklungsgrundlage gedacht, um für die Detektion und das Monitoring von Biomarkern zu dienen, die an Stoffwechselabläufen beteiligt sind. Darüber hinaus werden in Kapitel II innovative Biomarkerforschung bei häufigen Stoffwechselstörungen anhand von Longitudinalstudien, und in Kapitel III, der Nachweis von Mikrobiom-assoziierten Biomarkern bei PCOS nach Isoflavon-Intervention, als weitere Forschungsfelder dargestellt. Alle Studienansätze sind durch den besonderen Bedarf an einer Point-of-Care-Lösung (POC) miteinander verknüpft. Dies wird durch die neue Analysemethode über eine elektrochemische Detektion in Zukunft möglich. In dieser Arbeit wurden Daten von 1050 Patient*innen mit insgesamt 2800 Datensätzen gesammelt, sortiert, fehlerkorrigiert und über die Jahre kategorisiert. Ein Datensatz enthält u.a. mehr als 300 klinisch relevante Parameter, dazu kommen noch 650.000 Genotyp-Daten, NMR-Metabolom-Analysen und Fragebogenergebnisse. Die Ergebnisse dieser Doktorarbeit wurden bereits in einer Erstautorarbeit publiziert, eine weitere Erstautorarbeit wurde bereits eingereicht. Basierend auf den erarbeiteten Datensätzen konnten bereits zahlreiche weitere Veröffentlichungen zur Identifizierung und Validierung neuer Biomarker publiziert werden.

## Abstract in English

This thesis represents the scientific work done between August 2016 and November 2020 within the PhD programme AMBRA. Its main focus was the detection of biomarkers in common metabolic disorders including diabetes mellitus (DM), polycystic ovary syndrome (PCOS) and cardiovascular disease (CVD), as well as the complex interaction of biomarkers between these research areas. A better interdisciplinary understanding and development of new diagnostic approaches was also a purpose of this thesis. Therefore, chapter I, Biomarker detection with new electrochemical sensor systems, is meant as a developmental technical basis with the aim to serve as framework for the detection and monitoring of biomarkers involved in glucose metabolism.

Additionally, chapter II, biomarker research in common metabolic disorders using longitudinal study data, and chapter III, detection of PCOS biomarkers after isoflavone intervention, are also linked by using several biomarker approaches and the special need for a point-of-care (POC) testing solution. This will be possible done? by the newly developed analytical method in this thesis - electrochemical biomarker detection.

In this thesis, data from 1050 patients, including over 2800 datasets were collected, sorted, monitored and categorized over the years. The whole dataset includes more than 300 clinically relevant parameters and in addition 650.000 genotype analyses, NMR metabolomic results, and questionnaire data. Parts of this thesis was already published as one first author paper with an additional one currently in submission. It will also serve as a basis for many further publications to identify or validate new biomarkers.

# 1. Introduction

## 1.1.Diabetes mellitus

With more than 600 000 patients (15 %) suffering from diabetes mellitus type 1 or type 2 [DM, T1DM, T2DM] (3) in Austria and 6 % of DM patients in the total world population, these diseases are among the largest threats for the health care system and decrease an individual's life expectancy by ten years on average (4). DM is not only a financial burden, but also a personal and emotional one and is far from being fully understood. DM is defined as a group of metabolic diseases connected to chronic hyperglycaemia which results from defects in insulin action, insulin secretion or both (5).

Insulin as a metabolic active hormone affects many fundamental molecules in the body (carbohydrates, lipids and proteins), which results in metabolic abnormalities in patients suffering from DM. These abnormalities can have tremendous impact on the quality of life and life expectancy in DM patients - T2DM patients have a life expectancy reduced by 10 years in comparison to healthy individuals. In T1DM patients, the life expectancy is even decreased by 20 years (6). The most common diabetic complications are cardiovascular diseases, diabetic retinopathy and kidney disease. DM is also often accompanied by other common pathologies like high plasma lipids or high blood pressure, further damaging organ systems such as eyes, brain and nerves, heart and blood vessels or kidneys, bone and liver (7–10).

Beyond these general organ complications, DM has other substantial effects on almost all parts of the human body. Starting from bone and wound healing in combination with increased risk of developing mental health impairment, including cognitive dysfunction and neurologic damage, and of diabetic neuropathy (11–14).

Diabetes mellitus can be split into four main groups (15):

1. Type 1 diabetes mellitus (T1DM) is defined as loss of insulin production due to an autoimmune destruction of the insulin producing beta cells in the pancreas. The cause of this destruction is not entirely known, but heredity is an additional risk factor (16). The current state-of-the-art therapy is injection of adequate doses of insulin in combination with frequent measurement of blood glucose levels.

2. Type 2 diabetes mellitus (T2DM), starts with initially high insulin levels ("hyperinsulinaemia"). Several factors, including obesity, exaggerated carbohydrate, fat and/or alcohol intake, as well as the lack of glucose utilisation via exercise can lead to a constant elevation of blood glucose levels. As a result, increased insulin levels are required in order to reduce the glucose level. Cells (e.g. muscle, fat, liver) on the other hand develop a resistance to this high insulin level resulting in the so called insulin resistance (IR). The exact mechanisms of IR development are still under investigation, but publications have suggested that it is an appropriate response to nutrient excess. This response is linked to the mitochondria and more precisely the energy transport chain, the superoxide dismutase and the cells' struggle to return to an energy neutral state (17,18). T2DM accounts for around 90 % of all DM cases worldwide. It can range from rare forms of genetically determined insulin resistance with a relative insulin deficiency to an absolute insulin deficiency in the later course of the disease. T2DM is often associated with various metabolic comorbidities.
3. Gestational diabetes (GDM) is a glucose tolerance disorder with first appearance or diagnosis during pregnancy. Its detection and therapy are highly important due to its large impact not only on the mother, but also on the child throughout their lifetime.
4. Other "specific types of DM" summarise a range of various defects leading to diabetes. These forms are mostly different from the first three forms, like "maturity onset diabetes of the young" (MODY). This includes higher genetic heritability, occurrence of hormonal antagonists or non-responding insulin receptors despite normal insulin levels.
    a. Exocrine pancreatic disorders (e.g. cystic fibrosis, pancreatitis, hemochromatosis)
    b. Endocrinopathies (e.g. acromegaly, Cushing's syndrome, pheochromocytoma)
    c. Drug/chemically induced (e.g. alpha interferon, glucocorticoids, neuroleptics, pentamidine)
    d. Genetic defects of beta-cell function
    e. Genetic defects of insulin action
    f. Other genetic syndromes that can be associated with DM
    g. Rare forms of autoimmune-mediated diabetes.

### 1.1.1. History of diabetes mellitus

First recorded in ancient Egypt (circa 1550 BCE), DM has been known in many cultures (19). Polyuria in DM was described in Hindi Sanskrit texts as “madhumeha” or “honey urine” because of the patients’ sweet urine. This name was also used in documents from ancient China. At that time, there was no known connection between DM and the pancreas. Rather, “wasting-thirst” was split into three subgroups: the upper- (associated with the lungs), middle- (stomach), and lower- (kidneys) organs, which were treated with herbal mixtures (20). Since the late 1500s, involvement of the kidneys in DM was still believed in. With increased understanding of the human anatomy and complex structures by autopsies, a paradigm change started. Nearly 200 years later, Thomas Cawley discovered a link between the pancreas and diabetes which went unappreciated for 100 years (21). In 1889, Mering and Minkowski found out that urine of pancreatectomised dogs attracted flies but not urine of healthy ones. They then tested for sugar content and connected DM with the pancreas (22).

As already mentioned, treatment of DM was conducted by dietary intervention and herbal mixtures, blends of various substances (e.g. milk, beer, cucumber) but also phlebotomy and opium intake. As DM was also seen as losing nutrients to urine, patients were advised to eat as much as possible including large quantities of sugar. This opinion changed in the late 1700s to dietary restriction. The so called “starvation diet” indeed improved life expectancy and was at that time the viable way of helping the patients. In 1923, the Nobel Prize in Physiology was awarded to J.J.R Macleod and Frederick Banting. They extracted “insulin” from the pancreas of foetal calves, which was then used as medication. Until genetically engineered bacterial insulin was developed, pork and cattle organs remained the primary commercial source of insulin.

**Diagnosis of diabetes mellitus**

Although measuring glucose levels in patients can easily be done nowadays, diagnosing DM still takes some time. Testing for high blood glucose levels alone is not sufficient for an adequate DM diagnosis. The following diagnostic procedures are aligned with the ADA criteria (American Diabetes Association) (23)

**Fasting glucose**

The blood glucose level can reach > 140 mg/dl after meals also in healthy persons. Therefore, blood analysis needs to be done after at least eight hours of fasting. In case a fasting blood glucose level is too high, this is a hint for a disturbed glucose metabolism.

**Oral glucose tolerance test (oGTT)**

To detect not only DM but also its preliminary stage called prediabetes (preDM), and to gain better insight into the health status of the patient, a 2-hours-glucose test or oral glucose tolerance test (oGTT) is performed (24,25). After eight hours of fasting, 75 g of glucose are dissolved in 250 to 300 ml of water and swallowed by the patient. Blood is drawn after 30 min, 60 min and 120 min and glucose (for research purposes, including insulin) is measured: the higher the increase and the slower the decrease of blood sugar, the higher the chance of DM.

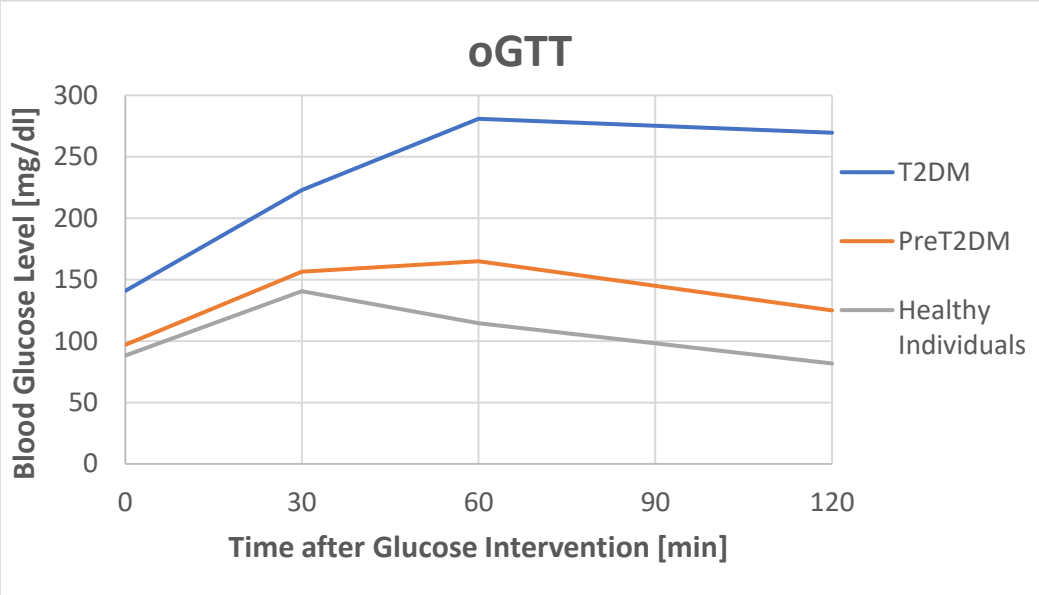


*Figure 1 Results from oGTTs in the BioPersMed subset cohort (see Chapter II). T2DM... type 2 diabetes mellitus (n=18), PreT2DM... Pre type 2 diabetes mellitus (n=32) according to ADA criteria (26), healthy individuals (n=31)*

- **Haemoglobin A1c (HbA1c)**

  The third tool to detect and manage DM is the HbA1c level (27). This value represents the proportion of glycated haemoglobin in the blood. Haemoglobin chemically binds glucose non-enzymatically and spontaneously. The higher the blood glucose over a longer period of time (3 months according to the lifetime of the erythrocytes), the higher the HbA1c level (28).

Therefore, HbA1c is a popular tool to not only detect DM but also to monitor the blood sugar management of patients long-term.

*Table 1 The stages of DM are defined by the World Health Organisation (WHO) either via fasting glucose, 2-hours glucose or HbA1c [35].*

| **Condition** | **Fasting glucose** | | **2-hours' glucose** | **HbA1c** | |
|---|---|---|---|---|---|
| ***Unit*** | *mmol/L (mg/dL)* | | *mmol/L (mg/dL)* | *mmol/mol* | *DCCT %* |
| **Healthy** | <6.1 (<110) | | <7.8 (<140) | <42 | <6.0 |
| **Impaired fasting glycaemia** | ≥6.1(≥110) & <7.0(<126) | | <7.8 (<140) | 42-46 | 6.0–6.4 |
| **Impaired glucose tolerance** | <7.0 (<126) | | ≥7.8 (≥140) | 42-46 | 6.0–6.4 |
| **Diabetes mellitus** | ≥7.0 (≥126) | | ≥11.1 (≥200) | ≥48 | ≥6.5 |

## 1.1.2. New biomarker developments for diabetes mellitus

Besides the already mentioned biomarkers in the diagnosis of DM, several biomarkers have been or are currently investigated for an even earlier and more precise risk prediction, like microRNAs (non-coding ribonucleic acids), markers of chronic inflammation/reactive oxygen species (ROS) or mannose (29–31).

Due to the special interest in this project, the following biomarkers are explained in more detail as follows:

- **C-peptide**

The protein C-peptide is a side product during insulin synthesis (part of proinsulin, Figure 2) and primarily determined in specific laboratories as part of the differential diagnosis of DM and functional tests.

It comprises 31 amino acids and connects the chains A and B within the proinsulin molecule.

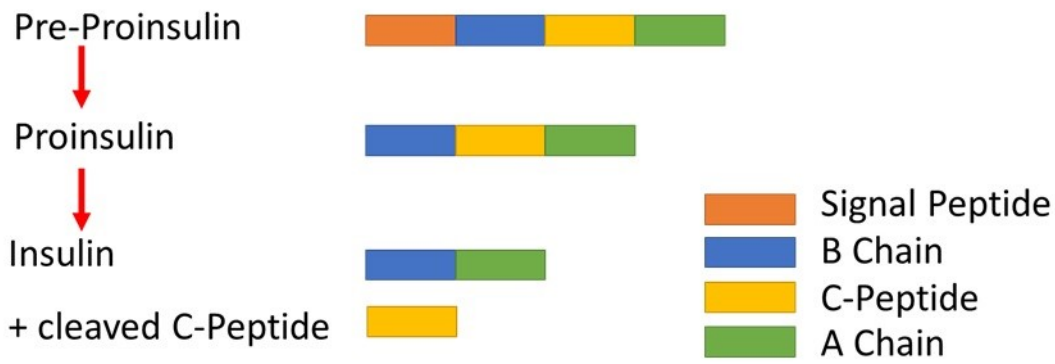


*Figure 2 Cleavage process which leads to the formation of C-Peptide in unimolar ratio to insulin.*

During the conversion from proinsulin, which itself can be a biomarker for T2DM, to insulin, the C-peptide is enzymatically cleaved off and then released into the blood together with insulin from the β-cells of the pancreatic islets (32). C-peptide has its own effects on carbohydrate metabolism and its absence may play a role in the development of diabetic organ damage. It is not contained in medically administered insulin preparations. Compared to insulin, the half-live time of C-peptide is 10 times higher. Serum levels below the normal range of 1.1-5 µg/l indicate a decreased β- cell function, as it is seen in T1DM. By contrast, levels above the normal range may indicate insulin resistance and can be used as a biomarker for early stages of T2DM.

The presence of C-peptide in the blood provides information about the body's own insulin production independent of medically administered insulin. These properties render C-peptide a potentially promising biomarker for biosensors for T1DM and T2DM prediction and monitoring (33).

- **Oxytocin**

Oxytocin has a wide variety of physiological and pathological functions but was up to now only associated with gestation and lactation or pituitary dysfunction. Oxytocin has been shown to improve insulin sensitivity via regulating adipokines such as adiponectin and leptin, and decreasing fat mass and thereby leptin production together with lipo- and glucotoxicity (34). Elabd et al. also published a β-cell regeneration effect of oxytocin (34). This hormone is reduced

in T2DM and in the preceding preT2DM and correlates negatively with parameters associated with T2DM e.g. fibroblast growth factor 21 (FGF21) or HbA1c (35).

### 1.1.3. Treatment of diabetes mellitus

Diabetes mellitus is a chronic disease. Despite many years of research, there is no definite cure for DM available. Treatment options on the other hand need to be differentiated between T1DM, with no insulin production, and T2DM with no response to insulin and later also almost no insulin production – dependent on severity.

**Therapy of T1DM**

The first line medical treatment for T1DM is an adequate substitution of the missing insulin in fast- or long-acting forms. Together with the measurement of respective glucose values, this provides a reliable long-term strategy in combination with lifestyle changes for the treatment of T1DM. Many different insulin options and molecules have been investigated and implemented over the years with the aim to tailor insulin application and delivery to the need of the individual patient (36).

**Therapy of T2DM**

The treatment of T2DM includes many approaches, such as pharmacological options and lifestyle changes comprising weight loss and physical activity for ameliorated glucose utilisation.

The main drug classes for a pharmacological therapy of T2DM treatment include:

- Alpha-glucosidase inhibitors (37)

  This class of drugs aim at preventing the uptake of sugar and starch from food by inhibiting the process of digesting these carbohydrates into uptake able monosaccharides.

- Sulfonylureas (38)

  An increase of insulin secretion via beta-cells is facilitated by sulfonylurea (eg. Acetohexamide, Glibenclamide, Glimepiride) .

- SGLT2 inhibitors (39,40)

  These inhibitors act on the sodium-glucose transport protein 2 (SGLT2) and alter the physiology of the nephron, thereby preventing the reabsorption of glucose in the kidney. This in turn leads to reduced blood glucose levels. A cardiovascular and metabolic

benefit for T2DM patients, manifested in decreased blood pressure, body weight, uric acid, and ketone bodies, has been described as positive side effect of SGLT2 inhibitors (41,42)

- Thiazolidinediones (43,44)

  By activating a group of nuclear receptors called peroxisome proliferator-activated receptors (PPARs), thiazolidinediones also known as glitazones, modulate gene transcription and lead to increased fatty acids storage in adipocytes and other tissues. Additionally, the transcriptionally increased insulin sensitivity forces the other cells in the body to use glucose as the main source of energy, thereby decreasing the blood glucose level.
- Insulin

  In late stages of T2DM, where physiologic insulin secretion by ß-cells is ceased and other pharmacologic approaches, as listed above, do no longer show sufficient effect on glycemia, exogenous administration of insulin becomes necessary.
- Metformin

  Metformin plays a special role in this project and its mechanism of action is therefore described in more detail below. Besides being used as first line treatment for T2DM, Metformin also serves as off-label medication for patients with polycystic ovary syndrome (PCOS). Various potential mechanisms of action have been described, but the key molecular mechanism of metformin action is still not fully understood, in spite of its more than 60 years history of use.

  The effect of metformin is presumably based on three mechanisms:
- Firstly, it lowers blood glucose levels by inhibiting hepatic glucose production (gluconeogenesis) (45), thereby counteracting insulin resistance in other organs. Metformin activates adenosine monophosphate-activated protein kinase (AMPK) via liver kinase B1, inhibits the glucagon-induced cyclic adenosine monophosphate (cAMP) production and increases the AMP/ATP ratio (46). It also has an effect on the gluconeogenesis by changing the nicotinamide adenine dinucleotide+ (NAD+):NADH ratio.

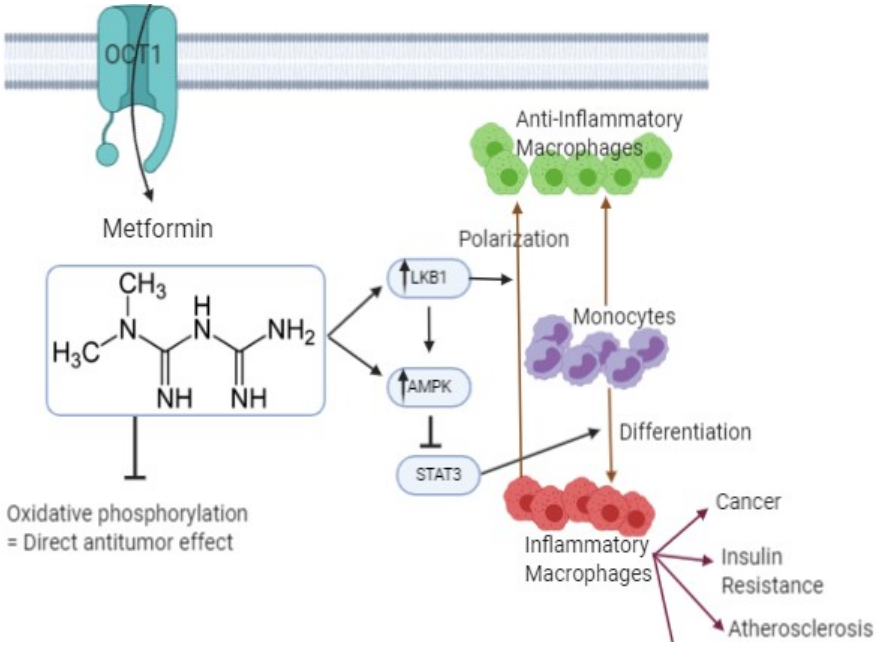


*Figure 3 Functional action of metformin. Transported via organic cation transporter 1 (OCT1) it regulates a wide range of metabolically active pathways* (202).

- Secondly, experimental studies have shown that metformin inhibits mitochondrial glycerol-3-phosphate dehydrogenase. As a result, fewer metabolites are available in the cytosol for the formation of new glucose and lactate is produced increasingly (47).

- Thirdly, metformin is thought to inhibit the absorption of glucose in the intestine and importantly to decrease insulin resistance, which improves the uptake into the muscle cells. It is also known to change the composition of the microbiome (48,49). However, both effects have not yet been reliably demonstrated.

- As already mentioned, beyond its use in DM, metformin is used as an off-label medication for the treatment of PCOS patients. Mainly acting on the attenuation of insulin resistance in these women, metformin has been shown to have an inhibitory effect on various enzymes involved in thecal cell steroidogenesis and a stimulatory effect on SHBG (sex hormone binding globulin) production in the liver. Metformin not only lowers androgen production, but also increases SHBG levels in blood, thereby leading to higher amount of bound steroid hormones and lower free circulating testosterone (50). By improving ovulatory cycles via decreasing circulating androgens

and causing a stabilising effect on the risk of miscarriages, metformin increases the rate of live births in PCOS women (51).

## 1.2. Glucose metabolism and hormones: Polycystic ovary syndrome (PCOS)

Affecting 5-20 % of women worldwide, PCOS is one of the most prevalent endocrine and metabolic disorders in women, starting in their adolescence (52,53). Several phenotypes with various degrees of hyperandrogenism, oligo/anovulation and polycystic ovarian morphology are known. Problems associated with PCOS include excess body and facial hair, acne, lack of regular cycles, delayed menses, pelvic pain, unfulfilled child wish, and sometimes even acanthosis nigricans (54).

The pathogenesis of the PCO syndrome has not yet been fully elucidated.

However, it has been demonstrated via mouse models that a hormonal imbalance in the womb during the embryonic development could contribute to the development of the syndrome in later life (55). Excessive doses of specific endocrine hormones (anti-Müllerian hormone (AMH), testosterone) were injected into pregnant mice, resulting in an increased incidence of PCOS in their offspring. High AMH levels lead to the stimulation of certain brain areas via corresponding signal cascades, which regulate the testosterone production. AMH levels in these mice were similar to the levels observed in PCOS women. This also explains the familial clustering of the disease, as the mechanism maintains itself via transfer to the next generation. When these mice were treated with a gonadotropin-releasing hormone (GnRH) antagonist, which lowers the secretion of both gonadotropins (luteinising hormone (LH) and follicle stimulating hormone (FSH)), the PCOS-like phenotype was abolished.

Though the aetiology is still under investigation, chronic pro-inflammatory status and a tendency towards insulin resistance (56–58) play a critical role in the development of harmful long-term consequences such as T2DM, an additional risk for pregnancy complications such as gestational diabetes (59), and an increased risk for cardio- (CVD) or cerebrovascular disease (60).

Lower insulin sensitivity has been found to be independent of BMI (61), while hyperinsulinemia and impaired glucose uptake were observed in a significant proportion of women with PCOS, even in non-obese women. Hyperinsulinemia exacerbates the clinical phenotype of PCOS through further stimulation of ovarian and adrenal androgen release, reduction of SHBG (62), independent of obesity (63).

## 1.3. Cardiovascular disease (CVD) – metabolic complications

Cardiovascular diseases (CVD) and their metabolic complications are some of the most important causes of disability and premature death worldwide.

With 17.8 million deaths, CVD were the most common cause of death in 2017. Thus, on a global average, 32 % of all deaths can be attributed to CVD (64). They also represent the top cause in the death statistics in Europe and Germany. In Europe, more than four million people die of CVD each year; 1.4 million of them are under the age of 75 years (65,66).

Considering the diversity of individual risk pathophysiology, a highly complex approach to identify novel cardiovascular biomarkers is needed together with the validation of already established CVD biomarkers in order to prove their scientific and clinical relevance. Accordingly, clinical parameters together with specific biomarkers are required to understand the underlying mechanisms of disease manifestation and progression. However, the detection of potential targets might then be used additionally to develop specific therapeutic approaches.

Western lifestyle, including unhealthy nutritional habits, physical inactivity, smoking and psychosocial distress are well-known major risk factors of CVD (67,68). A main cause of CVD is untreated arterial high blood pressure (hypertension). According to the WHO definition, a chronic systolic blood pressure of more than 140 mmHg and/or a diastolic blood pressure of more than 90 mmHg is considered as hypertension. Studies have shown that lowering blood pressure by 10 mmHg reduces the risk of CVD by about 20 % (69).

## 1.4. Biomarkers

Biomarkers are characteristic biological features that can be measured objectively. They indicate a biologically normal or pathological process in the human body.

A distinction is made between drug-related and disease-related biomarkers.

- Drug-related biomarkers show whether and how a drug will work in a specific patient and how his or her organism will metabolise it. In addition to known blood-derived systemic parameters (e.g. KRas mutation and cetuximab), an increasing number of pharmacogenomic biomarkers are currently developed.

- As so-called "risk indicators" or "predictive biomarkers", the disease-related biomarkers provide information on whether a patient is at risk of developing a disease, whether the disease has already manifested ("diagnostic biomarker") or whether a disease is likely to develop in individual cases ("prognostic biomarker"). Apart from already established and routinely used biomarkers a large number of potential novel biomarkers detectable in various body fluidsare gaining importance in different medical disciplines.

Biomarkers can be genes, gene products, cells, or molecules such as enzymes or hormones. Most commonly measured biomarkers in health and disease are blood-based biomarkers. These include red or white blood cell count, haemoglobin or lipid panel biomarkers like cholesterol, triglycerides (TG) and high- or low-density lipoproteins (HDL or LDL, respectively), as well as parameters of liver and kidney function. A comprehensive "metabolic" panel of biomarkers is a series of (mainly) blood tests to give the clinician a snapshot of the body's metabolism including tests for blood glucose, insulin or C-peptide and their metabolic agonists and antagonists.

Apart from blood, tissue samples are a highly important material for biomarker detection, especially in cancer. The tissue can either be fixed on a glass slide and the biomarkers of interest are visualised using antibodies or *in situ* hybridisation, or the tissue is lysed and used for further analyses (70–72), like RNA- or DNA-based biomarker detection, such as sequencing (73).

Although tissue extraction and *ex vivo* application of different laboratory techniques allow the detection of a comprehensive list of biomarkers, non-invasive methods to assess biomarkers that do not rely on tissue biopsies are needed and of special interest. Non-invasive approaches

not only allow easier access and use of point-of-care (POC) devices, but also enable a tighter measurement scheme in patients and a higher acceptance by the patients compared to invasive approaches. The possibility to analyse biomarkers from patient groups, where drawing blood or taking biopsies is not possible, opens the way for new biomarkers.

The three most interesting sources for biomarkers are urine, stool, and saliva, as they are non-invasively available in higher quantities and may provide a wide range of biomarkers for many diseases including kidney stones, urinary tract infections, hypertension, and diabetes mellitus. With the increasing knowledge about the impact of the microbiome on the host, this area became a newly developing field for biomarkers and treatment options (74–78). Saliva and stool are non-invasively accessible materials and therefore often used to analyse the oral/gut microbiome. However, other body microbiomes, such as the skin or the vaginal microbiome are currently of increasing interest for clinical applications (79,80).

These biomarkers are essential for the diagnosis of newly manifested diseases, but also for the monitoring of already existing chronic disorders. This enables potentially tighter treatment options and might therefore improve quality of life and lifespan in the patient.

In some cases, biomarkers are the only way of defining the difference between diseased and healthy persons, as the time gap between disease onset and clinical symptom onset might dramatically decrease the window of opportunity for an early treatment.

### 1.4.1. Need for biomarkers in common metabolic disorders

As the population increases and steadily ages, the need for prediction and management of metabolic disorders is an essential task for developed as well as developing countries. To set the scope of the financial costs of common metabolic disorders, 20 % of the statutory health insurance expenditures in Germany in 2007 were used for the treatment of diabetes mellitus (DM) and its accompanying and secondary diseases. The expenses in Germany for the treatment of DM and its consequences in 2005 were around 25 billion euros (81).

Depending on their additional complications (secondary diseases caused by DM), patients with T2DM cause 1.3- (no complications) to 4.1-fold (micro- and macrovascular complications) costs higher than the average costs of other persons within the statutory health insurance. Therefore, detecting common metabolic disorders like T2DM at an early state would allow for potential timely and relatively inexpensive interventions such as changes in eating behaviour or other lifestyle modifications (82).

### 1.4.2. New approaches to biomarker detection: electrochemical sensors and sensor development

A “sensor” itself is a device with distinct properties that allow a reaction to external stimuli, such as temperature, sound, light, pressure, movements, or magnetic fields. This reaction is in most cases an electric signal that can be read and amplified by other devices. From a wide range of different types of sensors, this work focuses on electrochemical sensors. This class of chemical sensors works in the presence of a biological analyte as a transducer element. The output of the sensor therefore correlates with the concentration of the target analyte allowing for a fast and reproducible measurement.

The main electrochemical methods used in these sensors are potentiometry, conductometry, voltammetry, coulometry and capacitance (see Table 2)(83).

*Table 2 Most common electrochemical methods used in biological sensors with their units and respective electrical properties (83).*

| Method | Units measured | Electrical properties monitored |
|---|---|---|
| Amperometry, voltammetry | I | Currents (amps) as a function of the applied potential |
| Capacitance | $F = C \cdot V^{-1}$ | Potential load (farads) |
| Conductometry | Ω | Resistance (ohms) |
| Coulometry | $C = I \cdot s$ | Current as function of time |
| Potentiometry | V | Potential difference (volts) |

*C: Coulomb - Specific number of electrons; F: Farads – capacity to store charge; I: Current - flow of charged particles; V: Volt - electric potential between two points; Ω: Ohm – Resistance of a substance*

The main methods used in this project were amperometry and voltammetry; therefore, they will be explained in context of biosensors in more detail.

To briefly explain the fundamentals of electricity, an energy source (e.g. a battery) has an electronic potential (V) which has the power to push electrons through a wire. The more powerful this push is, the higher is the unit of the energy source in volt. Using a water pipe as an analogue, voltage can be visualized as the height difference that makes the water flow down. The current (I), being the water in this example, are electrons moved via this potential. The corresponding unit is ampere, describing a specific number of electrons per second. The last important unit of an electrical system is ohm (Ω), which is defined by the resistance (R) between two points. These three parameters are interconnected, and their relation is described by the so-called “ohms law”. This law states that the strength of the electrical current flowing through an object is proportional to the electrical voltage.

$$I = \frac{V}{R}$$

The first electrochemical sensors were used in the 1950s to measure oxygen levels in the air to guarantee save working conditions and induce alarm in case of toxic gases. The rapid improvement in electrical engineering and subsequently microscope technology, which allowed for nanometre resolution, made production and designing of sensors easier and more cost effective (84).

One of the most frequently used sensors in the daily lives of thousands of people is the glucose sensor. It is important for patients with DM to perfectly dose their insulin. The sensor itself uses an amperometric approach to indirectly measure glucose. This indirect approach means that not glucose itself is measured, but glucose is oxidised to glucono-delta-lactone (GDL) and oxygen is reduced to hydrogen peroxide by glucose oxidase. By applying a defined current (300-600 mV) the movements of these electrons, that are proportional to the glucose level in the sample, can be detected. In amperometry, specimen X is oxidised at the anode. The lost electrons move through the solution until specimen Y at the cathode is reduced. This motion of electrons is measured.

### 1.4.3. Need for biomarker validation

As with every new biological breakthrough, but especially with the clinical use of biomarkers, comes the need for reproducibility and therefore validation. Due to a lack of specific regulations, no proper guideline for biomarker assay validation in general is established (85). In medicine, biomarkers must be validated for technical and clinical issues.

The technical verification procedure must be precise and well documented to allow reproducibility of the setup and operator-independent results. For inter-lab comparisons, the results must tightly overlap or only slightly differ in various laboratories. Furthermore, the clinical validity, importance and significance of a given biomarker in terms of diagnosis, prognosis, and risk assessment in a particular disease must be proven by independent clinical studies before its market launch and general distribution. Unvalidated study results can lead to inter-lab result differences and on the long run to wrong conclusions drawn from the data. This can not only be detrimental for patients, but can lead to mistrust of the lab work and, more importantly, to mistrust in clinical and translational science per se (86).

## 1.5. Thesis overview

This thesis, although being one coherent research question, was split into three chapters with the aim of presenting a structured insight into the project. The purpose of these chapters is the detection (chapter I), validation (chapter II), and finding (chapter III) of new biomarkers in the field of common metabolic disorders.

### 1.5.1. Chapter I: Biomarker detection with new electrochemical sensor systems

This part of the thesis was performed in cooperation with a semiconductor company, who delivered the technology needed for wireless connection as well as the knowhow in the field of electrical engineering.

We hypothesised that latest sensor and informatic developments can be used to detect new biomarkers. Additionally, these can be used to reanalyse already existing cohorts for an interdisciplinary and interconnected understanding of the patient health status.

One long-term goal of this project was the detection of predictive and monitoring biomarkers for DM in urine, using a low-cost POC detection system. Based on known biomarkers and detection limits in urine we decided for C-peptide as a potential biomarker candidate. Developmental work as well as proof of principle will be tested for this biomarker.

Until now, most of the low-cost devices to detect biomarkers either work with changes in colorimetric detection via antibodies (e.g. pregnancy tests) or a specific enzyme (e.g. glucose measurements). Our project uses an innovative approach via changes in current resistance according to the binding or non-binding of specific antibodies.

Importantly, one biomarker alone may not be sufficient for a specific risk/disease detection, as reported for several biomarker approaches (87,88). A follow-up project will therefore include additional urine-based biomarkers based on the tested method to improve the sensor.

The first sensors were standard gold screen printed electrodes (SPE) and were provided by the semiconductor company. These sensors were designed to measure the changes in current due to an increase in resistance via the binding of a candidate protein to a goldsurface-linked antibody in relation to a reference electrode.

## The BioPersMed cohort

For the identification of appropriate biomarkers and the validation of sensors, it was planned to use samples from the "BioPersMed" (Biomarkers for Personalized Medicine – see Chapter II) cohort study. This prospective, longitudinal study is still ongoing at the Medical University Graz and includes laboratory, genetic, functional. imaging, as well as psychological data of 1022 probands. Urine, saliva, stool microbiome, plasma and serum samples are stored under certified quality control at the BioBank Graz. Probands are followed up biannually with a telephone visit between the examinations.

The BioPersMed cohort is of particular interest for this PhD thesis, as it consists of 11.1 % T2DM, 25.6 % prediabetic and 63.3 % healthy persons at time of inclusion into the study. These persons were followed for several years checking for a potential T2DM manifestation during the observation period. The inclusion criterium for this study was having at least one cardiovascular risk factor, thus making it a perfect resource not only for this research topic but also for research planned in other common metabolic diseases.

## Background of electrochemical sensor conditioning

The gold surface of the electrochemical sensors first needs to be cleaned using $H_2SO_4$ and CV. The cleaning enhances the surface of the sensor and allows for linking with the antibodies. This linking can be done using different methods, chemisorption via thiol derivates, via bifunctional linkers or adapters like biotin and streptavidin. Either way, this linking process is based on three properties:

1) hydrophobic attraction between antibody and gold surface
2) dative binding between gold conducting electrons and the antibody or
3) ionic interaction of the negatively charged gold and positively charged antibody.

The gold surface is then activated using glutathione (GSH) (Figure 4A). GSH binds to the surface via the thiol group and allows for further binding via the carboxy group. Our bifunctional linker, namely carbodiimide (EDC) forms an intermediate compound with the carboxylic part which are then activated and reactive towards amines (Figure 4B). Thereafter, the complex binds to the amines in our liker N-hydroxy-succinimide (NHS) (Figure 4C). When the antibody is added, its primary amines bind to the ester (Figure 4D).

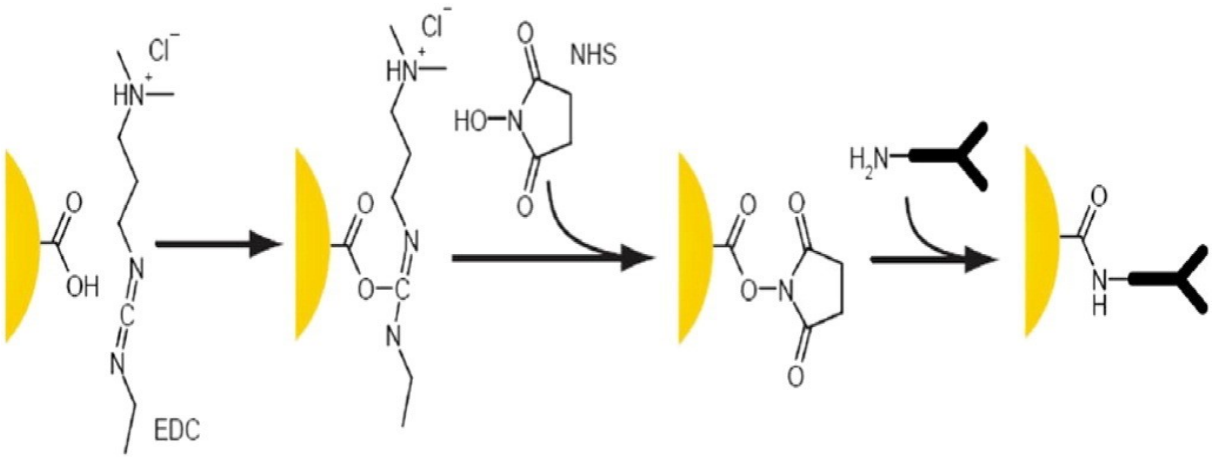


*Figure 4 Schematic figure of functionalisation of the gold surface with EDC/NHS. Adapted from Jazayeri et al 2016* (89) *(licence CC BY-NC-ND 4.0) .*

### 1.5.2. Chapter II: Biomarker research in common metabolic disorders using longitudinal cohort data

Cardiovascular diseases (CVD) and their metabolic consequences are the most important cause of disability and premature death (64). Modern lifestyle, including smoking, psychosocial stress, physical inactivity and unhealthy nutritional habits are key risk factors of CVD within different age groups as well as the triggers behind cardiovascular death (67,68). Reduction of these potential risk factors may avoid many CVD deaths (90). Unfortunately, an increasing number of T2DM cases, with a high lifetime-risk for the development of heart failure, persistent high stroke mortality, and many patients with CVD related risk factors remain undiagnosed and un- or undertreated (91–95). Therefore, detection of asymptomatic cardiovascular (CV) or metabolic risk already at an early stage remains a crucial task in the prevention of the onset and progression of CVD and related complications (96).

Considering the multiplicity of risk pathophysiology, an integrative approach is needed to identify novel and to validate established cardiovascular biomarkers for their scientific and clinical utility. Accordingly, practical biomarkers are required to facilitate (1) the understanding of underlying mechanisms of disease development and (2) the detection of potential targets for specific preventive therapies. For this purpose, there is an unmet need for a cohort of probands at CVD and metabolic risk early before clinical manifestation of cardiovascular disease.

In the BioPersMed cohort (Biomarkers of Personalized Medicine), we enrolled community dwelling and asymptomatic patients who are at risk for CVD in order to evaluate the predictive value of various biomarkers. This reflects different pathways of CVD and metabolic disease development using laboratory measurements, advanced imaging techniques, genetic investigations, and functional tests. The BioPersMed cohort is located at the Medical University of Graz (Austria) in a dedicated clinical outpatient research centre and the biobank (biobank.medunigraz.at).

The BioPersMed cohort includes 1022 people and more than four follow up visits. These visits are conducted every 2 years, with a total of 128 aliquots (e.g. serum, plasma, stool) per visit and patient. Questionnaires to assess lifestyle are filed and laboratory measurements, genetic and metabolomic screenings are performed. This renders the BioPersMed cohort a huge repertoire of longitudinal data for various scientific questions.
The aim of this study is therefore the use of this massive amount of data for biomarker research not only in the areas of cardiometabolic health but also interdisciplinary research for common metabolic disorders or specific research topics. As this cohort has additional endocrine parameters measures and PCOS criteria were checked it can be used to validate the findings of chapter III.

This cohort is also used to evaluate large-scale screening tools for the improvement of cardiovascular and metabolic risk stratification, early diagnosis, prediction of clinical outcomes, and long-term monitoring in an apparently healthy but representative at-risk population in a prospective manner.

### 1.5.3. Chapter III: Detection of PCOS biomarkers after isoflavone intervention in a prospective cohort*

The diagnosis of PCOS is primarily done by testing for the current Rotterdam criteria; based on recent publications on a tight connection of PCOS, its alterations in hormone and energy metabolism and the specific microbial composition, it is important to investigate these

*parts of this chapter have been published in Nutrients. (2020). Doi: 10.3390/nu12061622

approaches further (97). As already described, the microbiome has not only an important part in body regulations, but also an important impact on human wellbeing. With more than $10^{14}$ bacteria and archaea and their capacity to metabolize nutrients and food components in the gut, they not only harvest energy for the body, but produce hormones supporting our own organs (98,99). Their large metabolic repertoire with more than 3 million genes contributes enzymes that are not encoded by the human genome (98). Diseases can alter the microbiome and vice versa. Change in the microbial composition have an impact on changes in hormonal and enzymatic functions. We have already shown that PCOS and the respective phenotypes are associated with microbial changes in the gut (76,100).

In this PCOS cohort, clinical and laboratory parameters, food intake and stool microbiome data before and after 3 days of isoflavone intervention were collected. From 25 PCOS women and 25 healthy controls, aliquoted specimen were available. This study aimed at gaining better insight into the interplay between clinical PCOS phenotypes and stool microbiome. Specific strains could then be used as further predictive or diagnostic biomarkers or even for therapeutic approaches.

We hypothesized that a PCOS-associated gut microbiota dysbiosis exists, which is further involved in isoflavone production and biological processes. After a 3 days oral isoflavone intervention described by Setchell et al., we assessed the changes of metagenomic pathways, systemic glucose-metabolism associated parameters and microbiome composition (101). These parameters were then connected with metabolic and reproductive PCOS patterns.

Isoflavones might also be used as a prebiotic, which supports the growth of beneficial microbial strains in women with PCOS symptoms. Already known beneficial strains, so called “probiotics”, might improve microbial capacity to process isoflavones on their own/via their specific properties. (102).

## Connection of microbiome and PCOS

Recent evidence described important differences between the gut microbiome composition of PCOS patients compared to healthy individuals, reporting a much lower diversity and an altered phylogenetic profile compared to controls (103–105). This could potentially interrelate with the antiandrogenic and antioxidative effects of isoflavones, whose potential clinical effectiveness have been investigated in epidemiological reports and interventional trials (106–112).

Isoflavones, commonly found in soy products and other vegetables, are a subgroup within the flavonoid subtypes. They are naturally occurring substances, have chemoprotective properties and their activity is similar to hormones in plants (113,114). Epidemiological intervention trials and reports investigated their potential clinical effectiveness with and supported their beneficial effect in several diseases (107–109,111,115,116). However, not only positive regulations have been described. There are also studies describing an endocrine disruptor effect of isoflavones (117,118).

Some microbial strains are needed for highly important pathways including lipopolysaccharide and short-chain-fatty acid metabolization, energy adsorption and bile acid pathways (119,120). Differences in microbial strain composition in other diseases have already shown the importance of alterations in single strains in healthy and diseased subjects but also on different disease phenotypes. With focus on the clinical effects of PCOS, e.g. insulin resistance and inflammation, the detection of specific bacterial strains that have the capacity to ameliorate or influence PCOS symptoms is of high importance.

The predominating isoflavones in soy beans, genistein and daidzein, are weak ligands of the estrogen receptor (ER). They have been shown to positively influence antioxidant, estrogen-modulating and anti-inflammatory activity (111,121).

One of their metabolites, equol, derives from bacterial conversion of its precursor, daidzein, and shows promising biological effects along with more efficient absorption and extended half-life within the circulation when compared to its precursor (122). The bacteria involved, the biochemical conversion itself and the driving mechanism remain yet to be fully elucidated.

It has been proven that the gut microbiome, is capable of converting naturally occurring “xenoestrogens”, so called phytoestrogens, from dietary sources into metabolites which are hormonally active (112,121). Polyphenol compounds, such as isoflavones, could potentially be used to elicit this effect, not only for the antiandrogenic and antioxidative microbial metabolites, but also for a direct effect on microbiota composition, and positive effects on PCOS symptoms. Intracellular Ca2+ levels, among other hormonal effects, increase after equol binding to the G-protein-coupled estrogen receptor 1 (GPR30)(123). Furthermore, the common incretin effects after meals are reduced by equol, which might contribute to its metabolic influences (124).

So-called “equol producers” are individuals with the capacity to produce clinically relevant equol concentrations. These persons may benefit from the pharmacological activities deriving from isoflavone consumption. and the benefit may be greater in or even limited to these individuals as only these “equol producers” are capable of adequate equol production (121,125).

A method described by Setchell et al. identified these equol producers via the urinary equol:daidzein ratio as measured by mass spectrometry. The prevalence of equol producers in Western populations is approximately 35 % (101,121) with high proportions of up to 80% in Asian populations.

# 2. Materials and Methods

## 2.1. Chapter I: Materials and methods for electrochemical biomarker detection

### 2.1.1. Specific approach to sensor preparation –protocol development

Our first protocol was based on the work of Hafaiedh et al., where the first step in sensor preparation was the cleaning of the electrode (126). This work was used as an important basis because it was up to date, well-structured and documented, which is needed for reproducible experiments. The electrodes used were gold/gold/silver (working electrode (WE)/ counter electrode (CE)/ reference electrode (RE), Art.number: AC1.W1.RS, Datasheet attached) from the company BVT (Czech Republic).

Sensor preparation was performed in a multistep approach using boiling acetone, isopropanol in an ultrasonic bath and hot $HNO_3$ (Figure 5). Specific reactions of the sensors to these procedures were not known, so, we needed to first test these sensors' resistances against the cited chemicals.

Deionized water (DI) was used for washing. Acetone as well as propan-2-ol were used for lipid and solvent removal while $HNO_3$, an oxidising agent, was applied for the removal of metal contamination on the gold surface (see Protocol 1).

During our experiments we noticed a destruction of the electrode's isolation layer caused by the treatment with boiling acetone (Figure 5C). The observed damage could have led to unreliable results. Therefore, we adapted a different protocol by Khashayar et al. 2017 using milder reagents (127).

*Protocol 1 List of cleaning steps needed for the proper removal of contamination on the gold surface.*

| Reagent | Condition |
|---|---|
| **DI** | **RT** |
| **Acetone** | **56°C** |
| **DI** | **RT** |
| **Propan-2-ol** | **Ultrasonic Bath, RT** |
| **DI** | **RT** |
| **$HNO_3$** | **50°C** |

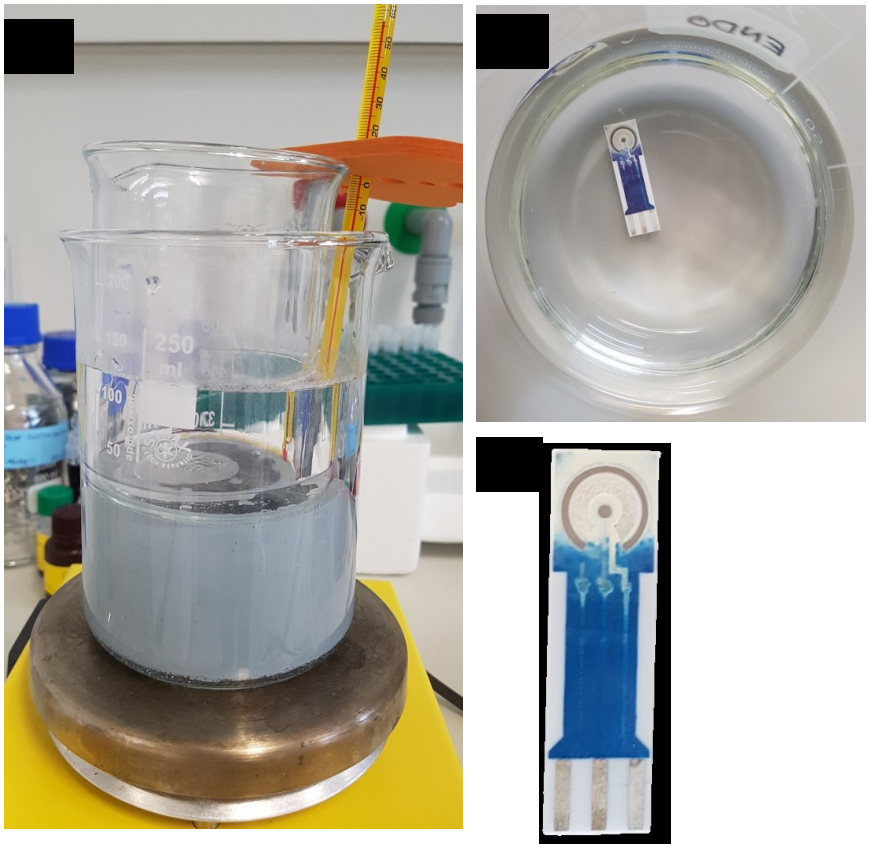

*Figure 5*
*a) Setup for boiling acetone and $HNO_3$ cleaning of the electrode*
*b) Electrode inside the cleaning chamber.*
*c) Electrode after the cleaning steps*

### 2.1.2. Protocol switch – Khashayar et al. 2017

This protocol gives a detailed description of the methods used.

**Sensor Preparation**

- Cleaning of the electrode

  The cleaning starts using 50 mM $H_2SO_4$ and cyclic voltammetry (CV) from –0.4 V to +1.4 V at a 100 mV/s scan rate as a cleaning step. 55 cycles were used to achieve a stable cyclic voltammogram which guarantees for a clean surface.

  In order to parallelise the cleaning step, which uses cyclic voltammetry as an excitation signal, a special stacked printed circuit board (PCB) device (Figure 6) was constructed in cooperation with our semiconductor company. By using the Arduino Uno SMD R3, a single board microcontroller, it is possible to apply the conditioning signals to 12 sensors at the same time, cutting time from ~30 min per electrode to ~30 min per 12 electrodes.

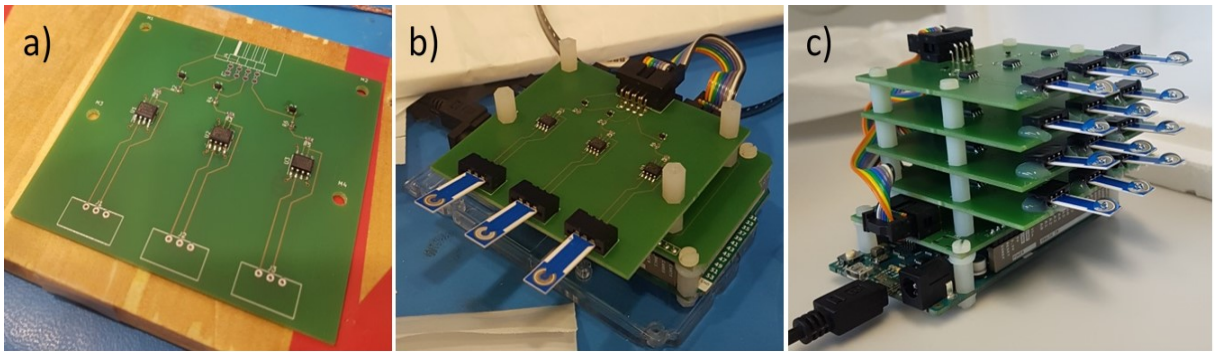


*Figure 6 First prototype of the Arduino based setup for parallelisation of the cleaning and AuNP deposition of the sensor. Printed circuit board (PCB) with conductive tracks, manually soldered converters (a) and with connection for the sensor (b) are ordered in layers of four (c) to clean and deposit on 12 sensors in parallel.*

- Electrodeposition

  Electrodeposition is the immobilisation of gold nanoparticles (AuNP) on the gold surface to increase the surface area and electron transfer between the candidate proteins and the electrode surface itself. 80 µl HAuCl4 with a 1.0 mM concentration in a 0.5 M H2S04 and 0.1 mM NaCl aqueous solution was pipetted on the dry and cleaned electrode surface. Subsequently, a CV scanning potential was applied in 0.1 V/s steps from -0.5 V to +1.5 V for 80 cycles.

- Activation of AuNP

  The activation of the AuNP modified gold surface was performed by adding 4 µl of 10 mM GSH to the WE and let dry at RT for 1h.

- Functionalisation

  For functionalisation of the gold WE 400 mM N-(3-Dimethylaminopropyl)-N′-ethylcarbodiimide (EDC) and 100 mM N-hydroxysulfosuccinimide sodium salt (Sulfo NHS) were mixed in a 1.5 ml Eppendorf tube and incubated for 20 min. before10 µg/ml of anti-mouse antibody was added and incubated for another 60 min at RT. 80 µl of this solution were thereafter deposited on the GSA-modified surface of the gold sensor and incubated for 2.5 h in a humid chamber to avoid evaporation. After gentle cleaning with phosphate-buffered saline (PBS), 10 µl of 0.2 % bovine serum albumin (BSA) in 0.1 M PBS were added to the surface to avoid non-specific binding of the antibody. The last step in preparation of the sensor was the cleaning with 0.1 M PBS followed by 0.1 M PBS 0.5 % Tween 20 (PBS-tween buffer) to reduce background noise.

### 2.1.3. First protocol - measurement using functionalised sensors

The first measurements were performed analysing mouse IgG spiked in PBS or deionised water and 0.1 mM $K_3[Fe(CN)_6]$, using differential pulse voltammetry (DPV) from +0.5 V to +1.1 V in 0.005 V/s steps. DPV uses short pulses (10-100 ms) and amplitude (1-100 mV) which are superimposed to a linear sweep leading to an overall stepwise increased voltage. The current is then measured. Duplicates of the concentrations 900 pg/ml, 300 pg/ml and 100 pg/ml were analysed according to the range of detection described by Khashayar et al. (127). In addition, comparative measurements with and without antibody as well as in PBS or in water were performed (see results Figure 16).

### 2.1.4. Protocol changes in cooperation with the Universitat Rovira i Virgili

With increasing company interest in biomarker detection using not only antibodies but also aptamers, we started a cooperation with the research group Interfibio (128,129). This group is located in Tarragona, Spain at the Department of Chemical Engineering, Universitat Rovira i Virgili (Head Prof. Ciara O'Sullivan, PhD). The close connection allowed for technology transfer in the field of electrochemistry and protein chemistry and enabled us to adapt our protocol, develop a more robust method and therefore increase reproducibility of our results. Due to the high cost of C-peptide as well as anti-C-peptide antibodies, we used human serum albumin (HSA) for protocol establishment instead.

### 2.1.5. Antibody experiments

Due to their easy accessibility, we decided to use antibodies and their fragments to establish our gold sensor-based electrochemical protein detection.

#### Indirect ELISA primary AB (A0433) anti-HSA-polyclonal from rabbit

These experiments were conducted to evaluate if we can use self-made antibodies in a sandwich type ELISA assay. This would allow for a cheap and easy test setup which, if successful, can then be transferred to the electrode. Thus, the first step was to validate the primary anti-HSA-polyclonal from rabbit (Merck, A0433) antibody. The HSA (A3782) as well as the secondary AB (A6684 anti HSA mouse) and the detection AB (A9044, anti-mouse IgG) were provided by URV together with the protocol (see also page Protocol 2 and the results on page 63). As negative control either no protein or no secondary AB was used.

The whole protocol uses 50 µl reagents per well an step except for the washing step were 200µl PBS-Tween was used

**Immobilisation**

1µg/ml AB (e.g. A0433) in carbonate bicarbonate buffer pH 8-9

Incubate 1 h 37 °C

Wash 3X PBS-Tween

**Blocking**

5 % skimmed milk in PBS-Tween 10mM 0.05% Tween 1 h 37 °C

Wash 3X PBS-Tween

Incubate with antigen (e.g. HSA A3782) 1 h 37 °C

Wash 3X PBS-Tween

**2nd AB**

Incubate with 2nd AB (e.g. A6684) 1 h 37 °C

Wash 3X PBS-Tween

**Detection AB**

Incubate with detection AB (eg. A9044) 1h 37°C

Wash 4X PBS-Tween

**Measurement**

Add TMB

Measure every 5 min at 650 nm

Stop reaction when signal is saturated

Stop with 1 M sulphuric acid (~15 min)

Measure at 450 nm

*Protocol 2 This protocol describes the steps to detect protein (HSA) using antibodies and TMB in an ELISA sandwich format.*

**Reaction buffer**: 200-500 ml of PBS: 0.1 M phosphate, 0.15 M NaCl, pH: 7.2-7.5

**Protein Solution:** Dissolve protein to be modified in reaction buffer to a concentration of 60 µM (2-10 mg/ml). For an IgG with 150.000 MW, 60 µM corresponds to 9 mg/ml.

**Deacetylation Solution**: 0.5 M Hydroxylamine, 25 mM EDTA in PBS, pH 7.2-7.5. Dissolve 1.74 g hydroxylamine-HCL and EDTA (0.475 g of tetrasodium salt or 0.365 g disodium salt) in 40 ml of reaction buffer. Add ultrapure water to a final volume of 50 ml

**Procedure for Sulfhydryl Modification of Proteins**

**Reaction of Antibody in SATA**

Immediately before reaction, dissolve 6-8 mg of SATA in 0.5 ml of DMSO (Result in ~55 mM solution) [in our case 4.4 mg in 314.5 µl of DMSO].

Combine 1 ml of protein solution with 10 µl of SATA solution. Mix contents and incubate reaction at RT for 30 min.
[Stock 9 mg/ml. Diluted to 3 mg/ml. Prepare 200 µl (20 µM)
66.4 µl of stock Ab + 133.6 µl of Reaction buffer
Add SATA 2 µl in the Ab Solution].

**Purify Acylated Protein from Excess reagents**

Using microcons pore size 50000. Centrifuge 15000 rpm 5 min. Wash 3X with 100 µl DI.

**Deacetylate SATA-Modified Protein to Generate Sulfhydryl Groups**

Combine 1.0 ml of SATA-modified (acetylated) protein with 100 µl of the deacetylation solution.
When finished, add 200 µl of reaction buffer to obtain the initial volume
Mix contents and incubate reaction for 2 hours at room temperature.

**Purify Sulfhydryl-modified protein**

Use a desalting column to purify the sulfhydryl-modified protein from the hydroxylamine in the deacetylation Solution. Desalt into reaction buffer containing 10 mM EDTA to minimize disulfide bond formation using the same procedure as in Section B. Promptly use the prepared protein in the end application. Before or after desalting, the protein may be assayed for sulfhydryl content using Ellman's reagent.

*Protocol 3 This protocol shows the experimental workflow for the production of HRP labelled antibody*

a) Horse radish peroxidase (HRP) activated antibody production (AB)
As HRP-labeled AB availability could not be guaranteed over the period of the project as well as considering the financial aspect of prelabeled antibodies, we decided to label our AB in-house. The protocol we used is adapted from the protocol provided by Thermo Scientific (130,131). See Protocol 3.

b) Generating Anti-HSA-Mouse F(ab)2 and Fab Fragments
Recent publications have shown the advantage of using only antibody fragments. These fragments, which can still detect the antigen, are for example F(ab)2. They are generated by breaking of the disulfide bond between the Fab parts and the light chain Fc using bromelain (see Protocol 4). The amount of thiol groups in antibodies, which could lead to unspecific linkage to the surface, therefore altering the antibody to be ineffective, are decreased in F(ab)2. After generation of fragments, the newly exposed sulfur can bind to the gold surface in a directed way, being more accessible to the antigen. F(ab)2 is further broken down using either L-cysteine or TCEP (see Protocol 4)generating two Fab fragments derived from the heavy chain of the former antibody (132–135).

As TCEP showed comparable results with L-cysteine, but production time is vastly reduced, we continued using only TCEP for splitting of F(ab)2 in the following experiments.

**Screen printed electrodes (SPE) for protein detection using antibodies**

After extensive testing of antibodies and fragments using ELISA, the next logical step was transfer of the protocol to the gold electrodes. As internal stability tests with the BVT electrodes showed problems with harsh reagents and URV had satisfactory results with electrodes from the company Metrohm DropSens (Spain)DropSense, we switched to their product (DRP-250AT and DRP-250BT, Datasheet attached). Therefore, only DropSense electrodes were used from this point on.

**Preparation of Column**
**Buffers**

2 l 0.15 M NaCl
40 ml Tris buffer + 50 mM EDTA (pH 7.0)
50 ml 0.01 M PBS (0.138 M NaCl + 2.7 mM KCl) pH 7.2
50 ml 0.01 M PBS (0.138 M NaCl + 2.7 mM KCl) pH 7.4
40 ml 0.1 M Phosphate buffer

50 ml of Silica was put into a column using a 20 ml syringe. The column was then slowly flushed with ~150 ml PBS. Thereafter, when the silica was settled, 0.15 M NaCl was attached via a tube and slowly dropped on the column over night (ON). The column should not run dry.

**Split of AB to F(ab)2**

50 µl of 0.5 M Tris buffer containing 50 mM EDTA
+500 µl of 1 mg/ml Anti-HSA-Mouse
+50 µl 10 mg/ml Bromelain in PBS
ON 37 °C

**Separation**

The split antibody was added to the column and after the solution was sunk into the silica, 0.15 M NaCl was slowly added. These fractions were collected in 1.5 ml tubes and measured for protein content.

**Fab Production**

**TCEP**

50 µl of 10 mM TCEP in PBS added to 50 µl 1 mg/ml F(ab)2 and is shaken 30 min. Thereafter added to 10 KD microcons and washed with 100 µl PBS. We got a concentration of 0.64 mg/ml.

**L-Cysteine**

1500 µl of 10 mM L-Cysteine in Phosphate buffer (10.3 pH) is added to 60 µl of 0.48 mg/ml F(ab)2 and incubated for 2h. Cleaned using microcons. The yield was 0.57 mg/ml.

Both Fab fragments were tested using ELISA in Maleinmate Plates.
Blocking using L-Cysteine 10 µg/ml
2nd AB 1:5700 Anti-HSA-Rabbit
Detection 1:5000 Anti-Rabbit IgG

*Protocol 4 This protocol describes the 4 steps to generate Fab, a part of the antibody, using TCEP or L-Cysteine.*

### Cleaning of SPE

The first step in this process was the cleaning of screen-printed electrodes (SPE) to remove chemical leftovers on the surface. This was performed to obtain more comparable data points and less variation of the results. There are different SPE cleaning methods with a wide range of harshness to the surface (136). As we already know that the SPE surface was not particularly robust, we skipped aggressive reagents, like piranha solution and explored four alternative cleaning methods: Ozone treatment, UV treatment, KOH treatment, as well as $H_2SO_4$ treatment.

### Detection of Human Serum Albumin (HSA) using DropSense electrodes

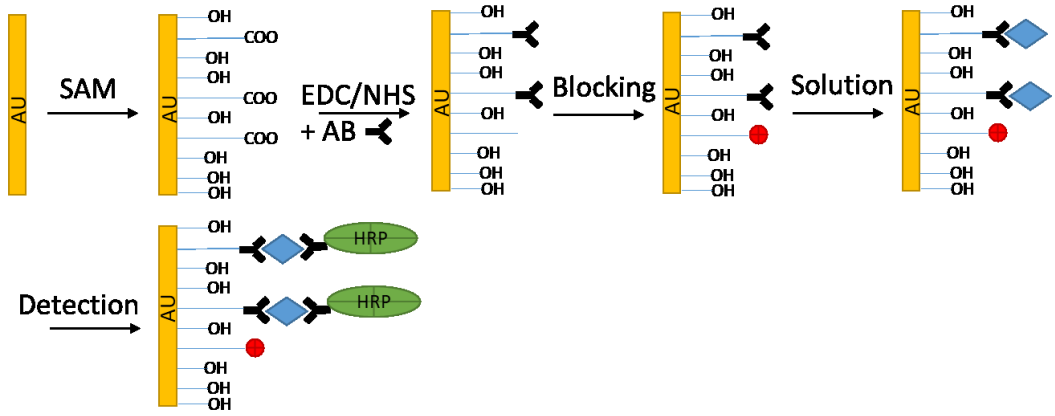


*Figure 7 Overview of the electrochemical detection of proteins on a gold surface. After cleaning the surface, a mixture of different length self-assembled monolayers (SAM) was added. These SAMs were linked via their thiol head group to the gold surface. The mixture also allowed for a better distancing of the protein thereafter. The COO-tail of the SAM then interacted with the N-(3-dimethylaminopropyl)-N'-ethylcarbodiimide hydrochloride (EDC) N-hydroxysuccinimide (NHS) which links antibodies to the chain. A blocking agent was then added to prevent unbound activated tails from binding proteins. After the surface was incubated with the solution, our protein of interest bound to the antibodies. The detection was then be done by comparing the resistant of the electrode before and after the solution. An increase after adding the solution meant that an additional isolation to due binding of proteins occurred. Another method of detection can be done by adding horse-radish-peroxidase-linked antibodies. These HRP Ab can bind to our protein and produce electrons which can be measured on the gold surface.*

The ELISA result (Figure 20) showed that, the system detection of albumin with the primary AB (A0433) Anti-HSA-Poly from Rabbit with an indirect approach was effective. From these CV as well as impedance settings seen in Protocol 5, a protocol for two different kinds of DropSense electrodes were constructed.

We expected no resistance of the bare clean electrode [Z′ over Z′′ correlation of 1] when measuring using impedance measurement (IM) (Figure 28).
After overnight (ON) incubation and cleaning, we expected a half circle and afterwards again a correlation. This half circle is the resistance of the layer (Figure 28).

**a) Experimental layout of HSA detection:**

CV and IM were performed regularly to verify if every step was carried out correctly. Measurement solution was 1 mM $K^3Fe(CN)^6$ [in 0.1 M Strontium Nitrate].

- 2 types of electrodes (AT: High Temp, BT Low Temp) 3 each
- Self-Assembled-Monolayer: 16 MHA (mercaptohexadecanoic acid) (448303 Sigma)
- 50 µl 1:1 400 mM NHS + 100 mM EDC [final:200 NHS 50 EDC]
- Anti-Albumin AB (A0433)
- Antigen HSA (A3782)

One electrode each (AT and BT) were incubated not with anti-albumin but with anti-streptavidin as control.

The protocol (see Protocol 5) was used for the functionalisation of the electrode. The ON treatment (step 6) visually destroyed the isolation layer (Figure 27) of the electrodes and the BT electrode detached from the sensor. Therefore, it was only performed for 3h in the following experiments.

1. Cleaning with DI (Deionized water)+dry $N_2$
2. 50 µl of 1 mM K3Fe(CN)6 in 0.1 M Strontium-Nitrate
3. Cyclic voltammetry(CV): -0.3 V to 0.4 V in 100 mV/s steps
4. Check for specific "gold peak" in 0.5 M Sulfuric Acid. [Only BT showed that peak]
5. DI + Dry $N_2$
6. 50 µl of 16 MHA (2.89 mg/10 ml) in ETOH 3h in humid chamber
7. DI-> ETOH-> Dry $N_2$-> Store ON
8. CV + IM
9. Clean EtOH + $N_2$
10. 50 µl 1:1 EDC+NHA for 30 min -> Wash DI + $N_2$
11. 30 µl of anti-HSA-AB [3.16 µl in 176.84 µl of 10 mM Na acetate buffer 5.0 pH, 32.8 mg/40 ml] on Electrodes, 2 AT and 2 BT electrodes
12. 40 µl of Anti-streptavidin
13. 1 h incubation followed by DI wash and $N_2$
14. Blocked with 1 M ethanolamine 30 min RT
15. 200 ng/ml HSA in PBST added 45 min RT
16. Wash PBS-T in beaker
17. Measure CV + IM

*Protocol 5 This protocol describes how to functionalise the electrode and verify every step using CV + IM.*

**b) Test of self-assembled monolayers (SAMs)**

The choice of SAMs generally has a high impact on the (gold) electrodes' capacity to bind antibodies. For linking antibodies to the gold surface differenct substances can be used. One approach is the use of self-assembled monolayers (SAMs) which consist of carbohydrates with different carbon chain lengths and a thiolgroup as a linker to the gold surface (16-mercaptohexanoic acid, 11-Mercaptoundecanoic acid). Substances with a different chain-length influence the way of antibodies function as it allows for better spacing between each antibody. Therefore, different length-mixed SAMs were tested to obtain an optimal mixture in order to optimise the protocol.

### 2.1.6. New protocol: production of gold sputtered electrodes

SPEs, although cheap and easily available, are not the only gold electrode-based option for protein detection (137). An alternative approach is the gold sputtered electrode (GSE), comprised by a very thin, but pure layer of clean gold with a known height.

GSE cleanness and gold purity are superior to SPEs with the downside of higher cost and longer production time. We decided to manufacture GSEs in order to directly compare measurement results with SPEs. GSE production was performed in a cleanroom.

A standard glass slide was covered with a commercially available positive photo-resistant (Figure 8a) substrate and activated using UV light and an iron template mask (Figure 8b). This self-created mask for a triplicate layout (Figure 32) was used to generate the pattern on the glass surface. It covers areas on the electrode from UV light where no gold circuitry should be in the final sensor.

After the following cleaning step, there was a sputtering step with a 30 nm titanium layer followed by a 10 nm gold layer on the surface (Figure 8d). The glass slide was then washed with acetone to dissolve the underlying photosensitive surface (Figure 8e and f) which leads to the formation of the pattern seen in Figure 31 page 74.

Finally, the electrodes were washed with ethanol, deionised water (DI) and blow-dried in nitrogen.

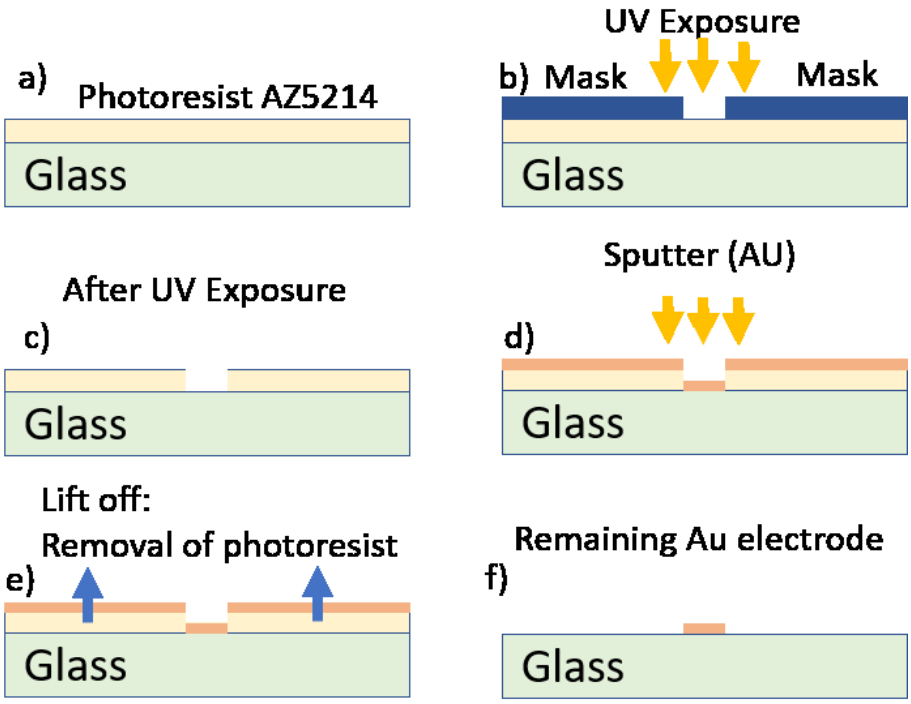


*Figure 8 Production of Gold Sputtered Electrodes*

### 2.1.7. Final protocol of the detection of HSA:

After electrode washing with ethanol, we applied deionised water and blow-dried in nitrogen. Fragments of the anti-HSA-mouse antibody were produced using 10 µl of 10 mM TCEP in PBS + 50 µl 1 mg/ml F(ab)2 (which was produced using 10 mg/ml bromelain), we added 10 µg/ml of the fragment for 3h. The electrodes were dried and stored at 4°C overnight. After blocking via mercaptohexanol (1 mM), glycerol 2,5 % and 1M $KH_2PO_4$ for 30 min., protein was added in 10K, 1K, 100, 10, and 0 ng/ml concentrations using a microfluidics system. Detection was done after 1 h incubation using 1:5000 Anti-HSA-Goat HRP produced by our cooperation partner at the University of Tarragona, Spain.

After washing with PBS-tween (100 µl/channel), the 3,3′,5,5′-Tetramethylbenzidin (TMB) was injected (10 µl/channel) and allowed to react for 2 minutes. The HSA binding event was quantified by measuring the reduction current of the HRP-oxidized TMB by pulse amperometry (0 V for 10 ms followed by −0.2 V for 500 ms). TMB acts as an electron donor.

As the production of the sputtered electrodes is generally more expensive and the fabrication of Fab fragments is time- and labour-intensive, we also tried to use another SPE electrode produced in Spain. This measurement allowed for multiplexing, as well as cheaper production.

We also tested the whole AB fragment on these SPE not only in PBS, but also more realistic setting by using synthetic urine.

### 2.1.8. HSA detection using printed circuit board (PCB) and whole antibody in synthetic urine.

The electrode arrays used in these experiments were manufactured by Fineline (Spain) using printed circuit board (PCB) technology. The electrode chip was manufactured using the typical FR-4 glass epoxy resin with a copper thickness of 30 µm as rigid substrate and with a surface finish of 3 µm soft gold, electrolytically deposited on a nickel layer of approximately 4 µm. This PCB-based chip incorporates 64 individually working electrodes, organised in four channels of sixteen electrodes each. The gold working electrodes have a circular shape of 1.0 mm in diameter and share a common gold counter and common gold reference electrode (Figure 9). The measurement was performed by Mary Luz Botero Gallego, MSc. and Josep Lluís Acero Sánchez, PhD from UVR based on the protocol for gold sputtered electrode.

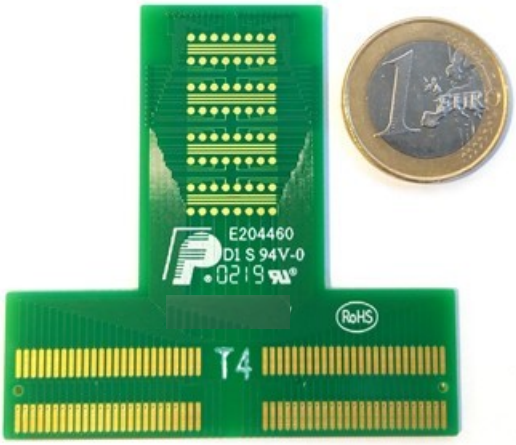


*Figure 9 PCB electrode array containing 64 gold working electrodes with one Euro to compare dimensions.*

Prior to functionalisation, the PCBs were rinsed in deionised water, blow dried with nitrogen, and exposed to a piranha solution (1 part of $H_2O_2$ and 3 parts of concentrated $H_2SO_4$) for 5 minutes. Afterwards, the arrays were successively rinsed in deionised water, ethanol, isopropanol and blow dried with nitrogen. Cleaned arrays were subsequently immersed overnight in a 1:1 mixture containing of a 0.5 mM solution of 11-mercaptoundecanoic acid (MUA) and 6-mercaptohexanol (MH), both prepared in ethanol.

Following extensive washing with ethanol, the arrays were immersed for 20 minutes in a solution of 200 mM N-(3-dimethylaminopropyl)-N′-ethylcarbodiimide hydrochloride (EDC) and 50 mM N-hydroxysuccinimide (NHS) prepared in 0.1 M MES buffer pH 6.5, rinsed with water and dried in a stream of nitrogen. A 100 µg/ml solution of α-HSA antibody (produced in rabbit) prepared in 0.1 M phosphate buffer pH 7.4 was immobilised onto the electrodes for 45 minutes at 25 °C. Following rinsing with deionised water, the arrays were blocked with ethanolamine (1 M in deionised water) for another 45 minutes at 25 °C.

Finally, the functionalised arrays were immersed in PBS-tween buffer under stirring conditions for 10 minutes, rinsed with deionised water and stored at 4 ºC until use. Negative controls consisted of electrodes blocked with ethanolamine as it binds to unreacted N-hydroxysuccinimide esters.

The detection assay was based on an enzymatic sandwich ELISA assay in which the immobilized antibody was exposed to the HSA target and subsequently, a secondary antibody conjugated with horseradish peroxidase (HRP) enzyme was added. The presence of the target is revealed by adding TMB substrate and measuring the current resulting from the reduction of the oxidized TMB by electrochemical pulse amperometry.

If the target were present, higher reduction currents would occur. Upon electrode array functionalisation, a polymeric microfluidic system developed at URV was assembled and mounted on the PCB array surface to form four individual microchannels for sample injection. Initially, the array was conditioned with 100 µl/channel of 10 mM phosphate buffered saline containing 0.05 % (w/w) tween 20 (PBS-tween). Functionalised arrays were exposed to various concentrations of HSA prepared either in PBS-tween or synthetic urine (30 µl/channel) for 45 min at 25 °C. After washing with PBS-tween (100 µl/channel), a 1:5000 dilution in PBS-tween of an HSA-HRP antibody (produced in goat) prepared at URV was injected (30 µl/channel) for 45 min at 25 °C. Following another washing step with PBS-tween (100 µl/channel), TMB enhanced HRP membrane substrate was injected (10 µl/channel), allowed to react for 2 minutes and the HSA binding event was quantified by measuring the reduction current of the HRP-oxidized TMB by pulse amperometry (0 V for 10 ms followed by −0.2 V for 500 ms).

## 2.2. Chapter II: Materials and methods for the detection and validation of biomarkers

### 2.2.1. Patient recruitment

The BioPersMed project is designed as a single-centre, prospective, observational study. Only asymptomatic subjects without diagnosed CVD but with at least one classical CV risk factor were eligible to participate. According to the published European Guidelines on cardiovascular disease prevention in clinical practice, classical CV risk factors besides of age and gender comprise (1) smoking, (2) elevated total cholesterol levels, and (3) arterial hypertension (138). Moreover, sedentary lifestyle, obesity, social environment, T1DM or T2DM, low HDL cholesterol, increased triglyceride levels, elevated fibrinogen, apolipoprotein B (apoB), lipoprotein(a), familial hypercholesterinaemia, increased high sensitivity (hs)CRP, preclinical evidence of atherosclerosis and chronic kidney disease [glomerular filtration rate (eGFR) ≤ 60 ml/min/1.73 m2] were regarded as additional potential CV risk factors. From October 2010 (first patient in) to February 2016 (last patient in), we enrolled a total of 1022 community dwelling adult men (55%) and women (45%) who live in the greater Graz area via an established recruitment network, consisting of general practitioners, peripheral hospitals, and, in most cases, through the outpatient clinics of the Division of Cardiology and Endocrinology & Diabetology.

Patients presenting with significant non-CVD independent of aetiology, or who were expected not to be able to complete study specific examinations, have been excluded from participation. Moreover, physical inability to adequately perform functional tests as well as pregnancy and serious mental health problems have been considered as exclusion criteria. Ethical approval for the BioPersMed cohort study has been granted by the Ethics Committee of the Medical University of Graz, Austria and is renewed every year (EC Nr. 24-224 ex 11-12). The BioPersMed study is conducted in compliance with Good Clinical Practice Guidelines Procedures (GCP) and complies with the Declaration of Helsinki and the Austrian laws. All participants in the BioPersMed cohort have been thoroughly checked for in- and exclusion criteria before the first phenotyping at baseline examination in order to avoid screening failures. A summary of all examinations is shown on page 51. All patients read signed an informed consent.

## 2.2.2. Follow up

The baseline exams are repeated every two years ("follow-up") additionally to interim telephone visits. According to the scheme, cohort participants will be monitored for the next decades and clinical outcomes are collected prospectively. All together 169 (17 %) participants dropped-out for various reasons. Causes for this premature unplanned termination of the study ranged from a change in residence (n = 5) to no longer having interest in study participation, limited personal time (n= 136) or new-onset of non-CV related diseases (accident: 3, cancer: 4, other: 9). 12 persons have died so far (cancer: 7, sepsis: 3, CVD: 2). In total, 1022 persons have been included in the baseline examination. After that 799 attended the follow-up two years post baseline examination. As of November 2020, 613 people have completed the second follow-up at four years after baseline visit, 440 completed the third follow-up at six years after the baseline visit. Eight years after the baseline visit, 120 participants completed the fourth follow-up (Figure 10). A small number of participants missed one follow-up but decided to continue to participate in the study. This issue explains the difference between the number of drop-outs and the amount of missing follow-up visits.

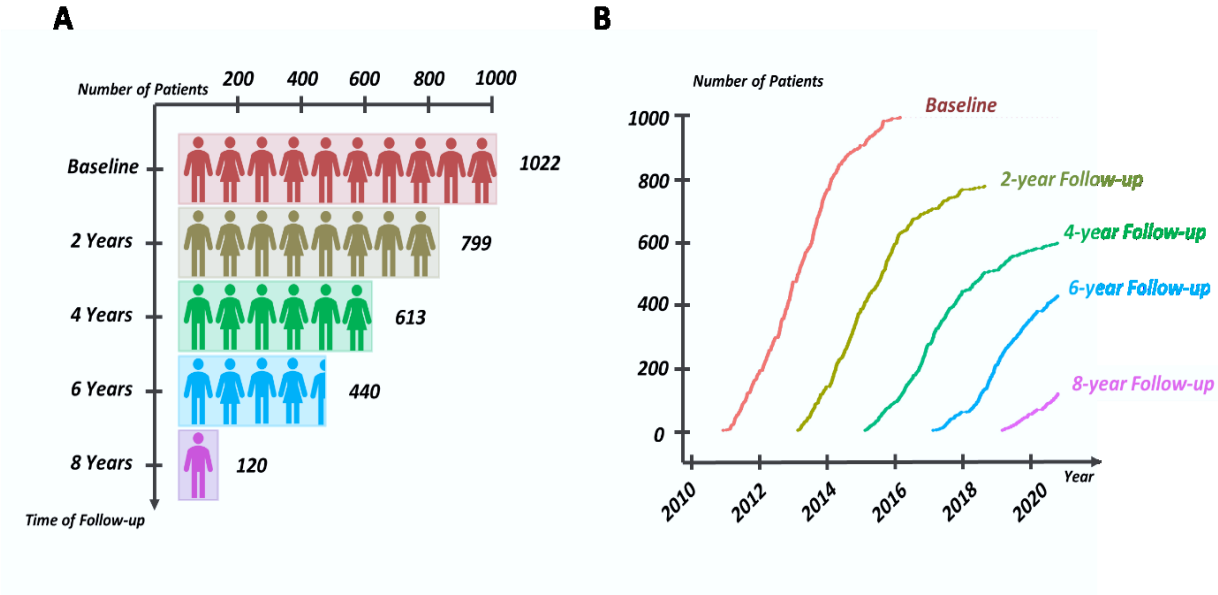


*Figure 10 Overview of the recruitment process for Baseline and Follow-ups every 2 years.*

### 2.2.3. Measured parameters in the BioPersMed cohort

At baseline and at two-years follow-up, an in-profundity diagnostic cardiovascular work-up was performed (Figure 11). The emphasis was set on reproducibility and standardisation. The measurements performed in this study include laboratory measurements of endocrine as well as cardiology parameters. A full list of measurements together with in-depth explanation is attached in the supplement. Additionally, genetic testing of all participants at baseline was done using Illumina´s Affimetrix SNP array. This array allows for the measurement of 650,000 single-nucleotide polymorphisms (SNPs).

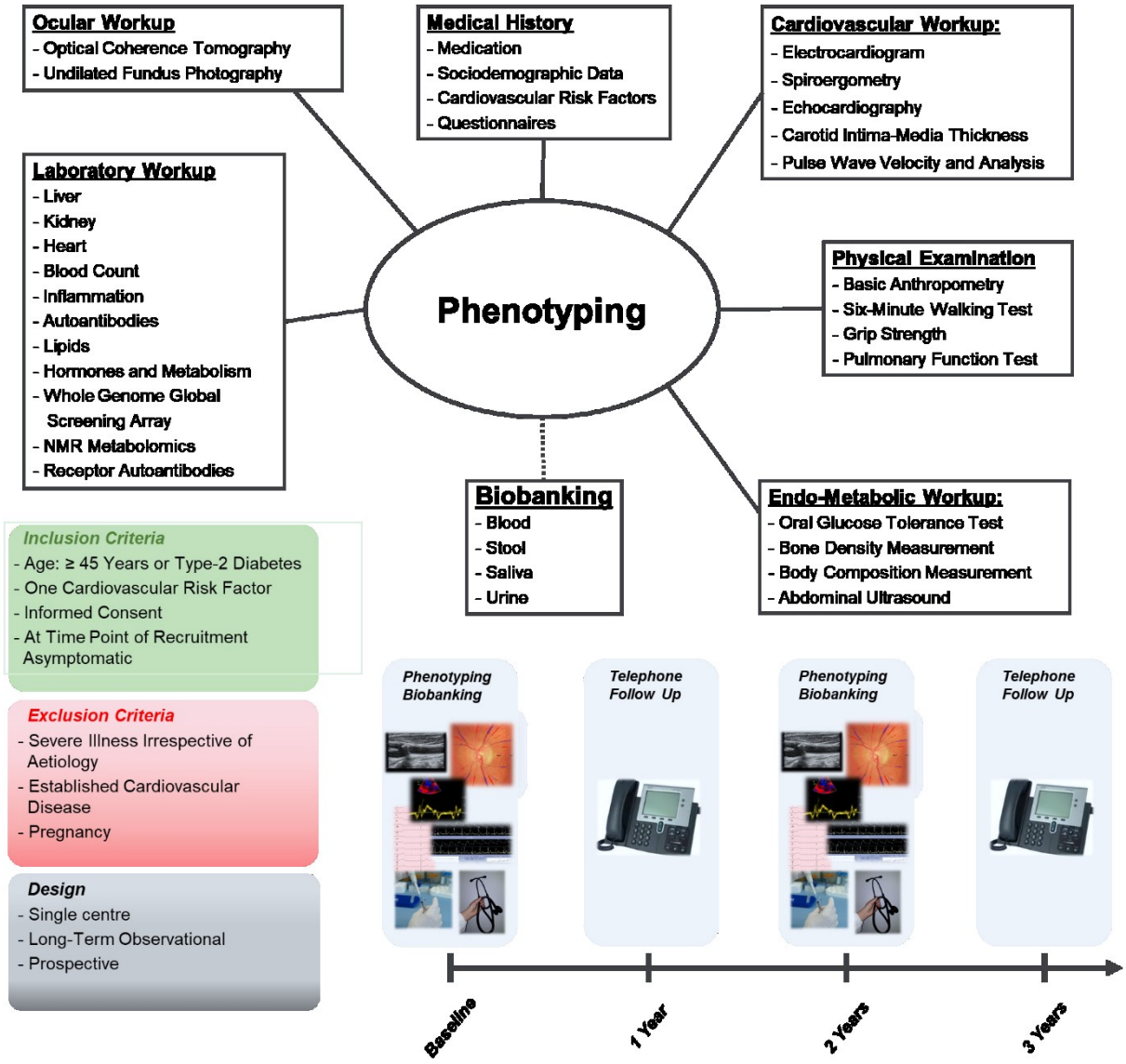


*Figure 11 Summary of the inclusion and exclusion criteria and design of the study. This figure also points out the phenotyping performed in the BioPersMed cohort.*

### 2.2.4. Data management

Laboratory data are stored as SQL using a Postgres database and automatically transmitted via an Open Clinica link or manually entered by study nurses. A user interface with dedicated fields for every entry helps to reduce entering errors.

Statistics have been calculated using RStudio Version 1.2.5033 (RStudio Inc., Boston Massachusetts, United States of America) (139). Normal distribution of data was tested and, if positive, Pearson-correlation calculated. In case of a violation of normal distribution, a non-parametric equivalent was used. A description of the data is given in the corresponding tables. Before analysis, an 80 % monitoring of the whole data set was performed by certified monitors. Biological and technical outlier were manually identified and corrected. R-Script for various data subset exports, sample matching, SNP pathway/protein connection as well as in-depth data analysis were self-made. As many research questions not only include baseline measurements of one laboratory (e.g. at the Endocrinology Lab Platform of the Medical University Graz) but needed to be interconnected with other timepoints and other laboratories via many different identifies a R was used to link these parameters horizontally (time) as well as vertically (laboratories). This allows for a holistic view of every proband. Missing variables can also be spotted more easily and, if needed, substituted with subsequent measurements, or extrapolated based on existing data.

```r
#loading needed library
pacman::p_load(tableone)
library(tidyr)
library(readxl)
library("MatchIt", lib.loc="\\\\klinikum-graz/home$/001/HaudumC/R/win-library/3.5")
library("kableExtra", lib.loc="\\\\klinikum-graz/home$/001/HaudumC/R/win-library/3.5")
#calculating LAVI from existing Biopersmed Data
biopersmed_merged_lab_export_new_visite$kof_bsa <-
0.007184*biopersmed_merged_lab_export_new_visite$pes_groesse^0.725*biopersmed_merged_lab_export_new_
visite$pes_gewicht^0.425
biopersmed_merged_lab_export_new_visite$kof_bsa[biopersmed_merged_lab_export_new_visite$kof_bsa<1]<-
NA
biopersmed_merged_lab_export_new_visite$lavi <-
biopersmed_merged_lab_export_new_visite$ecg_vol_la_vol_new/biopersmed_merged_lab_export_new_visite$k
of_bsa
#loading samples selected from Cardiology and combined with needed parameters from BioPersmed
biopersmed_AF_Proben <- read_excel("U:/Projects/PhD/BioPersMed_
Labordaten_stand_171116/Biopersmed_all_combined/cardiology/biopersmed_AF_Proben.xlsx")
Proben_AF <-
merge(biopersmed_merged_lab_export_new_visite[,c("ssid","Geb.date","study_event_oid","event_ordinal"
,"subject_age_at_event.x.11","event_start_date.x.11","pes_bmi","pes_gewicht","ecg_dim_la_es","ecg_vo
l a2 2ch","ecg vol la vol new","kd vorhofflimmern","ekg rhythmus","pes blutdruck dia","pes blutdruck
_sys","ecg_vol_lvef","lavi")],biopersmed_AF_Proben[,c("ssid","study_event_oid","event_ordinal","Ges"
)],by=c("ssid","study event oid","event ordinal"))
Cardio_start<-
merge(biopersmed_merged_lab_export_new_visite,biopersmed_merged_lab_export[,c("ssid","study_event_oi
d","event_ordinal","Geschl")],by=c("ssid","study_event_oid","event_ordinal"),all=TRUE)
#remove rows with no screening FU otherwiese fill gap will crash
Cardio_start<-subset(Cardio_start, !is.na(study_event_oid))
#creating groups to define dieseased and controll
Proben_AF$Group=1
Control_AF<-
Cardio_start[as.numeric(Cardio_start$lavi)<35&as.numeric(Cardio_start$ecg_dim_la_es)<40&Cardio_start
$kd_vorhofflimmern==2&Cardio_start$ekg_rhythmus==1&
!is.na(Cardio start$ecg vol a2 2ch)&!is.na(Cardio start$ecg vol la vol new),c("ssid","Ges","Geb.date
","study_event_oid","event_ordinal","subject_age_at_event.x.11","event_start_date.x.11","pes_bmi","p
es gewicht","ecg dim la es","ecg vol a2 2ch","ecg vol la vol new","kd vorhofflimmern","ekg rhythmus"
,"pes_blutdruck_dia","pes_blutdruck_sys","ecg_vol_lvef","lavi")]
Control_AF$Group = 0
#checking if colums are the same to allow for binding (=combination of rows of 2 sets) making one
dataset
names(Control_AF)
names(Proben_AF)
Pool_AF <- rbind(Proben_AF, Control_AF)
#delte samples with missing values
Pool_AF<-
na.omit(Pool_AF[,c("ssid","study_event_oid","event_ordinal","pes_bmi","subject_age_at_event.x.11","G
es","Group")])
#make the "random" reproducible"
set.seed(1111)
#searches for controls in our dataset mating the diseased in ges (gender), age and bmi with nearest in
a 1:1 ratio. And plots a summary of the results
match.it <- matchit(Group ~ subject_age_at_event.x.11 + Ges +pes_bmi, data = Pool_AF, method="nearest",
ratio=1.0)
a <- summary(match.it)
plot(match.it, type = 'jitter', interactive = FALSE)
match_AF <- match.data(match.it)[1:ncol(Pool_AF)]
#extract the matched samples from our pool and writes them as a csv file for samples extractiom from
the biobank
matched_AF_all_data<-
merge(match_AF[,c("ssid","study_event_oid","event_ordinal")],Pool_AF,by=c("ssid","study_event_oid","
event_ordinal"))
write.csv(matched_AF_all_data,"matched_AF_all_data_filtered.csv",sep = "/t")
#summery of how well the sample matching worked exported as means as a HTML file.
kable(a$sum.matched[c(1,2,4)], digits = 2, align = 'c',
      caption = 'Table 3: Summary of balance for matched data',"html", booktabs = T)
kable(a$nn, digits = 2, align = 'c',
      caption = 'Table 2: Sample sizes')
      caption = 'Table 2: Sample sizes')
```

*Figure 12 Example of a R-Script to extract matched BioPersMed controls for a set of known patients based on different variables (e.g. Age, BMI). Green lines starting with # are comments to explain the code to readers.*

## 2.3. Chapter III: Materials and methods for the detection of PCOS biomarkers*

### 2.3.1. Study Design

The intervention study was conducted at the Medical University Graz, Dept. of Internal Medicine, Division of Endocrinology and Diabetology in Austria. The protocol was approved by the local ethical committee (EK 26-347 ex 13/14). Written informed consent was provided by all participants; they were at least 18 years old.

PCOS was diagnosed according to the revised Rotterdam Criteria (2003) defined by the American Society for Reproductive Medicine (ASRM) and the European Society of Human Reproduction and Embryology (ESHRE). According to these criteria, at least two of the following symptoms needed to be present to diagnose PCOS: oligo- or anovulation, biochemical or clinical hyperandrogenism and polycystic ovarian morphology by ultrasound. The three diagnostic features were assessed and relevant disorders were excluded as published (103). Individuals in the control group did not meet any of the Rotterdam Criteria, with the exception of one case of isolated long-standing mild hirsutism with no other PCOS criterion, Ferriman–Gallwey score of 10 (normal reference <7) (140). This case is seen as a naturally occurring event in non-PCOS populations and did not significantly alter any outcomes (141). Pre-menopausal women were included in this study. Exclusion criteria for all women were antidiabetic, or antibiotic drug use, oral contraceptive within the preceding three months, periodontal-, acute or chronic gastrointestinal diseases, active infections at anybody site, a body mass index (BMI) <18 or >40, a known allergy to soy, and smoking (Table 3).

*Table 3 Anthropometric, metabolic, and steroid hormone parameters in women with PCOS and control women before isoflavone intervention.*

| | *Reference range* | *Controls (n=20)* | | *PCOS (n=24)* | | |
|---|---|---|---|---|---|---|
| | | median | IQR | median | IQR | p-value |
| ***Age*** | | 32 | 12.0 | 27 | 5.9 | 0.003** |
| ***Anthropometric parameters*** | | | | | | |
| *Body mass index* | 18.5-25.0# | 22.3 | 4.10 | 24.9 | 11.75 | 0.147 |
| *Waist to hip ratio* | < 0.85# | 0.80 | 0.06 | 0.82 | 0.077 | 0.439 |
| ***Metabolic parameters*** | | | | | | |
| *Fasting glucose (mmol/l)* | < 7.0† | 4.5 | 0.50 | 4.7 | 0.59 | 0.209 |
| *AUC glucose (mmolh/l)* | § | 10.2 | 4.52 | 10.9 | 3.61 | 0.273 |
| *Fasting insulin (pmol/l)* | 20.9-173.8 | 41.4 | 51.08 | 84.4 | 55.25 | 0.022* |
| *AUC insulin (mmolh/l)* | § | 353 | 427.3 | 691 | 562.0 | 0.009** |
| *HOMA2-IR* | < 2.0 | 0.8 | 1.05 | 1.7 | 1.20 | 0.027* |
| *Total cholesterol (mmol/l)* | < 5.2 | 4.6 | 0.64 | 4.5 | 1.13 | 0.699 |
| *LDL cholesterol (mmol/l)* | < 3.4 | 2.3 | 0.83 | 2.3 | 1.14 | 0.144 |
| *HDL cholesterol (mmol/l)* | > 1.0 | 2.0 | 0.42 | 1.7 | 0.49 | 0.006** |
| *Triglycerides (mmol/l)* | < 1.65 | 0.59 | 0.25 | 0.74 | 0.24 | 0.010* |
| ***Serum sex hormones*** | | | | | | |
| *FSH (IU/l)* | 0.5-61.2‡ | 9.2 | 8.11 | 7.5 | 2.73 | 0.178 |
| *LH (IU/l)* | 2.0-22.0‡ | 5.8 | 9.34 | 9.3 | 8.60 | 0.042* |
| *LH:FSH ratio* | § | 1.2 | 1.19 | 1.5 | 1.06 | 0.035* |
| *SHBG (nmol/l)* | 18 - 144 | 78 | 29.40 | 43 | 41.50 | <0.001*** |
| *AMH (pmol/l)* | 1.4-65.2 | 26.8 | 22.42 | 61.1 | 52.59 | 0.0002*** |
| *Total testosterone (nmol/l)* | 0.37-2.1 | 1.1 | 0.56 | 1.3 | 0.77 | 0.002** |
| *DHT (nmol/l)* | § | 0.34 | 0.24 | 0.46 | 0.528 | 0.096 |
| *Androstenedione (nmol/l)* | 0.89-7.5 | 2.6 | 1.61 | 4.2 | 2.69 | 0.0003*** |
| *DHEA (nmol/l)* | § | 13.7 | 11.37 | 21.4 | 12.40 | 0.015* |
| *DHEAS (µmol/l)* | § | 3.3 | 3.74 | 4.9 | 2.35 | 0.073 |
| *Free testosterone (pmol/l)* | § | 10.6 | 5.86 | 20.9 | 13.00 | <0.0001*** |
| *Free DHT (pmol/l)* | § | 1.3 | 1.03 | 3.0 | 2.19 | <0.0001*** |
| ***PCOS assessment*** | | **# of cases** | **% of cases** | **# of cases** | **% ofcases** | **p-value** |
| *Oligo-/Amenorrhoea* | | 1 | 5 | 17 | 71 | <0.0001*** |
| *Hirsutism* | | 1 | 5 | 11 | 46 | 0.003** |
| *PCOM* | | 0 | 0 | 22 | 96 | <0.0001*** |
| ***Dietary assessment*** | | **median** | **IQR** | **median** | **IQR** | **p-value** |
| *Total points* | | 69 | 27.0 | 68 | 31.8 | 0.318 |
| *Grains (% of total points)* | | 19 | 9.4 | 17 | 8.9 | 0.025* |
| *Dairy (% of total points)* | | 13 | 8.6 | 13 | 10.2 | 0.502 |
| *Meat/Fish (% of total points)* | | 6 | 6.4 | 7 | 6.8 | 0.649 |
| *Fruits/Vegetables (% of total points)* | | 17 | 11.4 | 19 | 12.6 | 0.856 |
| *Fats (% of total points)* | | 10 | 6.0 | 12 | 5.2 | 0.258 |
| *Soy (% of total points)* | | 1 | 1.9 | 1 | 2.5 | 0.658 |

*IQR, interquartile range; AUC, area under the curve; HOMA2-IR, homeostasis model assessment for insulin resistance; LDL, low density lipoprotein; HDL, high-density lipoprotein; FSH, follicle-stimulating hormone; LH, luteinizing hormone; AMH, anti-Müllerian hormone; DHT, dihydrotestosterone; DHEA, dehydroepiandrosterone; SHBG, Sex hormone-binding globulin; DHEAS, DHEA sulfate; PCOM, polycystic ovarian morphology. #as defined by the World Health Organization; †as defined by the American Diabetes Association; ‡depending on menstrual cycle phase; §reference range not defined. Normally distributed data were compared using unpaired student's t-tests. Non-normally distributed data were either log-transformed, followed by parametric testing, or compared using Mann-Whitney U tests. Categorical data were compared using Fisher's Exact tests. Adapted from* (142)

Twenty-five metabolically healthy controls and 25 eligible women with PCOS from 230 screened patients (Table 3) reported to the Medical University of Graz, outpatient clinic of the division of endocrinology and diabetology the morning after an overnight fast. Baseline blood samples were drawn (Table 3) and medical history and anthropometric data were obtained. A baseline sample of spot urine was provided. Six of initially 50 participants were excluded from the analysis, either due to previously undetected hyperandrogenemia (n = 3 controls), smoking during the study period (n = 2 controls) or low BMI <18 (n = 1 PCOS). Screening for equol producing capacity and microbiome analysis could not be performed in one control subject because the subject did not complete the second study visit.

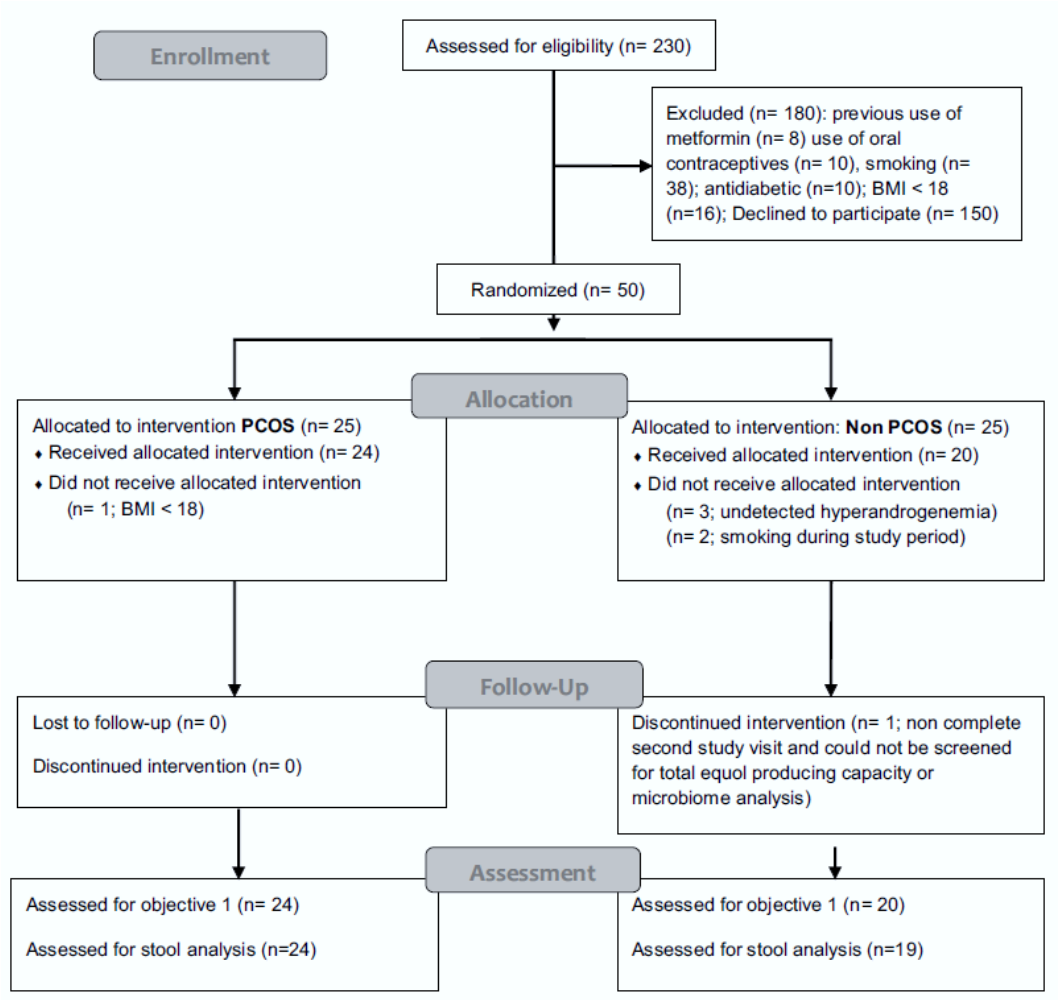


*Figure 13 Flow diagram from patient recruitment process to the final analysis.*

A 75 g oral glucose tolerance test (oGTT; Glucoral 75 Citron, Germania Pharmazeutika, Vienna, Austria) was performed, with blood sampling after 30, 60 and 120 minutes. Patients completed a food frequency questionnaire (FFQ), developed by the Clinical Medical Nutrition Therapy Unit, University Clinic Graz, adapted to include soy products, to validate the intake of major food groups (103).

After the first visit, an isoflavone intervention was performed according to an already published protocol to achieve steady-state serum concentrations as confirmed by Utian et al. (101,109). Participants consumed a soy drink (Joya© Choco Soy Drink 200 ml, Mona Naturprodukte GmbH, Vienna, Austria) twice a day (morning and evening) on three following days (approximately 25 mg of isoflavones per soy drink (110)). Stool samples were self-collected before the first soy drink using empty stool collection tubes with an inbuilt spatula (Praxisdienst GmbH, Longuich, Germany), stored at -16°C for a short time and returned to the outpatient clinic on cool packs on the morning following the last soy drink. At this time, post-intervention stool samples and urine were collected. The first and second study visits interval was 5 ± 1.3 (mean ± standard deviation) days.

### 2.3.2. Biochemical Measurements

Androstenedione, total serum testosterone, dihydrotestosterone (DHT), dehydroepiandrosterone (DHEA) and DHEA sulfate (DHEAS) were measured by liquid chromatography-tandem mass spectrometry (LC-MS/MS) as described by Lindheim et al. (103). Urinary daidzein, genistein and equol were measured using LC-MS/MS at LGC (Cambridgeshire, United Kingdom) according to a published method (143). Serum anti-Müllerian hormone (AMH), insulin, sex hormone-binding globulin (SHBG) were measured by automated chemiluminescence immunoassay (ADVIA Centaur XP, Roche, Rotkreuz, Switzerland). Serum luteinizing hormone (LH) and follicle-stimulating hormone (FSH) were measured by enzyme-linked immunosorbent assay (DiaSource, Louvain-la-Neuve, Belgium). Plasma high-density lipoprotein (HDL) cholesterol, total cholesterol, triglycerides, urine creatinine and glucose were measured by automated enzymatic colorimetric assay (Cobas, Roche, Germany). To evaluate the influence of isoflavone intervention on metabolic health we also examined changes in fasting insulin, fasting glucose and the homeostasis model measurement for insulin resistance (HOMA2-IR) in control (n=19) and patients (n=24) between T0 and T1.

### 2.3.3. Calculation of Indices

The calculation of "Body mass index" (BMI) was performed as $\frac{Weight\ (kg)}{Height\ (m)^2}$. The "homeostasis model assessment for insulin resistance" (HOMA2-IR) index was created via the HOMA calculator V2.2.3 designed by the Diabetes Trial Unit, University of Oxford, UK (dtu.ox.ac.uk/homacalculator, last accessed Sept 21, 2020). Area under the curve (AUC) for insulin and glucose was calculated from the oGTT data using the trapezoidal method. Free DHT and free testosterone were calculated from SHBG and total testosterone/DHT described previously [10]. Urine isoflavone concentrations were normalized to urine creatinine using the formula $100 \times \frac{[C]analyte}{[C]creatinine}$. Microbial metabolism of daidzein to equol was evaluated using the equol:daidzein ratio (E:D). An equol producer was defined as having a log10 (E:D) greater than -1.5 (101).

### 2.3.4. Next-generation sequencing of stool samples

DNA was extracted from stool samples using the MagNA Pure LC DNA Isolation Kit III (Bacteria, Fungi) on the MagNA Pure Instrument (Roche, Switzerland). Stool samples were thawed partially and a peanut-sized piece was homogenized in 500 µl 1x phosphate-buffered saline (PBS), according to the manufacturer's instructions. 250 µl of diluted sample was added to 250 µl bacteria lysis buffer in a sample tube containing MagNA Lyser Green Beads (1.4 mm diameter ceramic beads, Roche). Samples were homogenized (MagNA Lyser Instrument) followed by lysozyme treatment (Roth, Germany) at 37°C for 30 minutes, then proteinase-K (Roche) at 60°C for 1 hour. Lysates were afterwards incubated at 95°C for 10 minutes, cooled on ice for another 5 minutes, and high speed centrifuged. DNA was isolated by the MagNA Pure Instrument with manufacturer´s software. 100 µl supernatant volume was used. This sample was eluted in 100 µl elution buffer. PCR reaction was performed to amplify the region V1-2 of bacterial 16S rRNA gene using primers F27 (AGAGTTTGATCCTGGCTCAG) and R357 (CTGCTGCCTYCCGTA) (Eurofins Genomics, Germany) and the FastStart High Fidelity PCR System, dNTPack (Roche). 15µl of normalized and pooled PCR product were used as a template for indexing PCR to introduce barcode sequences to each sample according to Kozich et al (144). Amplicons of the bacterial 16S rRNA were sequenced on a MiSeq desktop sequencer (Illumina, Eindhoven, Netherlands) according to the manufacturer's instructions.

### 2.3.5. Processing of sequencing data

Fastq-join tool was used to join paired end reads and cutadapt 1.6 to remove primers. USEARCH 6.1 was used for reference based chimera detection (145).

Open reference operational taxonomic unit (OTU) picking was performed with the QIIME 1.9 pipeline on Medical University Graz in-house galaxy server using UCLUST against the greengenes 13.8 (146–148). Sequences were blasted in the NCBI database for further classification (149). Clustering, by UCLUST, was performed with a 97% sequence similarity threshold (150). The phylogenetic tree was generated with Fasttree. Analyses of alpha diversity were based on phylogenetic diversity (PD) whole tree as well as Shannon calculated in QIIME1.9. Beta diversity was calculated using Calypso Biomarker Discovery pipeline with QIIME 1.9 output (151). OTUs were filtered for abundance in at least two samples and an overall minimum abundance of ten.

### 2.3.6. Predicted metagenome analysis

PiCRUST (Phylogenetic Investigation of Communities by Reconstruction of Unobserved States) was used to predict differences in the functional composition of the metagenome between PCOS patients (n = 24) and controls (n = 19) and LEfSe (Linear discriminant analysis effect size) in combination with the QIIME1.9 (152,153). PiCRUST is done using 16S rRNA sequencing (Illumina, Netherlands) to predict the gene families contributing to the metagenome and identify the Kyoto Encyclopedia of Genes and Genomes (KEGG) bacteria pathways (154). We want to analyse the predicted metagenomic communities and the metabolic influence of a maximum number of OTUs. Therefore only singletons were removed for PiCRUST analysis. linear discrimination analysis was used by LEfSe to search for linear combinations of variables, e.g. bacteria, to generate two separate groups (155). These variables are used to calculate the effect size as a logarithmic LDA score (156).

### 2.3.7. Statistical analysis

SPSS Statistics Version 23 (IBM Inc., USA) was the statistical software for most tasks. Continuous data were screened for normality as well as equality of variance. All normally distributed data were compared using unpaired student's t-tests. Non-normally distributed values were either log-transformed, followed by parametric testing, or compared by Mann-Whitney U tests. All categorical data were compared with Fisher's Exact tests. Correlations

were tested with Spearman's correlations. Z scores (Z) were calculated from serum parameters using the standard mean of the samples ($\bar{x}$) and standard deviation (S) of the samples on normal distributed data (x), $Z = \frac{x - \bar{x}}{s}$ (157). The aggregated z-scores were calculated from the sum of every z-score in the categories of "androgens" and "fertility".

The effect size of variation of urinary equol concentration was calculated through two-sided, two-sample T test based on fold, expecting a urinary equol fold change of 7 when the fold change under the null hypothesis is 2 (101). In case of missing values, patients were excluded from the analysis for that variable. All data are expressed as interquartile range (IQR) and median. For the food frequency questionnaire, participant responses were assigned points based on the self-reported consumption frequency. Percentage of total points and total number of points in different food groups were compared between the groups.

# 3. Results

## 3.1. Chapter I: Results of the protein measurements for sensor development

### 3.1.1. Specific approach to sensor preparation – the development of a protocol

Three different electrode cleaning conditions (acetone, acetone and isopropanol, and acetone, isopropanol and $HNO_3$) were compared to electrodes rinsed in PBS only as control (Protocol 1). The measurements were performed with these BVT electrodes using Bode Plot (Figure 14), describing the phase change (degree) during an applied frequency change. This is used to determine the viability and integrity of the electrode (158). The results showed that cleaning with $HNO_3$ altered the electrode unusable. Beside the $HNO_3$ treated sensor, no changes were detectable compared to untreated sensors.

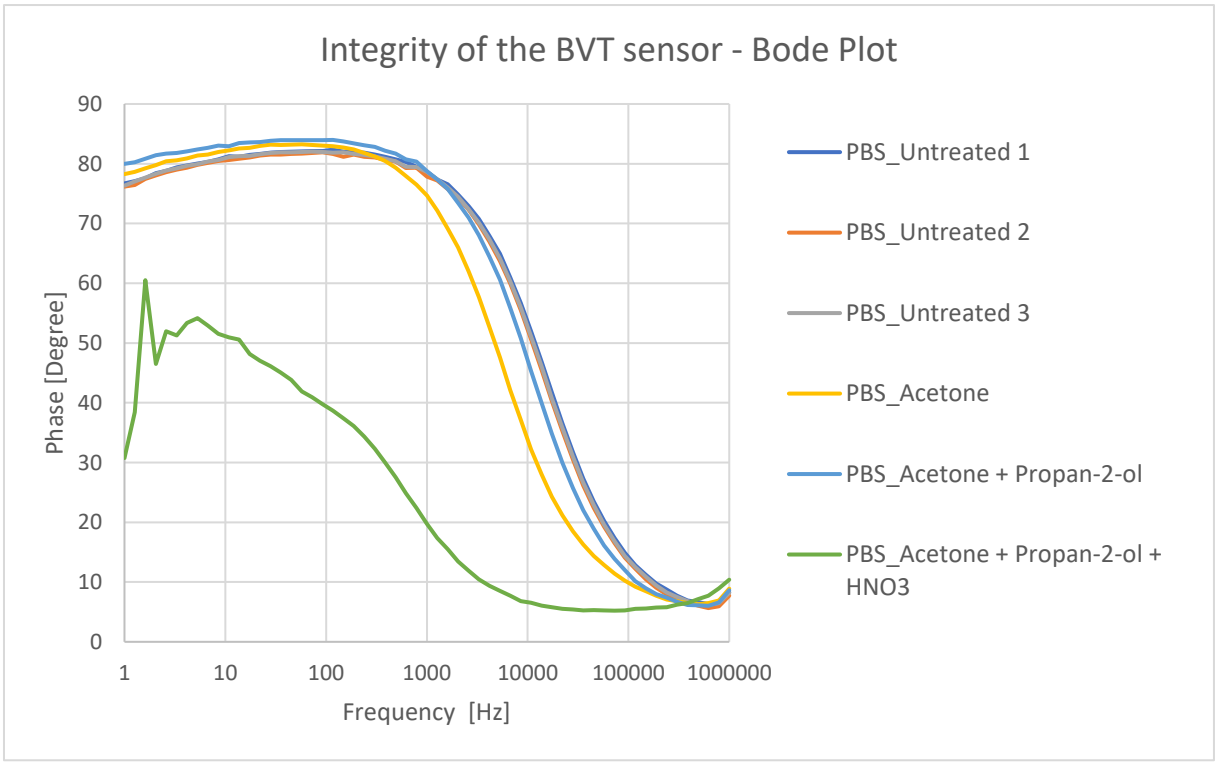


*Figure 14 The Bode plot describes the phase change during an applied range of frequencies. This gives insight into the viability and integrity of the BVT sensors. Three untreated sensors (untreated 1-3), one treated with acetone, one with acetone and propan-2-ol and one that underwent all cleaning steps were compared in PBS buffer solution.*

### 3.1.2. Protocol switch – Khashayar et al. 2017

The protocol used was described by Khashayar et al. 2017 (127).

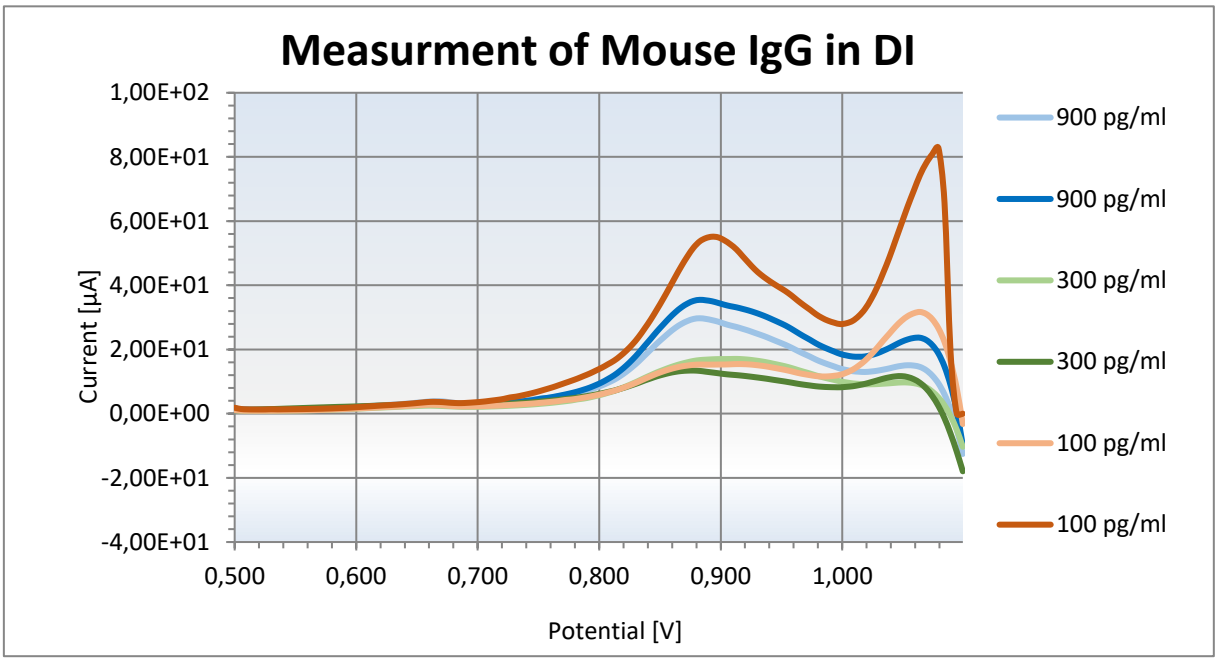


*Figure 15 Comparison of three different concentrations of mouse IgG in DI. and 0.1 mM $K_3[Fe(CN)_6]$ using DPV based on the protocol adapted from Khashayar et al. 2017*

Although there is a visible difference of the 0.880 V peak between the detection of 900 pg/ml and the other measurements, there is no differentiation between 300 pg/ml and 100 pg/ml. Sensor with 100 pg/ml showing a higher peak than the sensors measuring 900 pg/ml lead to the conclusion that there might have been an error in the cleaning or deposition steps of that sensor(Figure 15).

Concentrations measured in duplicates show that although the current at our peak of interest (0.880 V) correlates with the concentration and is reproducible, only a determination between high (900 pg/ml) and low (300/100 pg/ml) is possible at this point (Figure 16). Figure 16 partly replicates the results seen in Figure 15. However, we also observed a difference in current when measurements were performed in DI or PBS.

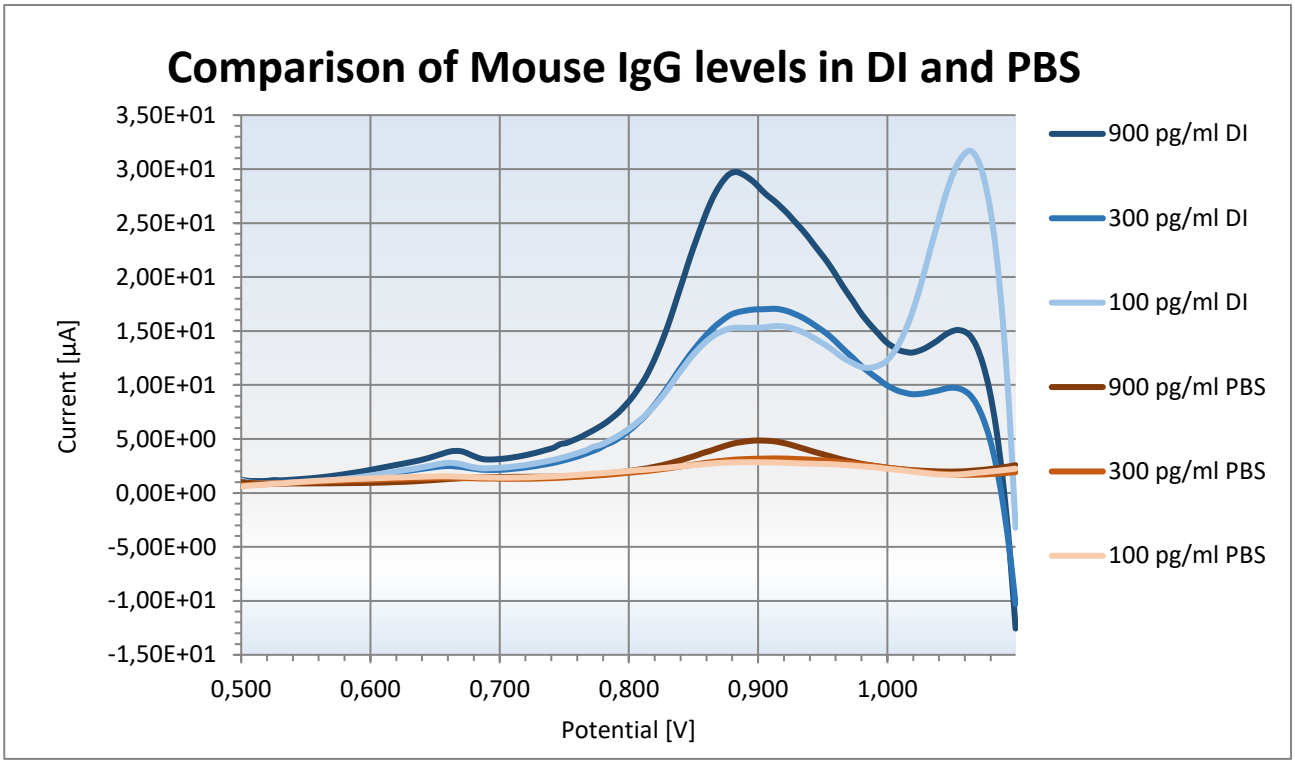


*Figure 16 Measurement of 900 pg/ml, 300 pg/ml and 100 pg/ml mouse IgG levels in DI and PBS using DPV.*

### 3.1.3. Antibody experiments

The sensor protocol was adapted during my research stay at the Universitat Rovira i Virgili,Tarragona, Spain.

**Indirect ELISA: primary AB (A0433) - anti-HSA-Polyclonal from Rabbit**

The indirect ELISA showed good results for the albumin detection system with the chosen primary AB (Merck, A0433) anti-HSA polyclonal from rabbit. The negative control with either no protein or no secondary AB showed no albumin detection, respectively.

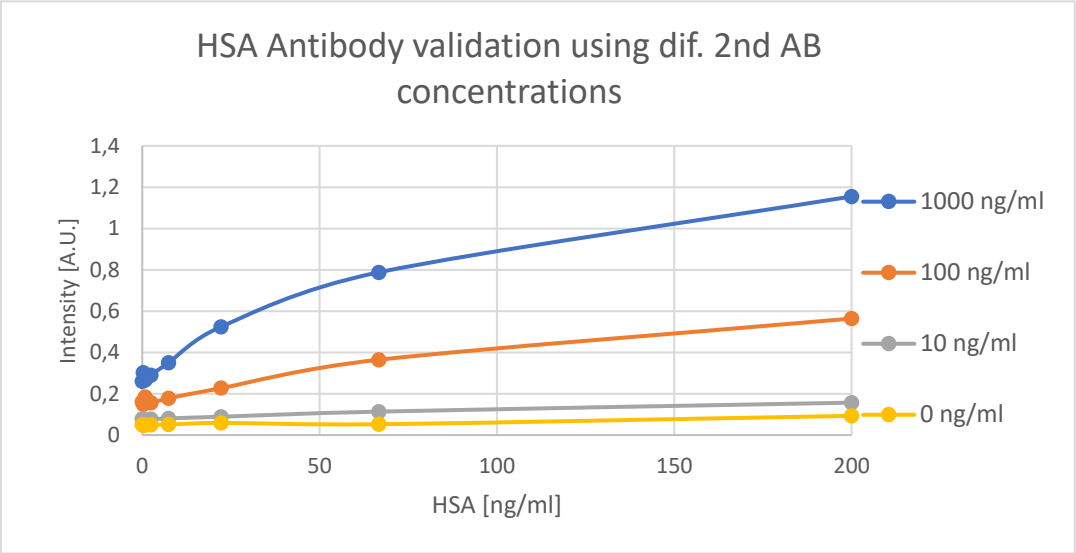


*Figure 17 Validation of HSA antibody using 1:20000 primary antibody and different concentrations of detection antibody in an ELISA format.*

**Generating anti-HSA-Mouse F(ab)2 and Fab fragments**

The fractions 15 to 20 generated by the column separation (Figure 18) contained a high amount of protein. This was determined by NanoDrop™ (Thermo Scientific) using 280 nm wavelength. The first peak is the F(ab)2. This finished product showed a concentration of 5 mg/ml and was stored in 50 µl aliquots at -20 °C. The following peaks are caused by products such as the Fc part of the antibody.

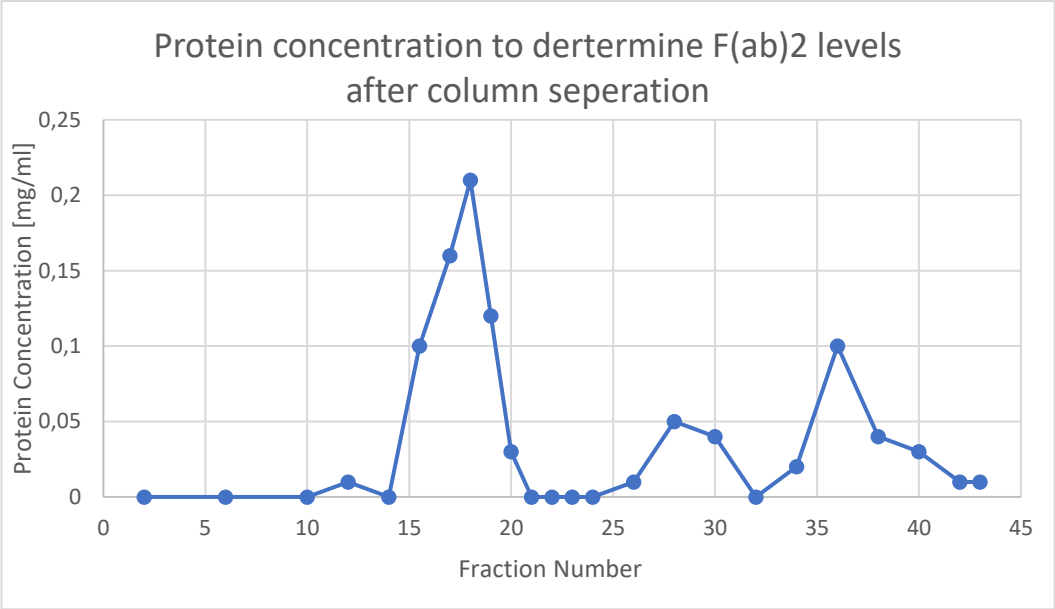


*Figure 18 Protein concentrations measured in each fraction generated by column seperation. Fractions 15 to 20 depict the expected F(ab)2 fragments.*

The usage of the F(ab)2 was compared to anti-HSA mouse on 96 well plates (Nunc, Thermo Fischer Scientific) in an indirect ELISA approach and showed similar results (159). The F(ab)2, besides the 1 ng/ml, worked as the intensity measured is higher than 1 (Figure 19). When compared to the full-length antibody (Figure 20) F(ab)2 showed similar intensity levels.

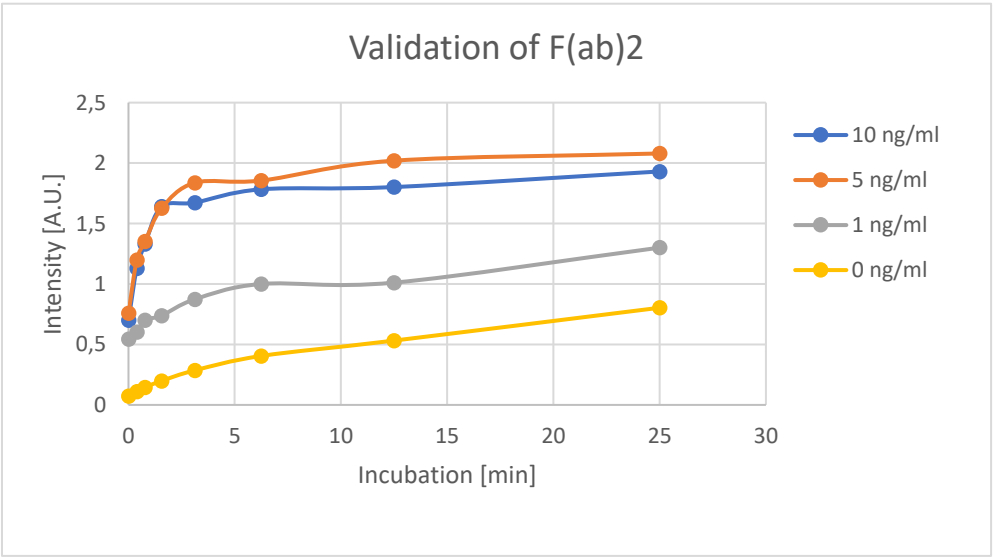


*Figure 19 Various concentrations of F(ab)2 were tested in an ELISA approach.*

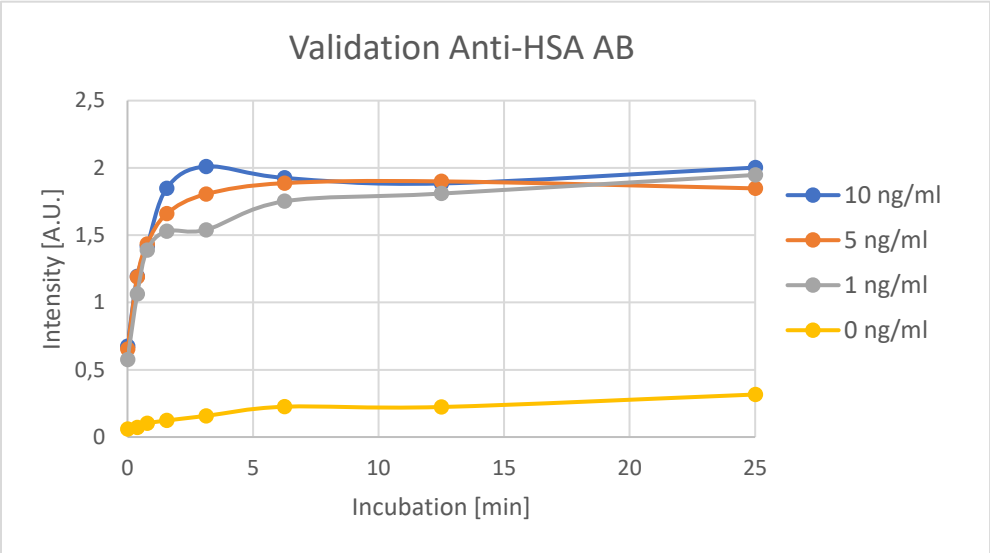


*Figure 20 Various concentrations of Anti-HSA AB were tested in an ELISA approach.*

Both methods for generating Fab from F(ab)2, TCEP and L-cysteine were tested for usage in an ELISA approach. Although both methods worked, there was a high background signal indicating insufficient blocking. Therefore, the experiment was repeated with 5% skimmed milk blocking and the results indicate a good background signal reduction.

### 3.1.4. Screen printed electrode experiments

**SPE-Setup: Cleaning of the Electrode**

The cleanness of a gold surface is defined by a high peak-to-peak (p-p) separation in the cyclic electrovoltagram. After rinsing with DI, the DropSense electrodes seemed to be already clean with a p-p of 50 mV (132 mV and 82 mV) (160). After the cleaning with ozone, the p-p was still 50 mV (122 mV and 72 mV, Figure 21) indicating that this cleaning did not improve the DropSense electrode. Furthermore, the peak height did not change significantly. The software used for measurement and visualisation was GPES Software 4.1 (Metrohm Autolab B.V., Netherlands).

The Dropsense electrode type AT, which were produced with higher temperature compared to BT, showed a good p-p <100 mV. Unfortunately, the Dropsense BT electrodes showed no peak after the cleaning with $H_2SO_4$ (
Figure 22).

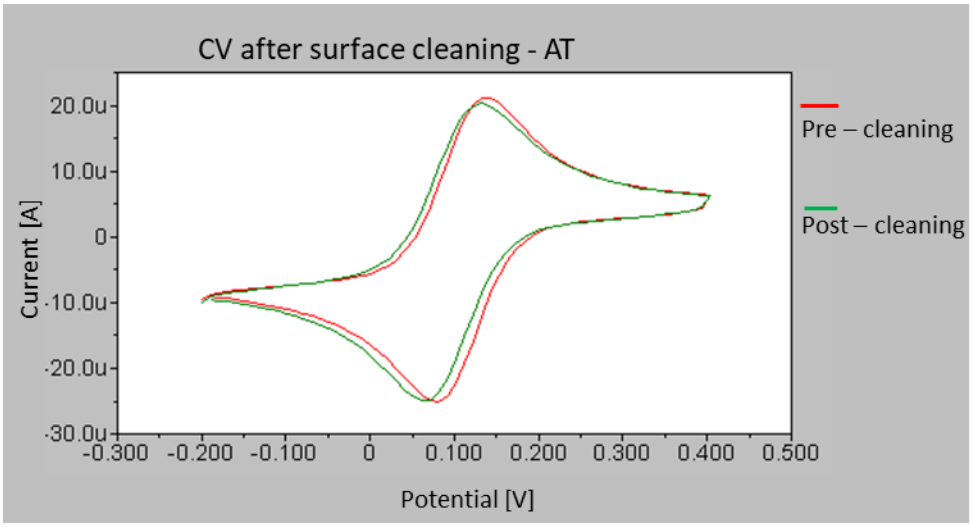


*Figure 21 The electrovoltagram of the DropSense AT electrode Ate01s03 before(red) and after (green) cleaning with H2SO4.*

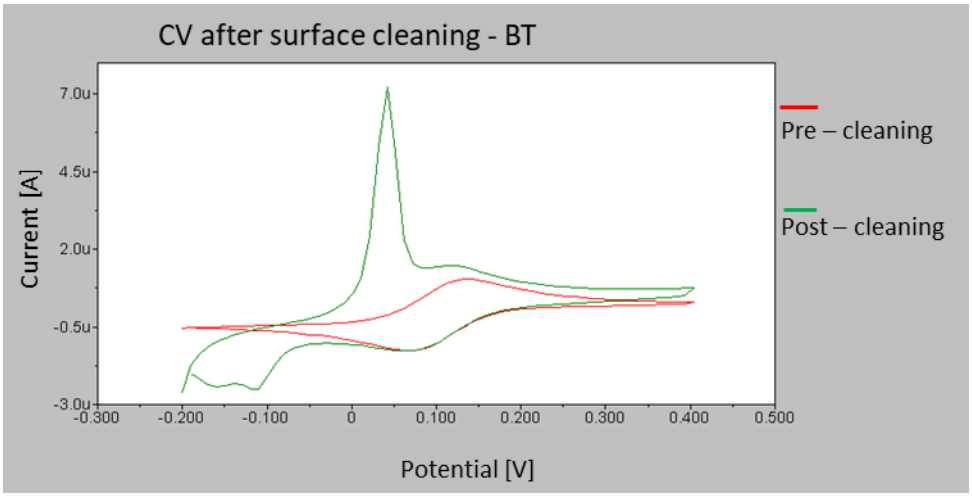


*Figure 22 The electrovoltagram of the DropSense BT electrode BVT_e01s03 before and after cleaning with H2SO4*

The electrovoltagram shows the reduction and oxidation peaks. This peak-to-peak separation should be around 0.08 V. The DropSense electrodes seemed clean from the beginning.

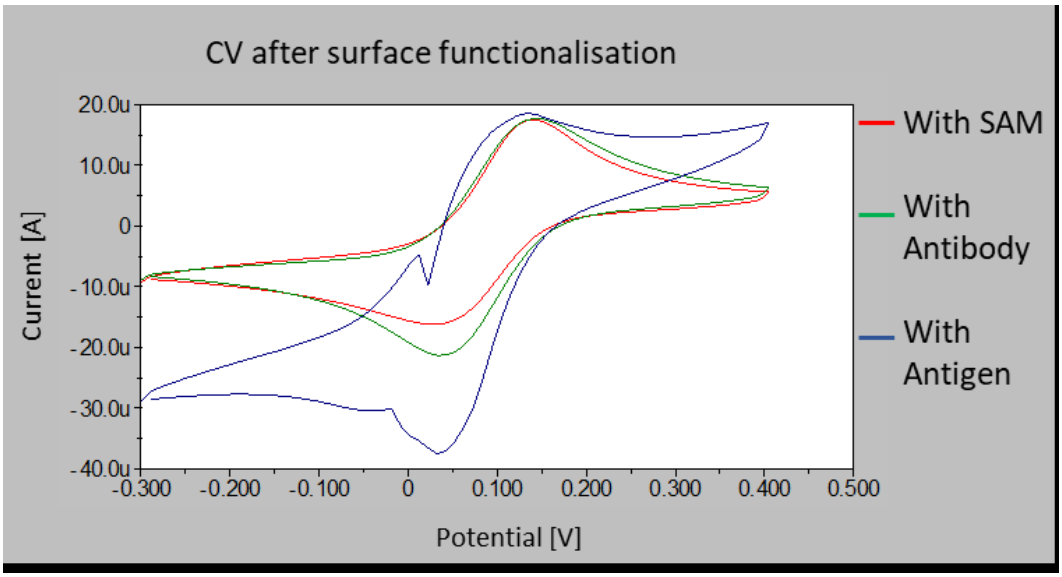


*Figure 23 CV of the AT electrode ATe01s02 after each step of the surface functionalisation and cleaning with UV light.*

The change in current at the reduction peak after Antigen addition (Figure 23, blue line) was not reproducible (Figure 24).

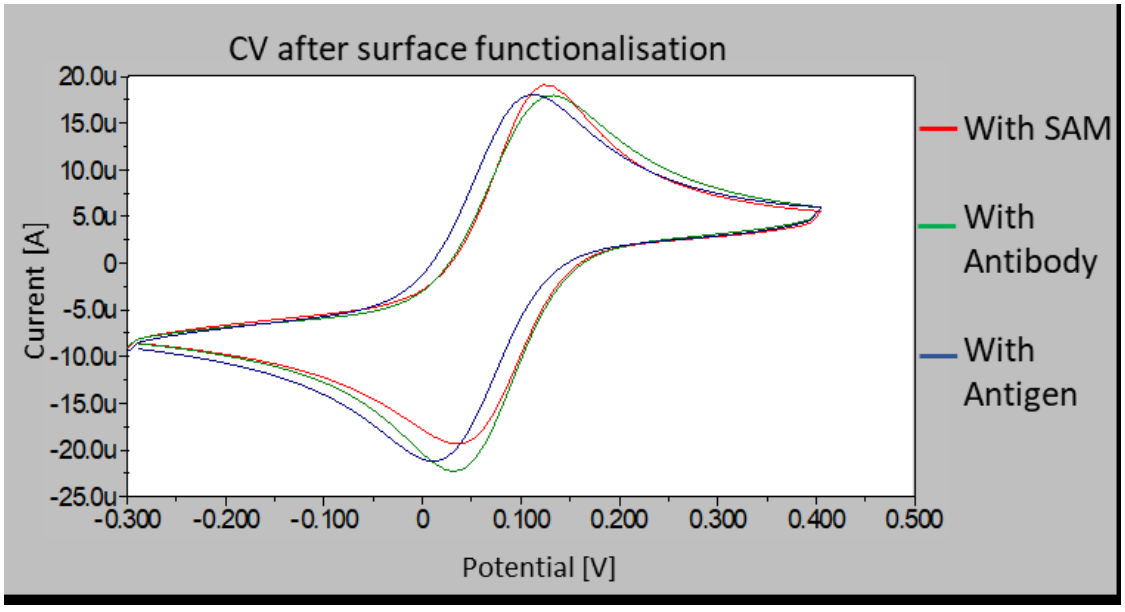


*Figure 24: CV of ATe03s02 after each step of functionalisation and cleaning with UV-light*

The UV cleaning seemed to destroy the reference electrode, similar to the treatment with $H_2SO_4$ (

Figure 22). The BVT electrodes were not robust enough to be used for cleaning (Figure 25, Figure 26).

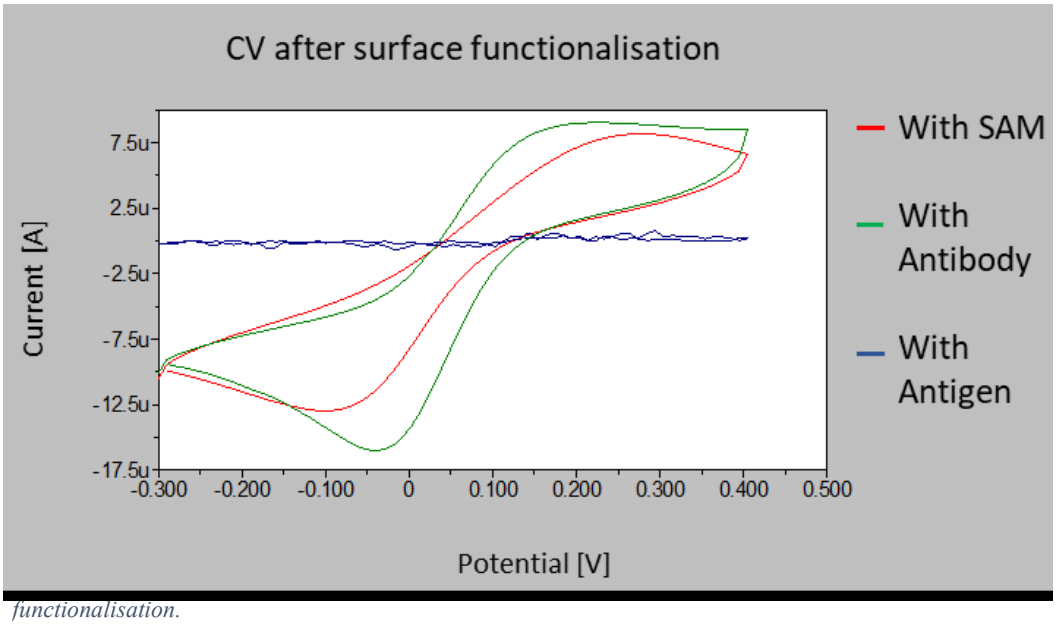


*functionalisation.*

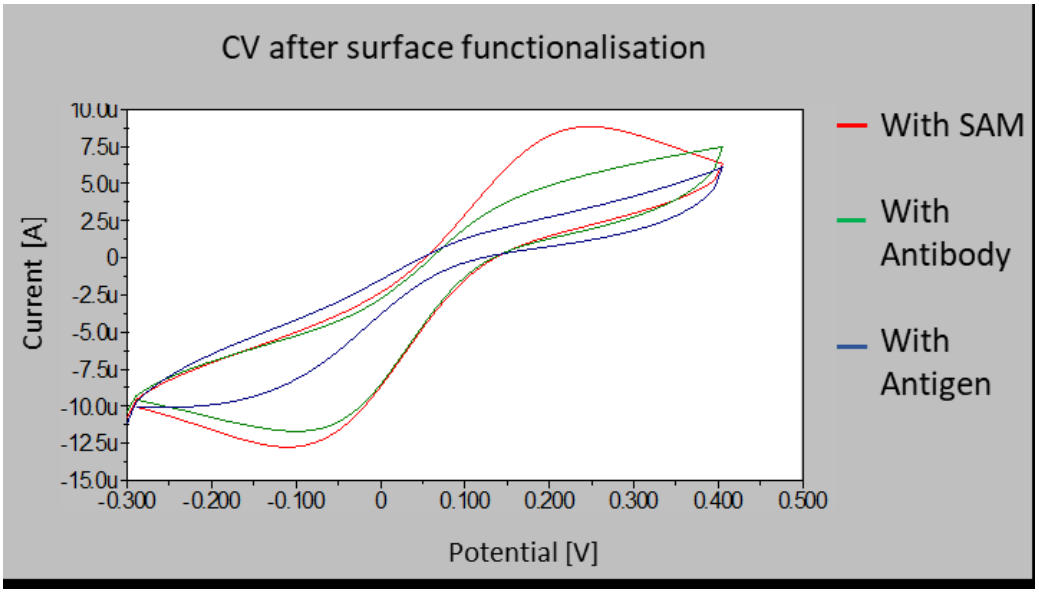


*Figure 26: CV of BTe02s02 after UV cleaning and after each step of the functionalisation.*


*Figure 27 : BT electrodes were destroyed by too harsh cleaning.*

With the electrode-cleaning experiments, we confirmed that DropSense electrodes were more robust than BVT electrodes (Figure 27). From this point on, we decided to work with DropSense electrodes only.

**Impedance results performed in potassium ferricyanide ($K_3Fe(CN)_6$)**

All electrodes (AT and BT) were tested for increased resistance after each step of the surface functionalisation. The data is analysed using cole-cole plot via frequency response analyser from Palmsense. Rs/ohm describes the resistance of the solution while Rp/ohm describes the resistance of the layer. A straight line indicates no resistance on the surface (=clean). Every addition (e.g. SAM, AB, AG) changes the resistance of the layer and is detectable by impedance measurements.

There was no difference between AB (red) and AG (green) lines (Figure 28). However, we observed a difference between the clean gold electrode (black) and the SAM (blue), indicating that the expected monolayer had formed. Nevertheless, there was no increase of resistance after adding AB.

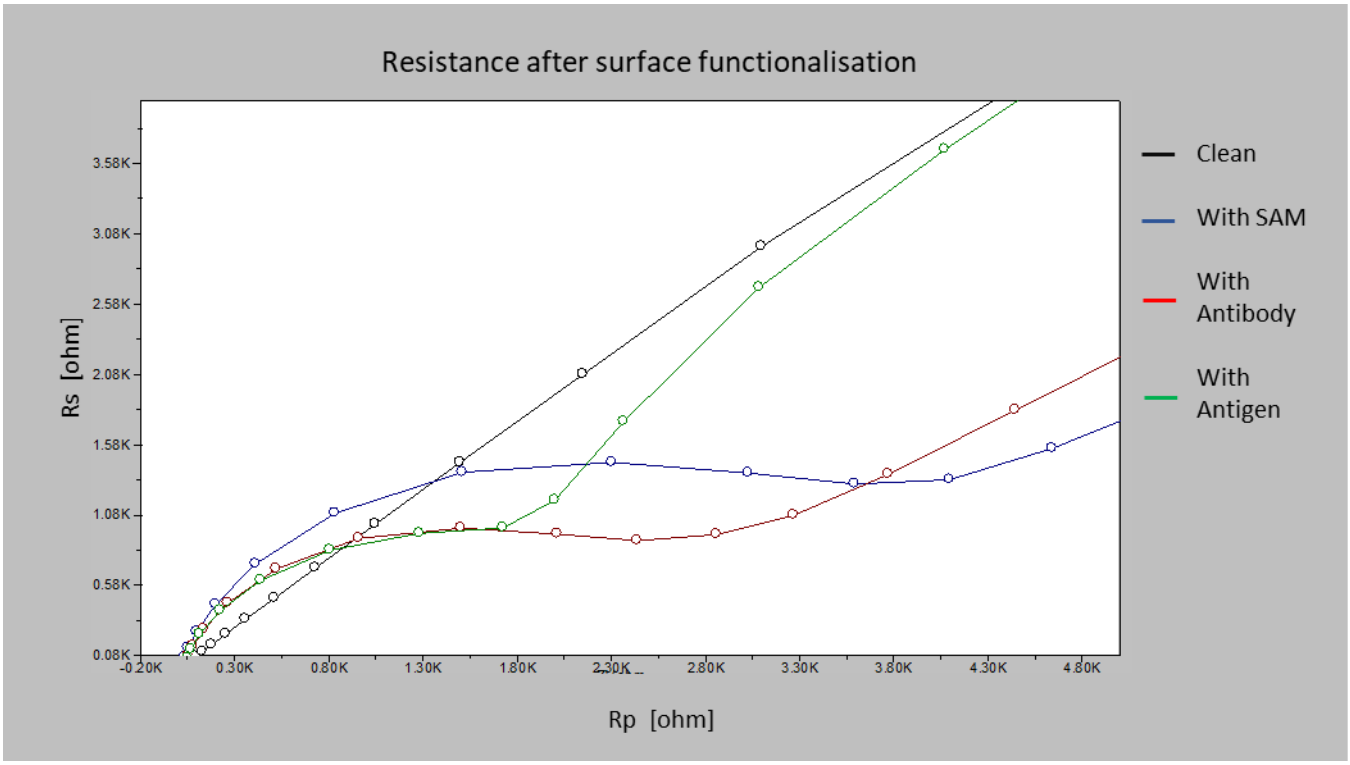


*Figure 28 The impedance results of the electrode ATe01s01 after each step of the functionalisation.*

Although the observed change in resistance indicates a successful formation of the 16 MHA SAM, either no AB binding occurred or the isolating effect of 16 MHA strong enough to block every extra resistance from the AB-AG complex.

Incubation time could also be a factor influencing the resistance. Therefore, we checked resistance for a period of up to 50 min, but no difference was detectable.

**Test of self-assembled monolayers (SAMs)**

- **Long chain mixed SAM:**
  10% 16- Mercaptohexadecanoic acid
  90% 11-Mercapto-1-undecanol

- Six BT electrodes were incubated 3h with long chain mixed SAM
- Three electrodes were checked for impedance and CV after every step to observe changes. Two of these were treated with 100 ng/ml protein, and one served as control without protein addition.
- Three electrodes were not checked. Two of these were treated with 100 ng/ml HSA, and one served as control without HSA protein.
- 1000 ng/ml anti-HSA Rabbit served as the sec. AB, and anti-Rabbit IgG (1:5000) was used for detection.

The amperometric measurement ("steps and sweeps") was done after 2 min of incubation with TMB. In this experiment we observed a blue colour (staining??) at the counter electrode but none at the working electrode, indicating an unspecific reaction.

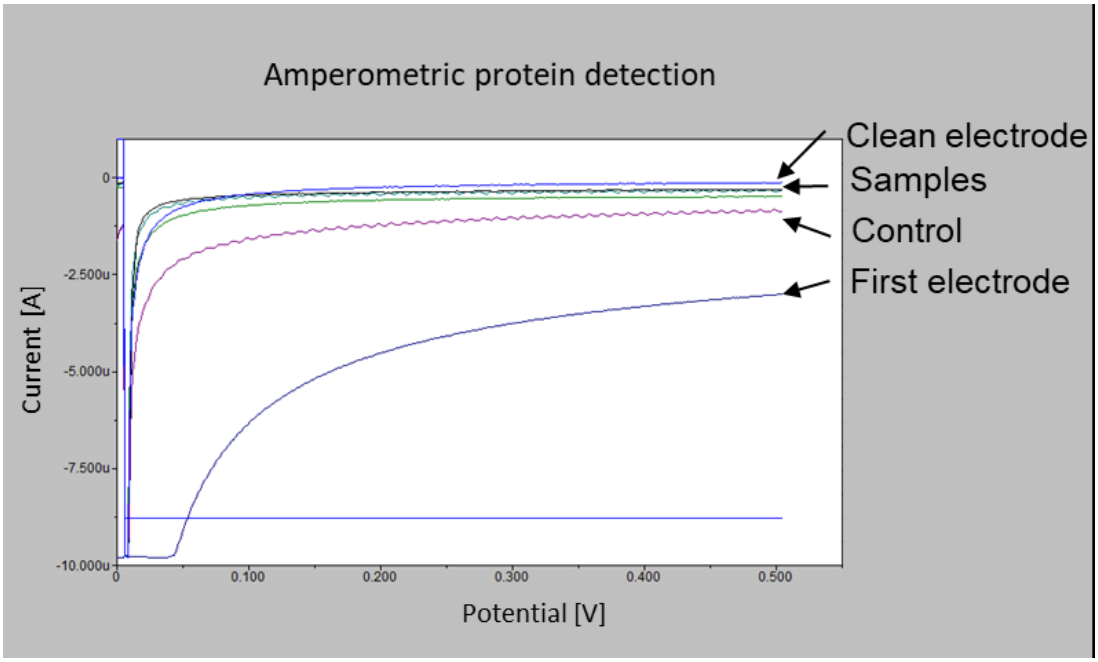


*Figure 29 Amperometric measurements of a clean electrode vs samples and control.*

Measurement of sample 3 was not visualised by the software. The result of sample 3 was similar to the samples 2,4,5. In summary, no difference between the samples and controls could be detected. The first electrode measured showed a low current and was thus not comparable to the other measurements (Figure 29).

- ***Short chain* mixed *SAM 1:***
  10 % 11-Meraptoacid 1 mM
  90 % 6-Mercaptohexanol 1 mM

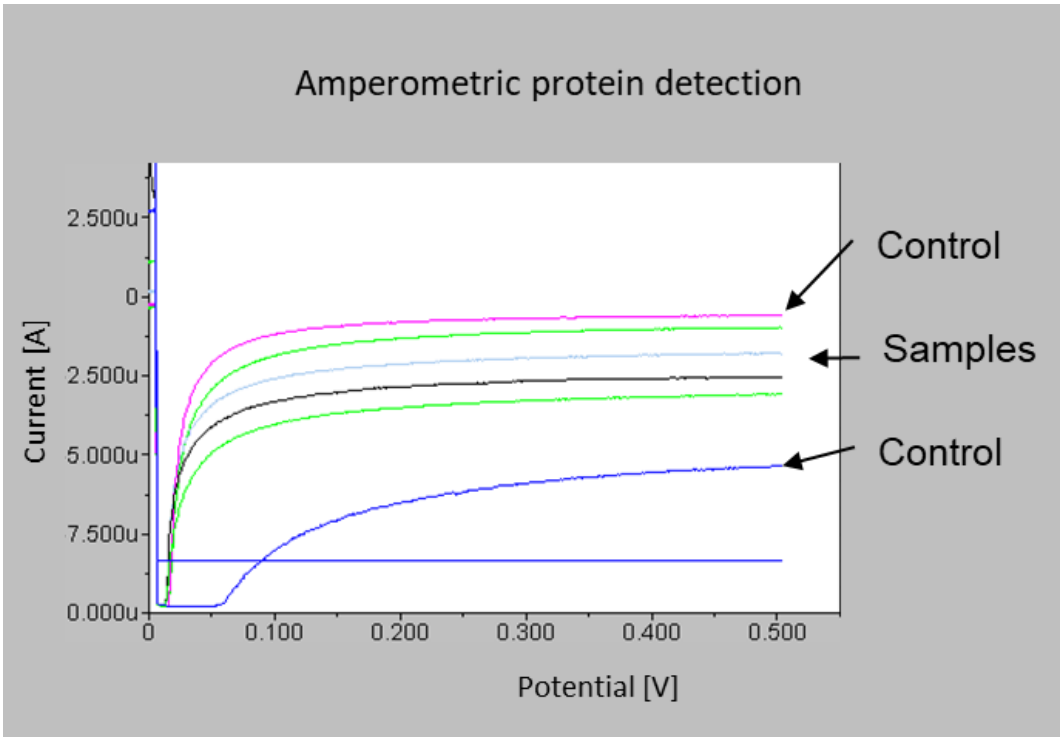


*Figure 30 The voltage over current graph shows no differences between control (blue, magenta) and samples when using short chain mixed SAM.*

### 3.1.5. Results of the gold sputtered electrode measurement

As already described on page 46, gold sputtered electrodes consist of a thin layer of gold, which was fabricated on a glass slide. The self-designed pattern (Figure 32, Figure 31) determines the electrode layout. The advantage compared to SPE is not just the flexible layout design but also a higher purity of the gold layer. The measurements were performed with four concentrations (channel 1-12 in triplicates, 10.000 ng/1000 ng/100 ng/10 ng) of HSA as well as 2 negative controls (channel 13-15 anti-Mouse-IgG-HRP + 10.000 ng/ml protein, channel 16-18 no protein).

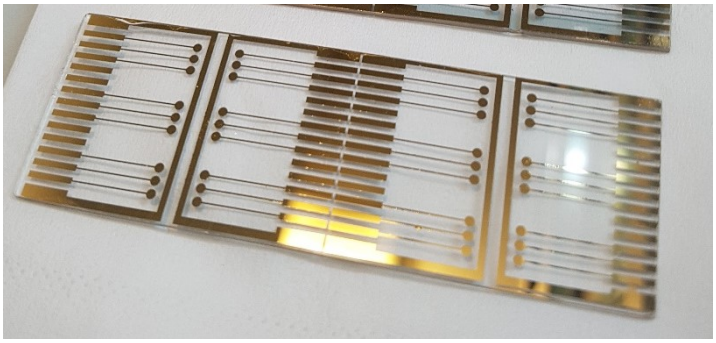

*Figure 31 Gold sputtered electrode at the URV facility in a cleanroom.*

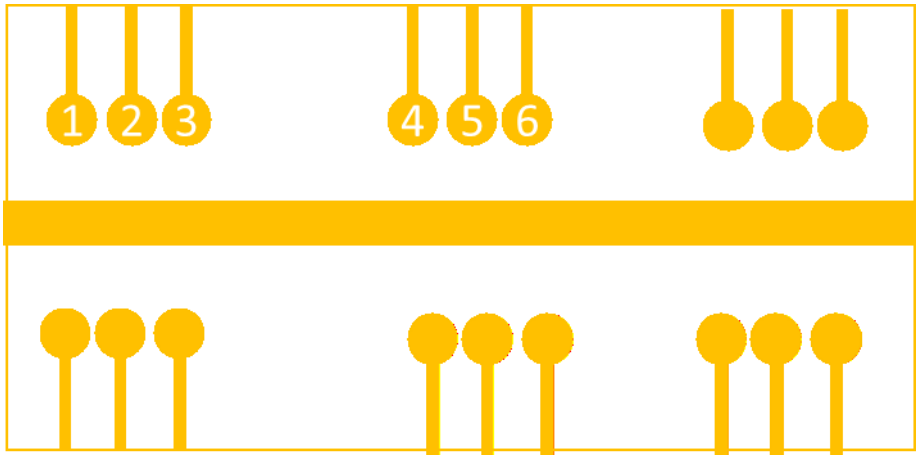


*Figure 32 Overview of the layout of the gold-sputtered electrode with 3 electrodes next to each other, forming triplicates.*

The electrode was incubated with TMB, as a detection reagent for 40 sec, 2 min and 4 min to see if time would influence the result. TMB acts as a substrate for HRP generating electrons that are measurable by applying a voltage.

Unfortunately, not all channels worked properly (Figure 33). Therefore, there was no possibility to repeat all measurements in duplicates or triplicates. The results are shown as the mean of the last 50 values from the Nova 2.1 software. The measurements indicating a time dependency as there was a slight change in current between 40 sec and 2 min. High non specific binding of 2$^{nd}$ AB as well as high background current with no protein indicating insufficient blocking. Therefore, blocking as well as incubation time of Fab was increased from 3 h to ON in the followup experiment (Figure 34)

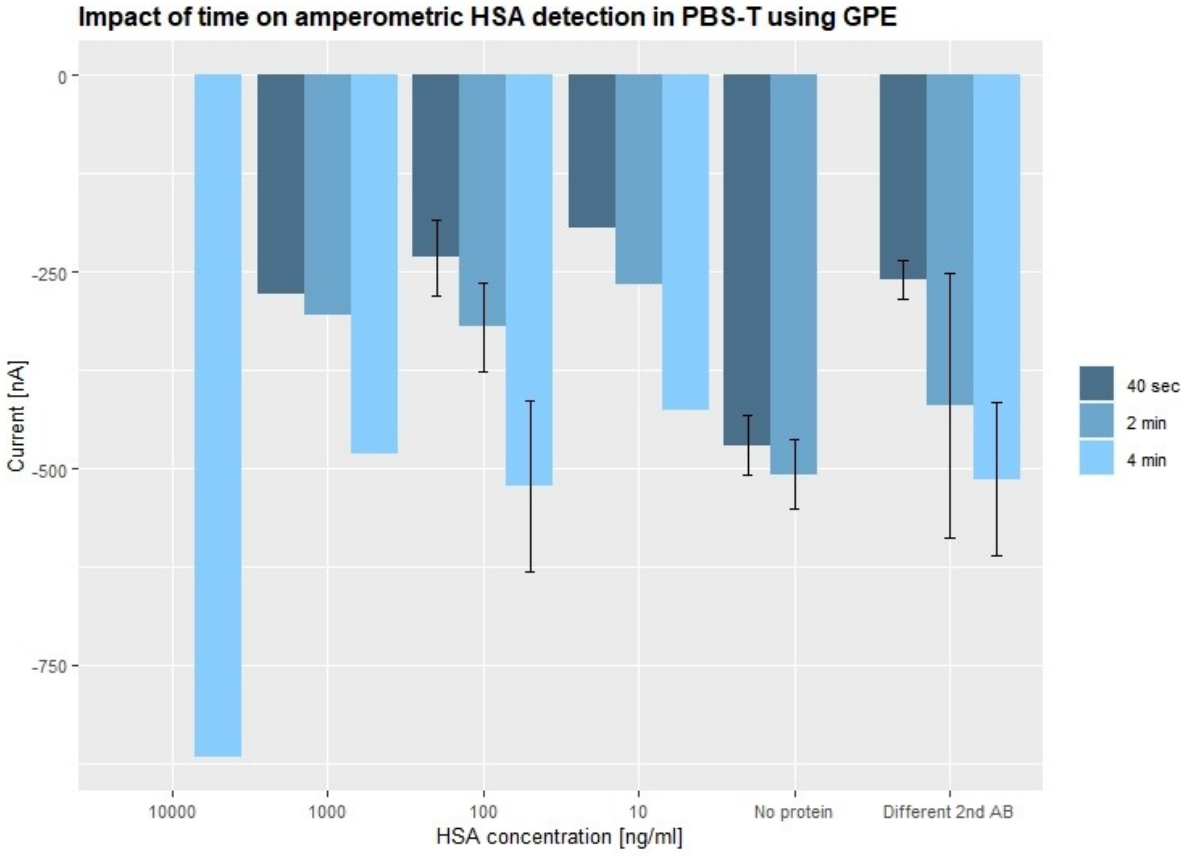


*Figure 33 The current measured with 6 different concentrations and the gold sputtered electrode using Fab.*

The measurement was repeated using a range between 300 ng/ml and 3 ng/ml in order to detect the impact of time on gold electrodes. There was again a difference in the lower concentrations when comparing 40 sec and 2 min incubation (Figure 34)

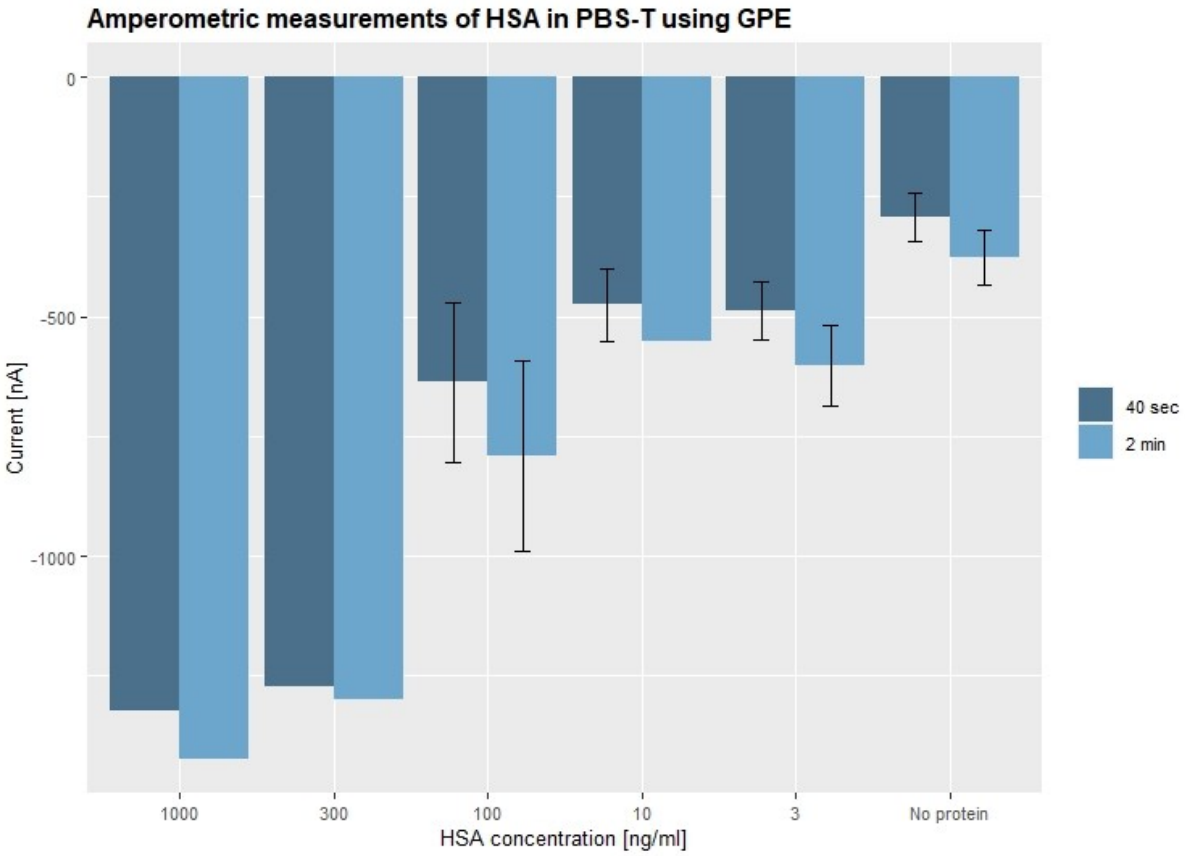


*Figure 34 Amperometric measurements of HSA in PBS-T and two timepoints. Each bar represents the mean of three measurements. Missing error bars indicating non-functional channels which lead to missing triplicate values.*

### 3.1.6. Measurement results of the printed circuit board (PCB) experiment

As the disadvantage of the gold sputtered electrodes is their high price, we used an already existing PCB electrode setup to reduce costs and compare the results.

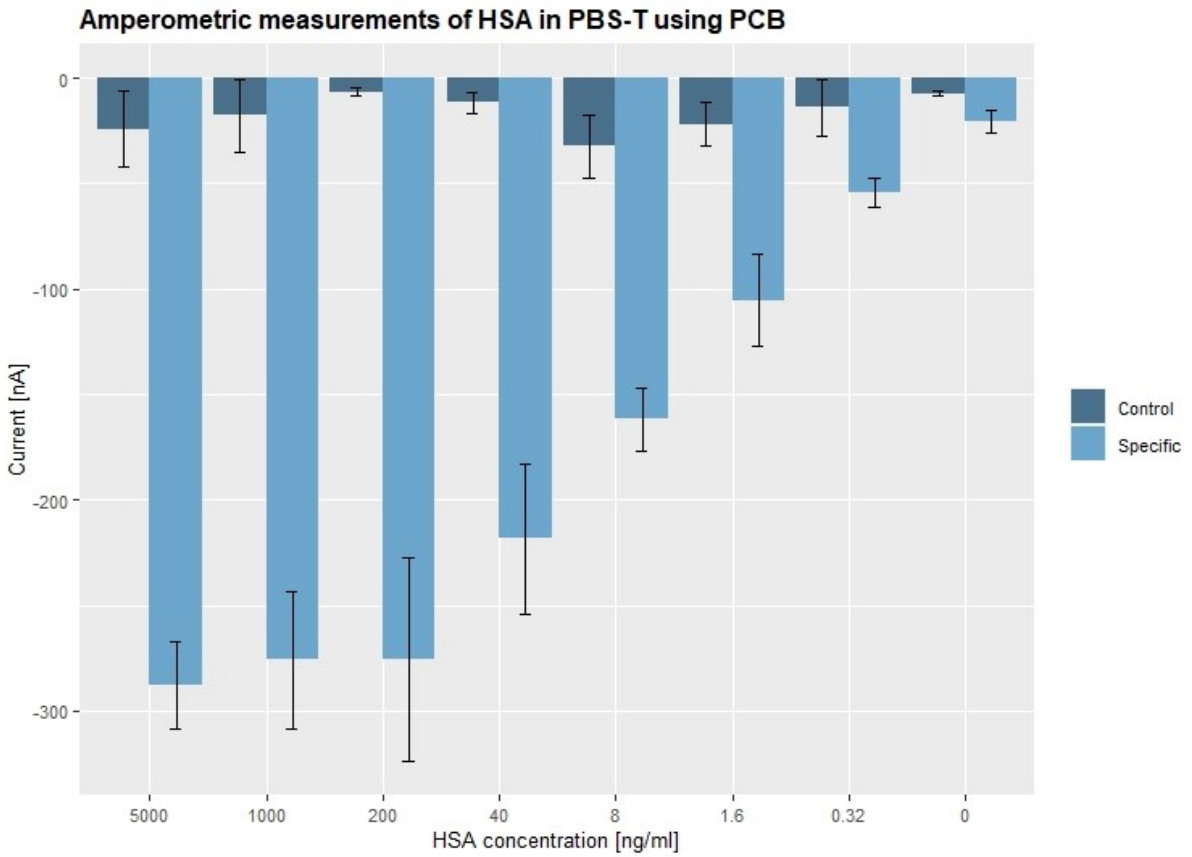


*Figure 35: Electrochemical detection of HSA in PBS-tween. Each bar corresponds to an average of eight electrodes.*

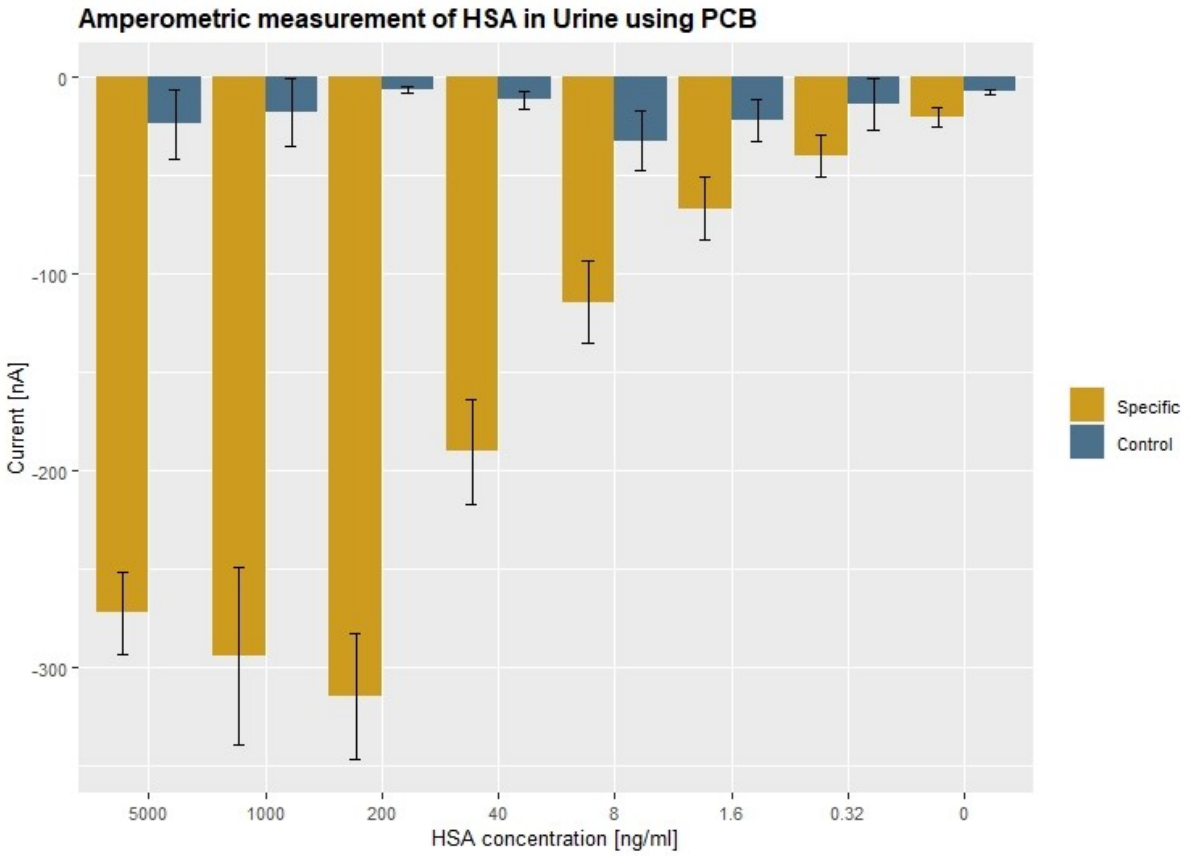


*Figure 36 Electrochemical detection of HSA in synthetic urine. Each bar corresponds to an average of eight electrodes.*

HSA was successfully detected in urine, exhibiting similar current levels than those obtained for HSA in PBS-tween (Figure 37). HSA binding data exhibited a typical sigmoidal response, as can be observed in the following figure (Figure 38). The limits of detection (LODs) obtained for HSA were of 2.4 and 12.5 ng/ml in the presence of PBS-tween and urine, respectively.

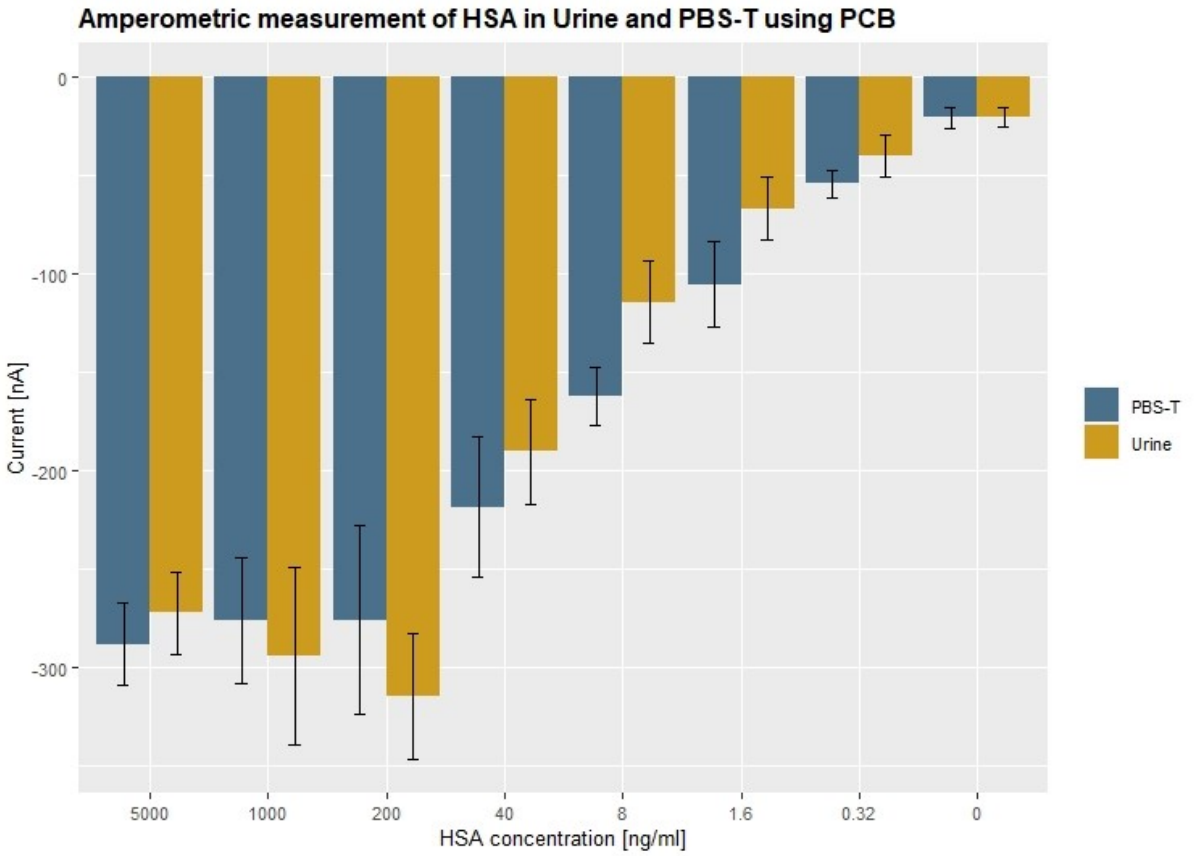


*Figure 37 Comparison of the electrochemical detection of HSA in both, PBS-tween and synthetic urine. Each bar corresponds to an average of eight electrodes.*

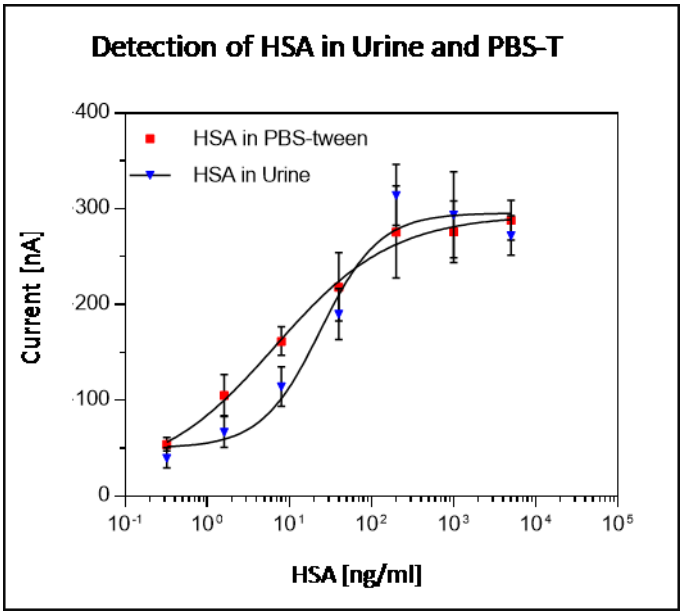


*Figure 38: Comparison of the electrochemical detection of HSA in both, PBS-tween and synthetic urine visualised as sigmoid curve. Each bar corresponds to an average of eight electrodes.*

## 3.2. Chapter II: Results of BioPersMed based biomarker research

### 3.2.1. Cohort overview

The main result of this cohort is up to now the data of a deep phenotype cohort profile. This showed that more than 25 % of the study cohort fulfilled the criteria of exhibiting a very high or high cardiovascular risk (96). A high number, nearly 30 % of the study population, could be identified as pre-diabetics.

The purpose of this results chapter is to give an overview of the baseline characteristics and findings.

The central Figure 39 shows an R-correlation plot of most measured biomarker at baseline. In this plot, biomarkers are not grouped (for example in organ systems); instead, clusters of high correlations were formed (blue indicates a positive correlation, red indicates a negative correlation, and white indicates no correlation) (161). Thereby, connections between different biomarkers of different organ systems can be revealed which may further serve as a basis for a multi-disciplinary in-depth analysis.

Such analyses already identified the so far unknown correlation between IGF1 receptor auto-antibodies with body composition and height (presented at the European Congress of Endocrinology in Barcelona, Spain 2018). Moreover, preliminary results and outcomes have been reported at 8 international and 5 national congresses in the fields of cardiology, endocrinology, diabetology, genetics, and osteology. The first presentations took place in 2015 – briefly before the patients' recruitment has been finished. Furthermore, data from the genome-wide association study of the BioPersMed cohort were already used as control data for a large keratoconus genomic study of researchers from the United Kingdom and the Netherlands and is currently under consideration for publication.

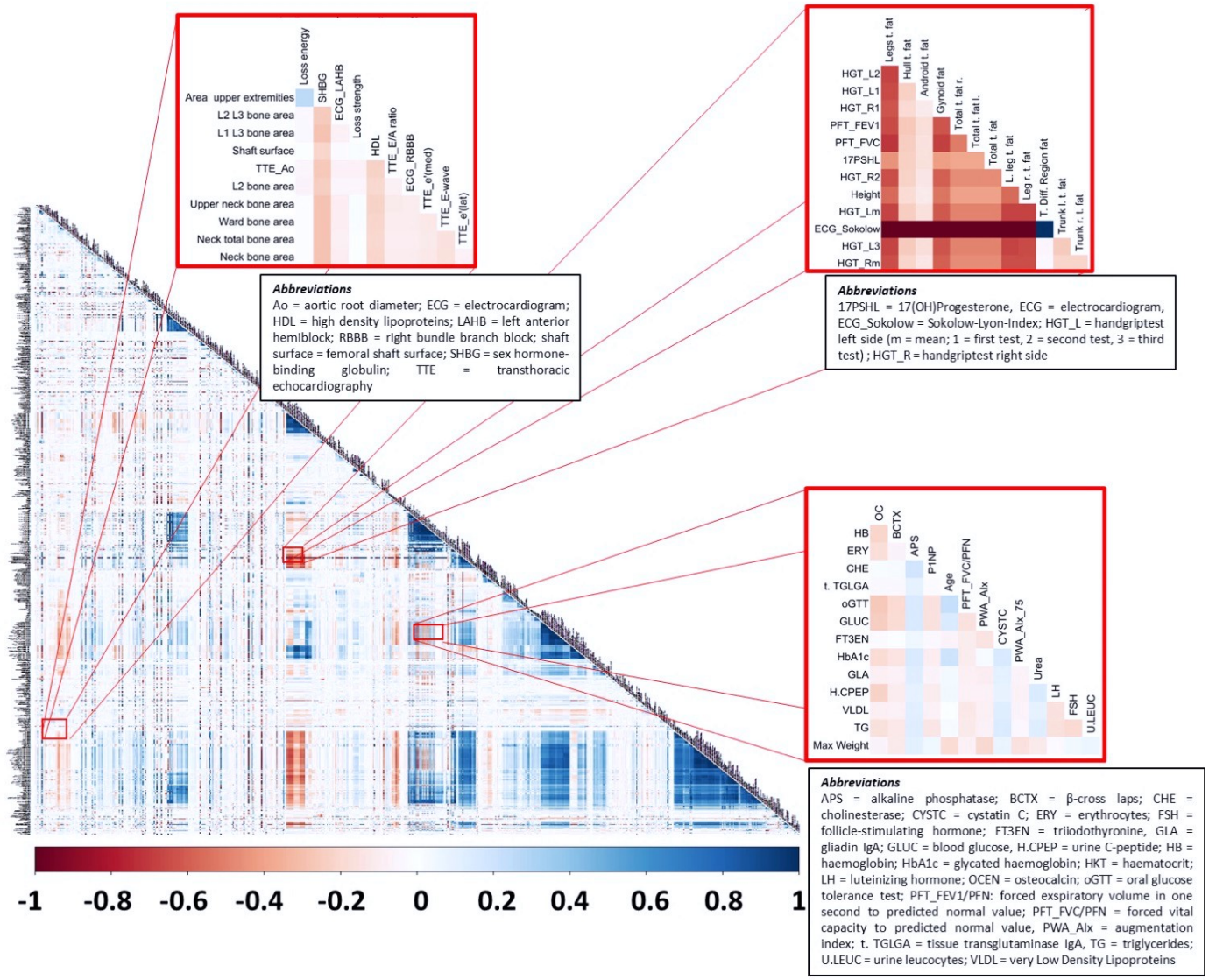


*Figure 39 Correlation plot of the main parameters of the biopermed cohort. Grouping was performed not according to systemic appearance (eg. bone markers grouped together) but a cluster according to correlation was forced. The highlighted clusters are correlations between parameters of different medical fields.*

## 3.2.2. Abstracts of interdisciplinary research done in BioPersMed

The scientific output of BioPersMed-related research has already been presented at several international congresses and will be published straight after the baseline paper. The following research topics were presented by the author to the scientific community.

#### 3.2.2.1. Diabetoporosity - Risk prediction in prediabetic patients

**Objective**

Both T1DM and T2DM not only bear micro- and macrovascular disease risk, but have a substantial effect on bone metabolism and strength. In this part of the study, we investigated the interaction between bone metabolism and densitometry parameters in the context of T2DM, healthy controls and especially prediabetic patients in a large cohort study, the BioPersMed study.

**Methods**

To identify putative alterations in bone metabolism between healthy (n=368), pre-diabetic (n=246) and diabetic patients (n=138), biochemical and clinical parameters of 752 female (n=424) and male (n=328) volunteers from the BioPersMed cohort were analysed. Bone metabolism markers (e.g. Osteocalcin, procollagen type 1 N-terminal propeptide (P1NP), C-telopeptide (CTX)) and calciotropic hormones such as 25(OH)vitamin D and parathyroid hormone (PTH) were associated with DXA-derived data (dual energy X-ray absorptiometry) for bone density, trabecular bone score (TBS) and body composition.

**Results and conclusion**

We can confirm the previous findings of "diabetoporosity" in diabetic patients. Although being older ($p<0.001$, No-DM: 56±8, pre-DM: 60±8, DM: 60±9 [y]) having increased total bone mass ($p<0.001$, No-DM: 2578±528, pre-DM: 2657±581, DM: 2839±514 [g]) than controls, but decreased TBS ($p<0.001$, No-DM: 1.35±0.12, pre-DM: 1.30±0.12, DM: 1.29±0.14 [a.u.]) and impaired bone metabolism e.g. osteocalcin (OC, $p<0.001$, No-DM: 23±7.5, pre-DM: 21±8.5, DM: 17±6.2 [ng/ml]). Of note, decreased OC ($p=0.004$) as well as TBS ($p=0.034$) already occurred in prediabetes patients to a lesser extent.

New imaging technologies, namely trabecular bone score (TBS), and bone turnover markers such as osteocalcin allow for a better phenotyping of patients for bone characteristics in T2DM and already in prediabetes.

DM patients, although having high DXA bone mass and T scores, suffer from an up to 10-fold increased bone fracture risk. Using the TBS score in DXA measurements as well as osteocalcin as biomarkers could help to give a better risk prediction together with other clinical risk factors in an individual risk setting to be used in personalized medicine.

### 3.2.2.2. Hereditary hypolactasia and bone properties

**Objective**

The aim of this study was to demonstrate the impact of variations in hypolactasia genetics on bone characteristics in men using DXA in 420 elderly men from the BioPersMed cohort. We found a strong connection between the -13910 T/C dimorphism (LCT) genotype and bone characteristics.

**Methods**

Biochemical and clinical parameters of 420 male volunteers (25 % CC, 48 % TC, 27 % TT) of the BioPersMed cohort (Biomarkers in Personalized Medicine, Medical University Graz) were analysed to identify putative differences between lactose intolerant (CC) and tolerant (TT, TC) men. Laboratory data in combination with DXA-derived measurements of bone density, dimensions and body composition were calculated in relation to the genetic status. Mann-Whitney-U-Test was used to check for statistical significance.

**Results**

Lactose intolerant (CC) men showed an overall decreased bone stability, with the main indicators being Z-Score ($p< 0.001$), T-Score ($p=0.003$), bone mineral density ($p=0.004$), bone mineral content ($p=0.045$) and bone mass ($p=0.040$), compared to tolerant (TT) men. Heterozygote (TC) men show a gene dose effect with decreased bone parameters, but to a lesser extent than CC genotypes. Interestingly, we found only a small change in the urinary calcium/creatinine excretion with borderline significance
($p=0.05$). No differences in age, vitamin D levels or medication between the groups were observed.

**Summary and conclusions**

In this study, we underlined the importance of genetic variations in the context of bone properties. In the setting of genetically determined hypolactasia, we were already able to show these variations in women and now in a bigger cohort also in men. Genome wide association studies (GWAS) in combination with food questionnaires will be linked with these volunteer's

data in the near future to investigate the impact other single nucleotide polymorphism (SNP) or nutritional changes for bone phenotypes.

## 3.3. Chapter III: Results of the detection of PCOS biomarkers

### 3.3.1. Patient characteristics

Both control and PCOS groups have been broadly characterized including laboratory and clinical parameters (Table 3). Controls were significantly older than women with PCOS ($p=0.003$) with a median of 5 years (32y vs 27y), all of them premenopausal. Waist to hip ratio (WHR) and BMI were not significantly different between the groups. In the assessment of lipid metabolism and glucose, women with PCOS showed a less favorable phenotype, with higher HOMA2 IR ($p=0.027$), fasting insulin ($p=0.022$) and area under the curve (AUC) insulin during the oGTT ($p=0.009$). Glucose tolerance was not impaired in the PCOS group. Women with PCOS had lower HDL cholesterol concentrations ($p=0.006$) and higher triglyceride ($p=0.010$) than healthy women.

As hypothesized, PCOS women showed abnormalities in serum concentration of steroid hormones and other reproductive markers. AMH ($p=0.0002$), LH ($p=0.042$), total testosterone ($p=0.002$), and DHEA ($p=0.015$) and androstenedione ($p=0.0003$) were significantly higher in women with PCOS than in the control group. Free DHT and median free testosterone were two- to three-fold higher in women with PCOS compared to control women ($p<0.0001$ for both). Women with PCOS reported oligo-/amenorrhoea, hirsutism, and polycystic ovarian morphology in 71 %, 46 % and 96 % of cases, respectively.
Women with PCOS reported a lower grain consumption than control group women ($p=0.025$). No statistically significant difference in any other assessed food group, including soy products were found.

### 3.3.2. Isoflavone metabolism and characteristics

We measured urine levels of genistein, daidzein, and equol before and after an intervention with isoflavone. Urine concentrations of all three compounds were low at baseline, reflecting an overall low intake of isoflavones, e.g. via soy products, in the study and in similar populations (Figure 40A) (162). Daidzein levels were significantly lower in PCOS women than in control women at baseline ($p=0.036$).

After three continuous days of moderate amount of soy protein (13.2 g/day) consumption, urine concentrations of all three compounds significantly increased in the whole cohort ($p<0.0001$ for genistein and daidzein and $p=0.003$ for equol). Differentiation between non-equol producers and producers was performed according to the work of Setchell et al., using log10(E:D) ratio of -1.5 as threshold (Figure 40B) (101). In this cohort, the equol producers prevalence was 30 % (13/43) (Figure 40C). Twenty-one % (5/24) of women with PCOS were classified as equol producers, compared to 42 % (8/19) of control women (Figure 40C). This difference was statistically not significant ($p=0.120$).

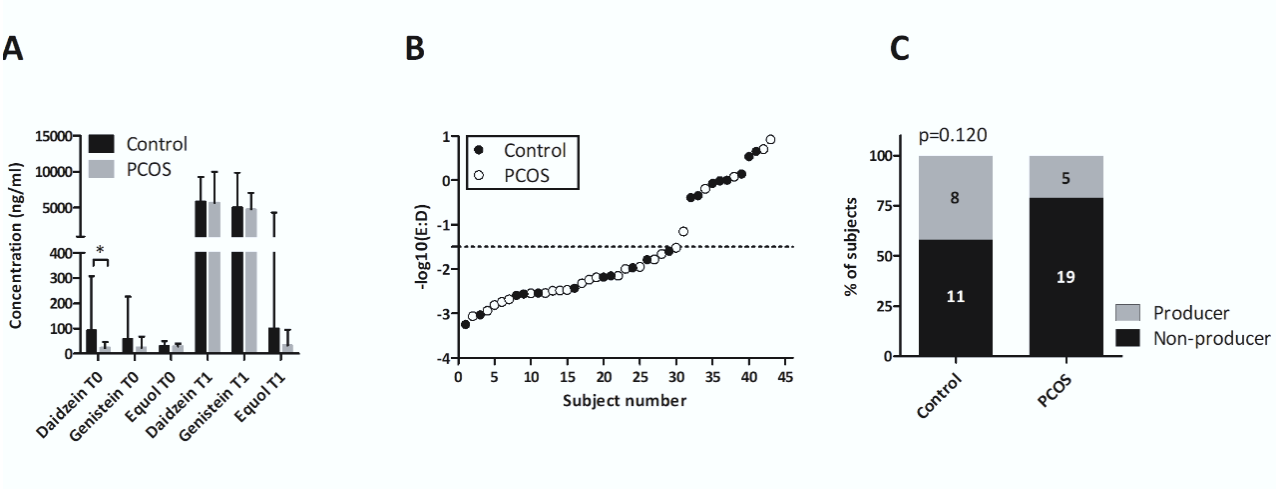


*Figure 40 The bacterial isoflavone metabolism in women with PCOS and control women. A: Genistein daidzein, and equol concentration in urine before (T0) and after (T1) a three-day isoflavone intervention performed via oral soy consumption. Data are visualized as median and IQR. B: Characterization of equol producers and non-producers using log10(equol:daidzein). Equol producers were defined as having a quotient >-1.5. C: Comparison of equol producer prevalence in control and PCOS groups with the number of subjects in each category is indicated both segments. Figure adapted from Haudum et al. 2020* (163).

## 3.3.3. Metabolic changes after isoflavone intervention

We found decreased fasting insulin ($p<0.01$), glucose ($p=0.01$), as well as the associated HOMA2-IR ($p<0.02$) levels in PCOS patients after isoflavone intervention. This effect was not observed in control women ($p=0.70$, $p=0.48$, $p=0.72$).

Additionally, equol producers showed a variation of urine equol concentrations 5-fold higher than non-producers which translates to a sample size independent effect size of 0.98. This was associated with lower serum free and total testosterone, AMH, androstenedione and WHR levels (Figure 41A). Participants age was significantly associated with the increase in equol after soy consumption. This makes age a possible confounding factor. When examining control

and PCOS groups separately, only the association of AMH and change in equol concentration remained significant (Figure 41B, C). In women with PCOS, increased T0 genistein levels were associated with a decreased LH:FSH ratio (Figure 41C).

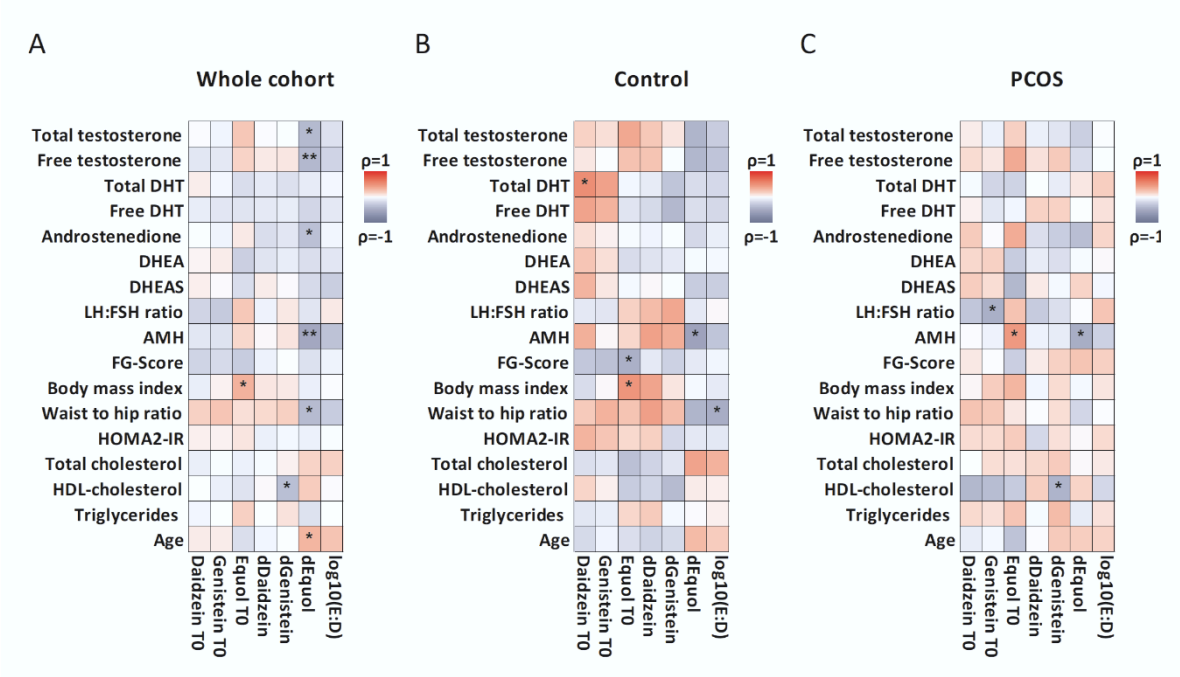


*Figure 41 The correlations of parameters related to reproductive function, isoflavone metabolism, and lipid and glucose metabolism. A. Control and women with PCOS. B. Control group only. C. PCOS group only. AMH, anti-Müllerian hormone; d, change from baseline to T1 after isoflavone intervention; DHEA, dehydroepiandrosterone; DHEAS, DHEA sulfate; DHT, dihydrotestosterone; FG-Score, Ferriman-Gallwey Score; HDL, high-density lipoprotein; HOMA2-IR, homeostasis model assessment for insulin resistance; LH:FSH, ratio of luteinizing to follicle-stimulating hormone; T0, baseline value. Spearman's ρ determines the color of cells and significant correlations are marked as follows: *p<0.05; **p<0.01; ***p<0.001. Figure adapted from Haudum et al. 2020* (163).

Standardized z-scores of the distilled values of fertility and androgen markers were used to further investigate the effect of an equol rise on these respective markers (164,165).

These z-scores of free and total testosterone as well as androstenedione and DHT were summarized to the "androgens" category. AMH and LH:FSH ratio were grouped to the category "fertility". Both categories correlated negatively with the rise in equol (-0.364, p=0.021, -0.396, p=0.021 accordingly) in the whole cohort. This effect is still present after Bonferroni correction (p*<0.025). The control or PCOS women showed no further significant differences.

## 3.3.4. Predicted metagenome

The baseline (T0) assessment showed a decreased microbial alpha diversity (PD whole tree p=0.023, Shannon, p=0.035) in PCOS women compared to controls (Figure 42).

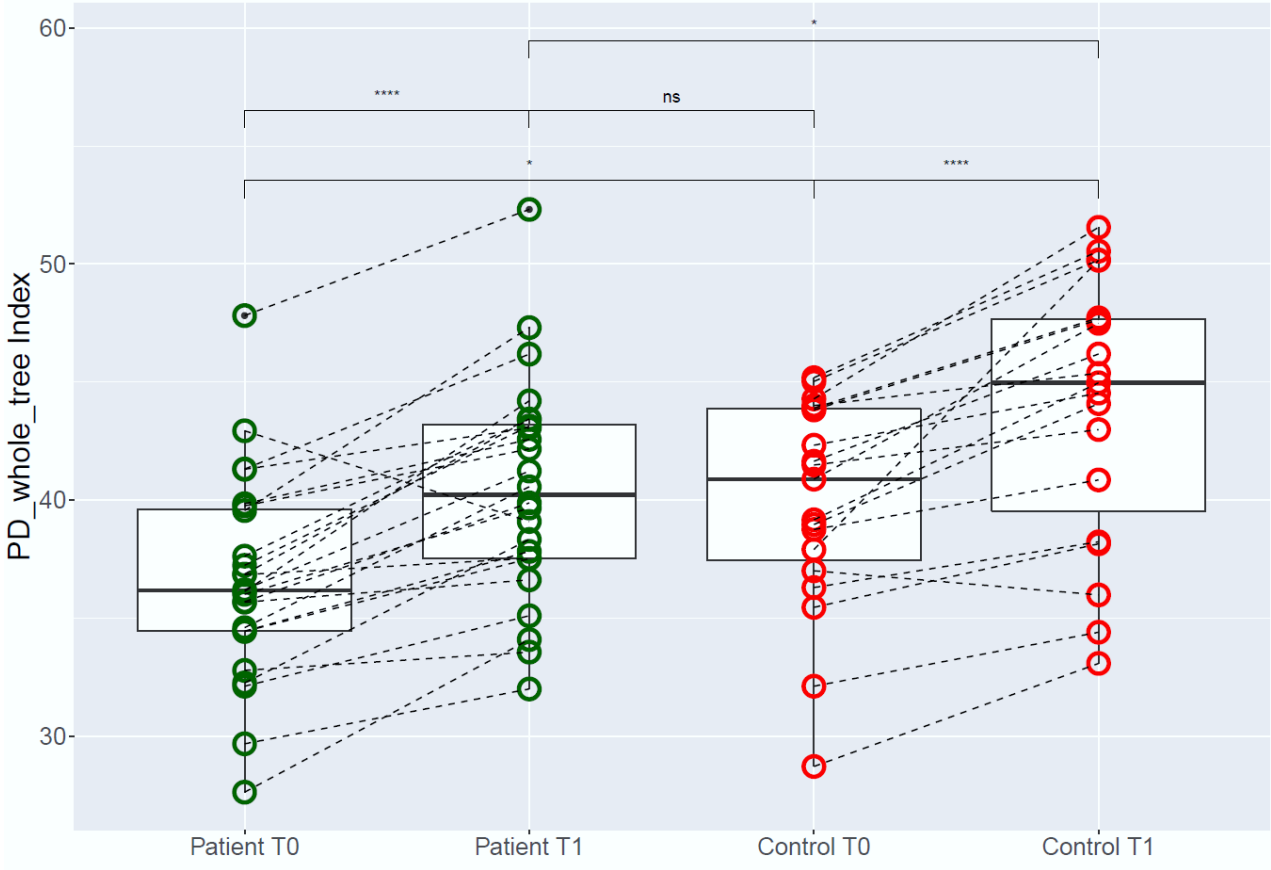


*Figure 42 Change of alpha diversity of patients and controls before (T0) and after (T1) oral isoflavone intervention. Differences in patients (**p=0.005) and controls (*p=0.02) between T0 and T1 were statistically significant using student's (paired) t-tests. There was a difference of diversity between both in T0 (*p=0.023) and T1 (*p=0.035) between controls and PCOS patients. However, there was no change between controls at baseline and patients after the intervention (ns, p=0.669). Figure adapted from Haudum et al. 2020* (163).

After the isoflavone intervention (T1) via soy consumption, the microbial diversity of the gut increased significantly in both groups. Although diversity after intervention was higher in healthy women compared to women with PCOS (PD whole tree p=0.035, Shannon p=0.036), microbial diversity in the PCOS group could be increased to controls' baseline levels (Shannon p= 0.0528, PD whole tree p=0.669).

The beta diversity determined by Bray-Curtis dissimilarity depicted no clustering before or after the 3-days isoflavone intervention (Figure 1Figure 43).

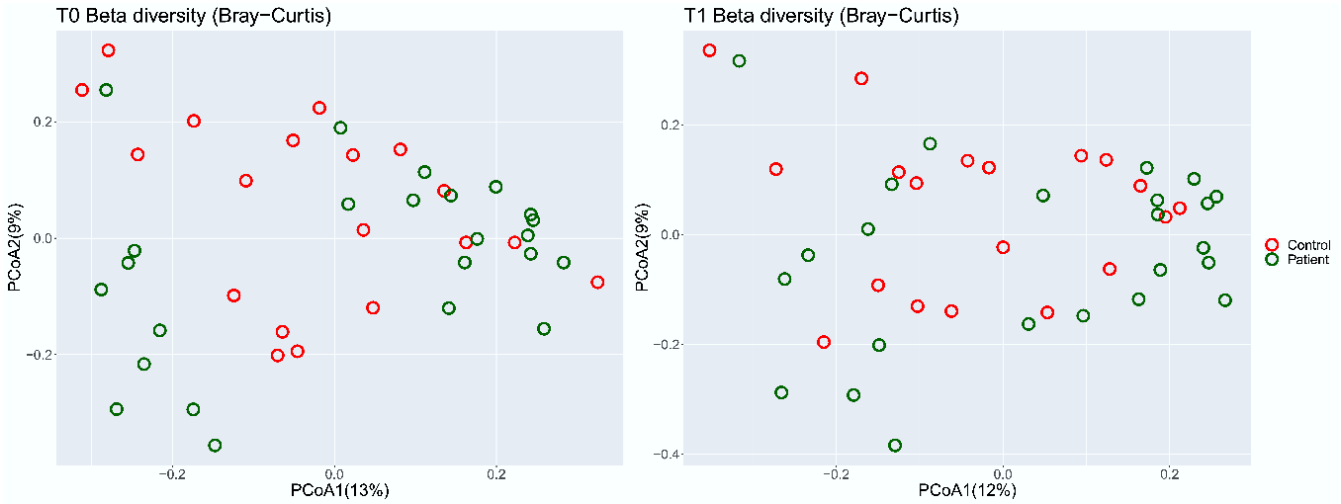


*Figure 43 The beta diversity (Bray-Curtis) showed no clustering before (T0) and after (T1) isoflavone intervention. Figure adapted from Haudum et al. 2020 (163).*

The LEfSe result for both, T0 (Figure 44 and T1 (Figure 45), present the top five bacterial strains contributing to each phenotype. The main contributor for PCOS changed from Oscillospira strain (186841) before soy intervention to *Parabacteroides distasonis* (1025011) after. We used the Calypso Biomarker Discovery pipeline to validate the family S24-7 as a biomarker for the control group in both baseline (T0) and after intervention (T1) with an area under the ROC curve (AUC) of 0.79 and a corrected and adapted p value of 0.001.

The strains *Megasphaera massiliensis* (357302 as well as 358887, Figure 44) were also main contributors for the PCOS phenotype. Of note, analysis-using blast determined 357302 as *Megasphaera massiliensis NP3.* The strain number 358887 showed high similarities (blastn, 99.7 %) with a close relative of *NP3*, archived as *DISK18*.

Metagenomic techniques were used to predict differences in the functional expression of the gut microbiome in the PCOS and control groups. The PiCRUST data were built from a rarefied OTU table. These QIIME results had a high mean sampling depth of 70165 starting from 30988 to 91475 and for reliable comparison were rarefied to 30980.

Using the metagenomics techniques on these rarefied result, we not only found pathway changes representing typical hallmarks of PCOS, including carbohydrate absorption and digestion (p= 0.02, -45.8 %) and mineral absorption (p= 0.04, -35.4 %). Additionally, associations to new pathways involved in the functionalization of plant metabolites like flavonoid biosynthesis (p=0.02, -45.4 %), as well as carotenoid biosynthesis (p=0.02-56.3 %)

were found. This indicates a metagenome change with disrupted capacity to metabolize an important class of secondary plant metabolites (146).

The isoflavone intervention shifted each of the mentioned KEGG pathways in the predicted metagenome of PCOS women towards the control group features at baseline. This is visualized by less carbohydrate absorption and digestion (p=0.02, -43.0%), and flavonoid biosynthesis (p=0.03, -43.7 %). On the other hand, there was no statistically significant difference of mineral absorption (p= 0.195, -24.4 %) as well as carotenoid biosynthesis (p=0.266, -21.5 %) between the patient and control groups after the intervention.

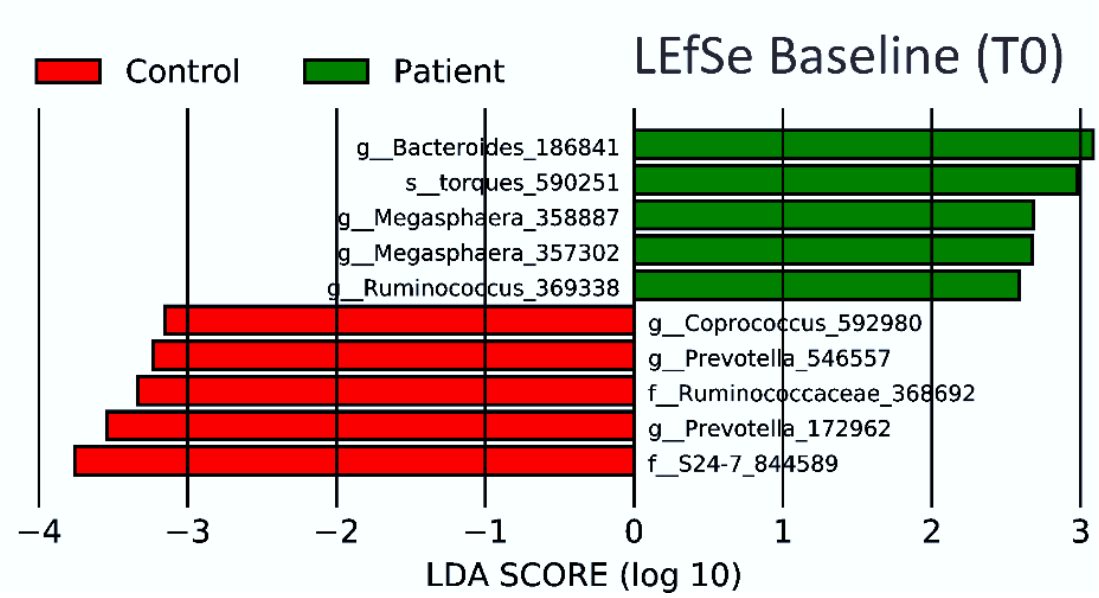


*Figure 44 LEfSe results before isoflavone intervention in the patient (green) and the control (red) groups. This analysis visualizes the contribution of strains to the PCOS phenotype. Letters, f(amily), g(enus), or s(train), at the beginning of the name represents the most accurate known scientific classification of this strain. Figure adapted from Haudum et al. 2020* (163).

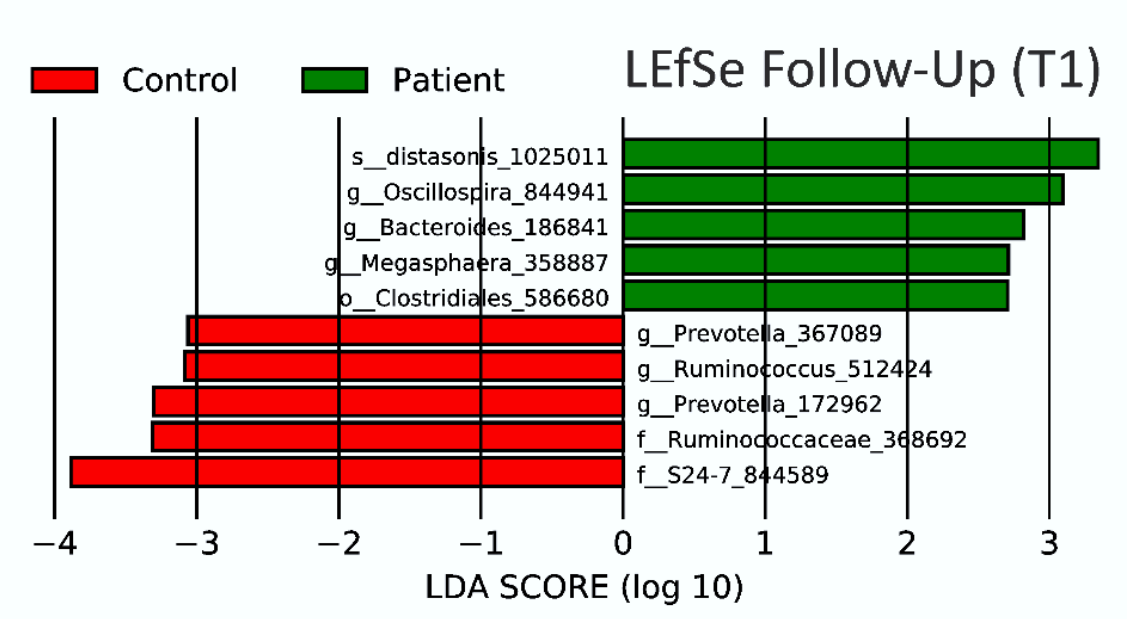


*Figure 45 LEfSe results after 3 days isoflavone intervention. Only a marginal change in LDA of OTU in the control group T0 compared to T1 was detected. This is in contrast to PCOS patients, where every OTU has been found to be different except for the Oscillospira strain (186841). Figure adapted from Haudum et al. 2020* (163)

# 4. Discussion

## 4.1. Chapter I: Discussion on biomarker detection using electrochemical sensors

This chapter of the dissertation project summarises that the system used for electrochemical biomarker detection on protein basis reached sufficient reproducibility in PCBs, not only in buffer solution but also in urine. The possibility to work with 64 electrodes at once allows for future multiplexing and reduced costs compared to gold sputtered electrodes, which is favourable for mass production.

The detection limit, although being already low, should be decreased in the future for a wider range of detection. This will be done by further optimising the protocol to ensure the capacity to detect small changes in clinical patients.

The results presented in this chapter are a milestone for the electrochemical detection of proteins for this project. They were presented to the company partner and were rewarded with additional funding in a separate project for further four years. This time will be used to adapt the protocol for C-peptide and creatinine and to integrate the sensor technology of the company partner.

As the electrode of choice for this project, being PCB, SPE or gold sputtered electrodes, was not determined, a testing of all three systems will be needed. We anticipate a cheap mass-manufactured PCB design with a batch-to-batch reproducibility better than SPE.
Alternative methods for detection, e.g. using aptamers, were already discussed in the project and will be tested further on (166). This aptamer approach could also be used to detect biomarker candidates from chapter II and III and might be used for an integrative device. The advantages of aptamers in comparison to antibodies in the fields of reproducibility, cost and shelf life are very promising (167,168).

### 4.1.1. Future perspective

As already discussed, this electrochemical research is planned to be used for the manufacturing of a low-cost POC system for biomarker detection in common metabolic disorders. Although there is a long road ahead, the most important milestones have been achieved. A test of a functional sensor pre-prototype using a mobile phone as a readout was already performed. The next step will be the adaptation of the protocol to allow for a wider range of biomarkers, validation of existing biomarkers in larger cohorts as well as the inclusion of a systems integrator allowing for a functional mass-production ready prototype.

## 4.2. Chapter II: Discussion of cohort results

With the dataset “BioPersMed” increasing over time, we are now at the point to reach critical mass and use these parameters with an interdisciplinary approach and the longitudinal dataset to generate promising clinical follow-up results. The link between several clinical areas has already started, and the results are more than promising. This fruitful research connection and the biobank as a basis for quality-controlled sample collection and storing is the perfect basis for long-lasting research projects. However, every big project has its downfalls and problems. The start of the BioPersMed cohort 2010 was not without struggle and, retrospectively, relatively improvisational. The patient recruitment as well as patient visit scheduling was initially not really synchronised between the groups (e.g. between the Divisions Endocrinology & Diabetology, Cardiology, Hepatology) which led to an inappropriate high number of different visit stages per patient. Not only the visit scheduling was initially not concerted, but there was also no systematic indexing of patients at the beginning between the Divisions. Fortunately, this system was changed by professional IT experts. Now, there is only one visit per patient per

timepoint allowing also for a better correlation of the parameters for many years.

### 4.2.1. Future perspective

The next step is to generate scientific value from this collection of patient derived data and samples. The baseline paper of BioPersMed is already finalised and is to be submitted in due time. This also allows for follow-up papers on specific research questions which have already been worked on to be published. In the future, the time between follow-ups will be increased from currently 2 years to 4 years to decrease the costs of the cohort study.

In addition, a BioPersMed steering committee will observe all duties for further data and biobanking conditions, research projects and cooperations.

## 4.3. Chapter III: Discussion on microbial intervention and biomarkers in PCOS

This chapter aimed to investigate the influence of isoflavone supply on microbiota composition and metabolic profiles in women with PCOS and in controls. We found a significant improvement of insulin and fasting glucose in the PCOS group, but not in the control group after this short-term isoflavone intervention. In fact, pancreatic insulin secretion after oral glucose uptake has been shown to improve after equol consumption in vivo (169). Additionally, a recent in-vitro study showed an inhibitory effect of equol on the production of intestinal glucagon-like peptide-1 (GLP-1) even with a rise in cellular Ca2+ levels, using GLUTag cells, a model of intestinal enteroendocrine L-cells (123). This could be the reason why an incretin/equol interaction may modulate glucose metabolism and insulin secretion.

While numerous publications have addressed potential effects of isoflavone rich food on various chronic diseases, isoflavones should not be equated with estrogens. Circulating levels of phytohormones even from small soy consumption may exceed endogenous estrogen levels by orders of magnitude (170).

Although experiments have been performed to correlate PCOS in rats and isoflavone, only a handful have investigated the connection between the isoflavones intake and PCOS in humans. These studies showed improvements in plasma lipid and androgen profiles after long term (3- to 6-months) isoflavone interventions in women with PCOS (106,107,171–175). These studies did not provide information about gut microbiota and metagenomics analysis as presented in our study to further characterize bacterial diversity (125) and the regulation of insulin resistance and ovarian dysfunction (63). Studies on hormonal effects of soy and its endocrine effects referring to different phases in life of women remains scarce and lacks reproducible studies. Only one meta-analysis found isoflavone consumption to reduce circulating levels of LH and FSH (170). This corresponds to our findings of higher genistein baseline levels in PCOS patients with a lower ratio of LH:FSH.

We saw effects after this short-term intervention, but the duration of isoflavone consumption needed for potential influences is debated. Two studies revealed changes in fecal bacterial community after 16 - 25 weeks of exposure (176,177). Nakatsu et al. investigated postmenopausal women and found bacterial variations on equol producers already after one week (178). In our trial, the predicted metagenome analyses demonstrated a convergence of

microbiome properties in PCOS women to those of controls within three days of isoflavone intervention.

If such an immediate effect resulted from an equivalent increase in equol producing bacteria has recently been investigating (125). Women with PCOS therefore may benefit from consuming more isoflavone-containing foods, independent of their initial capacity to produce equol. Women defined as equol producers may benefit directly from equol binding to DHT, which prevents androgen receptor activation, or via a decrease in steroidogenic enzyme expression. This has been shown in vitro and in a PCOS rat model (121,179). A more indirect effect is that the capacity to produce equol could be an indirect biomarker designated to the presence of bacteria in the gut, which exert beneficial influences on reproductive and metabolic processes.

With around 35% of equol producers in our study it fits well with previous reports on Western populations (180). Of note, potentially due to the limited sample size of our study we found only a borderline significance that PCOS women were half as likely to be equol producers compared to healthy control women.

An additional aspect of our study supports previous findings (107), indicating variations of urinary equol concentrations following isoflavone challenge, with an effect size in this study of 0.98. This points not only to a new diagnostic feature for PCOS women, but may also be the basis for potential pro- or/and prebiotic interventions.

Our evaluations of the baseline (T0) measurements (Figure 42) confirm recent publications arguing gut microbial alpha diversity decrease in PCOS women in comparison to healthy controls (53,181). Our data are also align with the concept that a fast adapting diet induces change of the microbiome (182–185). Although alpha diversity in PCOS women after invention (T1) is not as high as in the control group, this improvement was similar to the alpha diversity found in hormonally healthy controls before the intervention.

Bacterial strains which attributed to the healthy control group (T0, T1) - including S24-7 from the genus *Bacteroidales* - have already been documented as being the key species for starch binding and metabolising and have been linked to homoeothermic plant eating hosts (186). When comparing the control group using LEfSe, before and after isoflavone intervention only little differences were noted.

On the other hand, women with PCOS, only had *Megasphaera* 358887 and *Bacteroides* 186841 (Figure 44 and Figure 45) in common with their baseline LEfSe result. The most prominent OTU contributing to the PCOS phenotype after isoflavone intervention was however classified

as *Parabacteroides distasonis* (Figure 45). This bacterial strain has been documented to modulate the hosts metabolism by decreasing hyperglycaemia and weight gain, therefore improving metabolic syndrome and obesity in mice additionally has this strain the capacity to metabolize flavonoids in humans (187). To our best knowledge, we are the first to connect metabolic changes in women with PCOS to *Parabacteroides distasonis*. We also found out that the microbiome of PCOS patients contains several uncultivable members of the *Bacteroides* and *Ruminococcus* genus with yet unknown function.

Results obtained by LEfSe indicate a differentiation of controls and PCOS patients by the abundance of features classified as *Megasphaera massiliensis,* in women with PCOS. It has already been described that *Megasphaera massiliensis DISK18* has the capacity for forming biofilm as well as the producing important oxidative stress response markers (e.g. heat shock protein 33, chaperone dnaK gene cluster, superoxidase reductase), phosphate and carbon starvation proteins (e.g. Pho H , stringent starvation a & b), vitamins (e.g. vitamin B complex) and cofactors (188,189).

While some of the potentially important bacteria remain uncultivable to date, future approaches of microbiome research will possibly reveal their influence on the specific regulations and pathophysiology in PCOS. These strains could also be used as biomarkers for the detection of PCOS or equol producers and the result may be linked to metabolic profile of the patients. But more research on the use of strains as potent biomarkers needs to be performed.

Using recent advances in metagenomic analysis, we were able to highlight a significant contribution of equol production on pathways relevant for PCOS These pathways include carbohydrate digestion and absorption. This might directly connect to the modulation and/or manifestation of clinical symptoms in PCOS.

Predicted metagenome changes in this interventional study included predefined KEGG pathways such as the “carbohydrate digestion and absorption pathways”. It is defined as the digestion of complex carbohydrates to simple monosaccharides by a multitude of enzymes before final uptake in the small intestine (154,190). The absorption process is tightly linked to the potassium dependent (co-) transporter SGLT1 (sodium/glucose cotransporter 1). These induce quick insertion and activation of GLUT2 (glucose transporter 2), which facilitates the exocytosis of glucose in enterocytes (191,192). These KEGG “flavonoid biosynthesis and mineral absorption” were significantly reduced in PCOS phenotypes, as well as “carbohydrate digestion and absorption pathways” while “stilbenoid, diarylheptanoid and gingerol biosynthesis” was slightly increased.

These xenoendocrine molecules have been associated with neuroprotection, cancer prevention and cardiovascular health (193–196).

The KEGG “mineral absorption pathway” stands for bacterial properties of active and passive minerals transport through the intestinal mucosa. This system is known to use specific transport proteins, such as ferritin or vitamin D-dependent calcium-binding protein and might contribute to the specific features of metabolism in PCOS patients (197–200).

These changes in metabolic KEGG pathways enlighten an as yet unknown phenomenon in PCOS, which fits to the already described DOGMA (“Dysbiosis of Gut Microbiota”) hypothesis. This demonstrates a close connection of a dysbiosis of the gut and PCOS phenotype. (201).

Limitations of this study are the small character and its limited sample size. Furthermore, some of our results might be connected to the confounding factor of age, as the PCOS group was younger than the control. Age showed a significant positive correlation with equol production capacity. This relatively small 5-year difference should however not underpin large age-dependent changes in all of these premenopausal women. In summary, since the overall size of our cohort was relatively small, the risk of confounding factors may be more prominent, and our results need to be interpreted with caution and warrant further validation in a larger study.

### 4.3.1. Future development of biomarkers in medicine

The urgent need for new biomarkers, new sensor methods and additional validation cohorts in medicine and especially in common metabolic disorders is greatly supported by this project. However, this thesis generated additional tools and ideas to help patients cure and care as well as scientist and clinician. Many parts of this project are promising for the further developments by interdisciplinary teams of scientists., always keeping in mind not only the scientific advancement but also the clinical patient, who should benefit from these developments on the long run. Together with scientists and clinicians, the industry partners in this project fulfill the role of guides and discussion partners for technical and feasibility aspects. Working on a new biomarker is an important goal but has to be harmonized with potential markets and funding for a successful transfer from bench to bedside.

The BioPersMed project provides a continuous cohort for the validation of a combination of biomarkers for cardiovascular, metabolic, endocrine and many other common diseases, which

allows for the development of mutual biomarkers and a cross-validation between diseases. The rare possibility to follow patients over many years allows for an early detection of biomarkers in apparently healthy patients before the onset of a disease. The high number of study participants also allows for a sound validation of potential biomarker. In addition, the biobanking strategy of BioPersMed allows for a potential biomarker detection in several body materials such as blood, urine, faeces or saliva.

This cohort will also be used for the validation of the sensor established in this project. The number of biomarkers and the availability of urine as sample material of interest makes it a perfect collection for our approach.

With the knowhow we got in developing a sensor for the detection of protein-based biomarkers, our developments will also allow to focus on further biomarkers of interest, e.g. biomarkers out of the PCOS study. The strains defined in our work will give us more information on the isoflavone metabolizing capacity of our patients, but further bioinformatical research will help do identify microbiome-based biomarkers for the diagnosis and further treatment of PCOS.

**Bibliography**


1. Donald G, Lucas G. The Empire Strikes Back. Del Rey; First Edition/First Printing (April 12, 1980); 1980.
2. Pratchett T. A hat full of sky. 2004. 278 p.
3. Kautzky-Willer A, Harreiter J, Bancher-Todesca D, Berger A, Repa A, Lechleitner M, et al. Diabetes mellitus – Anleitungen für die Praxis Austrian Lipid Consensus 2016 - Gestationsdiabetes. Cent Eur J Med Wien Klin Wochenschr [Internet]. 2016;128(2):103–12. Available from: https://www.oedg.at/pdf/Diabetes-mellitus-Anleitungen-fuer-die-Praxis-2016.pdf
4. Griffith R by JR. Williams Textbook of Endocrinology, 10th edition. J Pediatr Adolesc Gynecol [Internet]. 2004 Jun;17(3):217–8. Available from: https://linkinghub.elsevier.com/retrieve/pii/S1083318804000993
5. Kharroubi AT. Diabetes mellitus: The epidemic of the century. World J Diabetes. 2015;
6. Diabetes Uk. Key statistics on diabetes. Diabetes. 2010;
7. Bell DSH. Heart failure: The frequent, forgotten, and often fatal complication of diabetes. Diabetes Care. 2003.
8. World Health Organization. Global Report on Diabetes. Isbn. 2016;
9. Piccoli GB, Grassi G, Cabiddu G, Nazha M, Roggero S, Capizzi I, et al. Diabetic kidney disease: A syndrome rather than a single disease. Review of Diabetic Studies. 2015.
10. Federation ID. IDF Diabetes Atlas Eighth edition 2017. International Diabetes Federation. IDF Diabetes Atlas, 8th edn. Brussels, Belgium: International Diabetes Federation, 2017. http://www.diabetesatlas.org. 2017.
11. Yang Y, Hu X, Zhang Q, Zou R. Diabetes mellitus and risk of falls in older adults: a systematic review and meta-analysis. Age Ageing. 2016;
12. Starup-Linde J, Lykkeboe S, Gregersen S, Hauge EM, Langdahl BL, Handberg A, et al. Differences in biochemical bone markers by diabetes type and the impact of glucose. Bone. 2016;
13. Ferrari S. Diabetes and Bone. Calcif Tissue Int [Internet]. 2017 Feb 8;100(2):107–8. Available from: http://link.springer.com/10.1007/s00223-017-0234-y
14. Marin C, Luyten FP, Van der Schueren B, Kerckhofs G, Vandamme K. The impact of Type 2 diabetes on bone fracture healing. Frontiers in Endocrinology. 2018.
15. WHO. Diabetes Fact Sheet Nº312. NMH Fact Sheet February 2010. 2015.

16. Chiang JL, Kirkman MS, Laffel LMB, Peters AL. Type 1 diabetes through the life span: A position statement of the American Diabetes Association. Diabetes Care. 2014.
17. Hoehn KL, Salmon AB, Hohnen-Behrens C, Turner N, Hoy AJ, Maghzal GJ, et al. Insulin resistance is a cellular antioxidant defense mechanism. Proc Natl Acad Sci U S A. 2009;
18. Henriksen EJ, Diamond-Stanic MK, Marchionne EM. Oxidative stress and the etiology of insulin resistance and type 2 diabetes. Free Radical Biology and Medicine. 2011.
19. Peet TE, Bryan CP. The Papyrus Ebers. J Egypt Archaeol. 1931;
20. Zhang H, Tan C, Wang H, Xue S, Wang M. Study on the history of Traditional Chinese Medicine to treat diabetes. European Journal of Integrative Medicine. 2010.
21. Cawley T. A Singular Case of Diabetes, Consisting Entirely in the Quality of the Urine; with an Inquiry into the Different Theories of That Disease. London Med J [Internet]. 1788;9(Pt 3):286–308. Available from: http://www.ncbi.nlm.nih.gov/pubmed/29139716%0Ahttp://www.pubmedcentral.nih.gov/articlerender.fcgi?artid=PMC5545243
22. v. Mering J, Minkowski O. Diabetes mellitus nach Pankreasexstirpation. Arch für Exp Pathol und Pharmakologie. 1890;
23. American Diabetes Association. 2016 American Diabetes Association (ADA) Diabetes Guidelines Summary Recommendation from NDEI. Natl Diabetes Educ Initiat. 2016;
24. Information NC for B, Pike USNL of M 8600 R, MD B, Usa 20894. Glucose tolerance tests: What exactly do they involve? 2016 Dec 30 [cited 2020 Aug 4]; Available from: https://www.ncbi.nlm.nih.gov/books/NBK279331/%0Ainternal-pdf://0.0.2.221/NBK279331.html
25. R.A. D, M. A-G. Assessment and treatment of cardiovascular risk in prediabetes: Impaired glucose tolerance and impaired fasting glucose. Am J Cardiol. 2011;
26. 2. Classification and diagnosis of diabetes: Standards of medical care in diabetesd2019. Diabetes Care. 2019;
27. Miedema K. Standardization of HbA1c and optimal range of monitoring. In: Scandinavian Journal of Clinical and Laboratory Investigation, Supplement [Internet]. Taylor & Francis; 2005 [cited 2020 Aug 4]. p. 61–72. Available from: https://www.tandfonline.com/doi/abs/10.1080/00365510500236143
28. WHO. Use of glycated haemoglobin (HbA1c) in the diagnosis of diabetes mellitus. Diabetes Res Clin Pract [Internet]. 2011 Sep;93(3):299–309. Available from:

https://linkinghub.elsevier.com/retrieve/pii/S0168822711001318

29. Vasu S, Kumano K, Darden CM, Rahman I, Lawrence MC, Naziruddin B. MicroRNA Signatures as Future Biomarkers for Diagnosis of Diabetes States. Cells. 2019;
30. Luc K, Schramm-Luc A, Guzik TJ, Mikolajczyk TP. Oxidative stress and inflammatory markers in prediabetes and diabetes. Journal of Physiology and Pharmacology. 2019.
31. Mardinoglu A, Stančáková A, Lotta LA, Kuusisto J, Boren J, Blüher M, et al. Plasma Mannose Levels Are Associated with Incident Type 2 Diabetes and Cardiovascular Disease. Cell Metabolism. 2017.
32. Vangipurapu J, Áková AS, Kuulasmaa T, Kuusisto J, Laakso M. Both fasting and glucose-stimulated proinsulin levels predict hyperglycemia and incident type 2 diabetes:A population-based study of 9,396 finnish men. PLoS One. 2015;
33. Yi L, Swensen AC, Qian WJ. Serum biomarkers for diagnosis and prediction of type 1 diabetes [Internet]. Vol. 201, Translational Research. Mosby Inc.; 2018 [cited 2020 Sep 10]. p. 13–25. Available from: /pmc/articles/PMC6177288/?report=abstract
34. Elabd S, Sabry I. Two Birds with One Stone: Possible Dual-Role of Oxytocin in the Treatment of Diabetes and Osteoporosis. Front Endocrinol (Lausanne). 2015;
35. Akour A, Kasabri V, Boulatova N, Bustanji Y, Naffa R, Hyasat D, et al. Levels of metabolic markers in drug-naive prediabetic and type 2 diabetic patients. Acta Diabetol. 2017;
36. Aschner P. Insulin Therapy in Type 2 Diabetes. Am J Ther. 2020;
37. Moelands SVL, Lucassen PLBJ, Akkermans RP, De Grauw WJC, Van de Laar FA. Alpha-glucosidase inhibitors for prevention or delay of type 2 diabetes mellitus and its associated complications in people at increased risk of developing type 2 diabetes mellitus. Cochrane Database of Systematic Reviews. 2018.
38. Sola D, Rossi L, Schianca GPC, Maffioli P, Bigliocca M, Mella R, et al. Sulfonylureas and their use in clinical practice. Archives of Medical Science. 2015.
39. Qiu H, Novikov A, Vallon V. Ketosis and diabetic ketoacidosis in response to SGLT2 inhibitors: Basic mechanisms and therapeutic perspectives. Diabetes/Metabolism Research and Reviews. 2017.
40. Garcia-Ropero A, Badimon JJ, Santos-Gallego CG. The pharmacokinetics and pharmacodynamics of SGLT2 inhibitors for type 2 diabetes mellitus: the latest developments. Expert Opinion on Drug Metabolism and Toxicology. 2018.
41. Usman MS, Siddiqi TJ, Memon MM, Khan MS, Rawasia WF, Talha Ayub M, et al.

Sodium-glucose co-transporter 2 inhibitors and cardiovascular outcomes: A systematic review and meta-analysis. Eur J Prev Cardiol. 2018;

42. Bonora BM, Avogaro A, Fadini GP. Extraglycemic effects of SGLT2 inhibitors: A review of the evidence. Diabetes, Metabolic Syndrome and Obesity: Targets and Therapy. 2020.
43. Nanjan MJ, Mohammed M, Prashantha Kumar BR, Chandrasekar MJN. Thiazolidinediones as antidiabetic agents: A critical review. Bioorganic Chemistry. 2018.
44. Soccio RE, Chen ER, Lazar MA. Thiazolidinediones and the promise of insulin sensitization in type 2 diabetes. Cell Metabolism. 2014.
45. Madiraju AK, Erion DM, Rahimi Y, Zhang XM, Braddock DT, Albright RA, et al. Metformin suppresses gluconeogenesis by inhibiting mitochondrial glycerophosphate dehydrogenase. Nature. 2014;
46. Rena G, Pearson ER, Sakamoto K. Molecular mechanism of action of metformin: Old or new insights? Diabetologia. 2013.
47. Berg J, Tymoczko J, Stryer L. Biochemistry, 5th edition. Biochemistry. 2002.
48. Elbere I, Kalnina I, Silamikelis I, Konrade I, Zaharenko L, Sekace K, et al. Association of metformin administration with gut microbiome dysbiosis in healthy volunteers. PLoS One. 2018;
49. McCreight LJ, Bailey CJ, Pearson ER. Metformin and the gastrointestinal tract. Diabetologia. 2016.
50. Attia GR, Rainey WE, Carr BR. Metformin directly inhibits androgen production in human thecal cells. Fertil Steril. 2001;
51. Morley LC, Tang T, Yasmin E, Norman RJ, Balen AH. Insulin-sensitising drugs (metformin, rosiglitazone, pioglitazone, D-chiro-inositol) for women with polycystic ovary syndrome, oligo amenorrhoea and subfertility. Cochrane Database of Systematic Reviews. 2017.
52. Meier RK. Polycystic Ovary Syndrome. Nurs Clin North Am [Internet]. 2018 Aug;53(3):407–20. Available from: http://www.nature.com/articles/nrdp201657%0Ahttp://www.ncbi.nlm.nih.gov/pubmed/27510637
53. Liu R, Zhang C, Shi Y, Zhang F, Li L, Wang X, et al. Dysbiosis of gut microbiota associated with clinical parameters in polycystic ovary syndrome. Front Microbiol.

2017;

54. Lause M, Kamboj A, Faith EF. Dermatologic manifestations of endocrine disorders. Translational Pediatrics. 2017.
55. Tata B, Mimouni NEH, Barbotin AL, Malone SA, Loyens A, Pigny P, et al. Elevated prenatal anti-Müllerian hormone reprograms the fetus and induces polycystic ovary syndrome in adulthood. Nat Med [Internet]. 2018 Jun 1 [cited 2020 Aug 4];24(6):834–46. Available from: https://www.nature.com/articles/s41591-018-0035-5
56. Azziz R, Carmina E, Chen Z, Dunaif A, Laven JSE, Legro RS, et al. Polycystic ovary syndrome. Nat Rev Dis Prim [Internet]. 2016 Dec 11 [cited 2019 Jan 15];2(1):16057. Available from: http://www.nejm.org/doi/abs/10.1056/NEJM199509283331307
57. Kelly CCJ, Lyall H, Petrie JR, Gould GW, Connell JMC, Sattar N. Low grade chronic inflammation in women with polycystic ovarian syndrome. J Clin Endocrinol Metab. 2001;
58. Diamanti-Kandarakis E, Dunaif A. Insulin resistance and the polycystic ovary syndrome revisited: An update on mechanisms and implications. Endocr Rev. 2012;
59. Goldrat O, Delbaere A. PCOS: update and diagnostic approach. Clin Biochem [Internet]. 2018;62:24–31. Available from: https://doi.org/10.1016/j.clinbiochem.2018.09.001
60. Dokras A. Cardiovascular disease risk in women with PCOS. Steroids. 2013;
61. Landay M, Huang A, Azziz R. Degree of hyperinsulinemia, independent of androgen levels, is an important determinant of the severity of hirsutism in PCOS. Fertil Steril. 2009;
62. Ferk P, Teran N, Gersak K. The (TAAAA)n microsatellite polymorphism in the SHBG gene influences serum SHBG levels in women with polycystic ovary syndrome. Hum Reprod. 2007;22(4):1031–6.
63. González F, Rote NS, Minium J, Kirwan JP. Reactive oxygen species-induced oxidative stress in the development of insulin resistance and hyperandrogenism in polycystic ovary syndrome. J Clin Endocrinol Metab. 2006;
64. Roth GA, Abate D, Abate KH, Abay SM, Abbafati C, Abbasi N, et al. Global, regional, and national age-sex-specific mortality for 282 causes of death in 195 countries and territories, 1980–2017: a systematic analysis for the Global Burden of Disease Study 2017. Lancet. 2018;
65. Ciaccio EJ, Lewis SK, Biviano AB, Iyer V, Garan H, Green PH. Cardiovascular involvement in celiac disease. World J Cardiol. 2017;

66. Townsend N, Wilson L, Bhatnagar P, Wickramasinghe K, Rayner M, Nichols M. Cardiovascular disease in Europe: Epidemiological update 2016. European Heart Journal. 2016.
67. Patel SA, Winkel M, Ali MK, Narayan KMV, Mehta NK. Cardiovascular mortality associated with 5 leading risk factors: National and state preventable fractions estimated from survey data. Ann Intern Med. 2015;
68. Mach F, Baigent C, Catapano AL, Koskinas KC, Casula M, Badimon L, et al. 2019 ESC/EAS Guidelines for the management of dyslipidaemias: Lipid modification to reduce cardiovascular risk. European Heart Journal. 2020.
69. Ettehad D, Emdin CA, Kiran A, Anderson SG, Callender T, Emberson J, et al. Blood pressure lowering for prevention of cardiovascular disease and death: A systematic review and meta-analysis. Lancet. 2016;
70. Swanson PE. Foundations of Immunohistochemistry. Am J Clin Pathol [Internet]. 1988 Sep 1;90(3):333–9. Available from: https://academic.oup.com/ajcp/article/90/3/333/1820683
71. Nanci A, Wazen R, Nishio C, Zalzal SF. Immunocytochemistry of matrix proteins in calcified tissues: Functional biochemistry on section. European Journal of Histochemistry. 2008.
72. El-Heliebi A, Hille C, Laxman N, Svedlund J, Haudum C, Ercan E, et al. In situ detection and quantification of AR-V7, AR-FL, PSA, and KRAS point mutations in circulating tumor cells. Clin Chem. 2018;64(3).
73. Wang Z, Gerstein M, Snyder M. RNA-Seq: A revolutionary tool for transcriptomics. Nature Reviews Genetics. 2009.
74. Lindheim L, Bashir M, Münzker J, Trummer C, Zachhuber V, Pieber TR, et al. The salivary microbiome in polycystic ovary syndrome (PCOS) and its association with disease-related parameters: A pilot study. Front Microbiol. 2016;
75. Tang WHW, Kitai T, Hazen SL. Gut microbiota in cardiovascular health and disease. Circulation Research. 2017.
76. Torres PJ, Siakowska M, Banaszewska B, Pawelczyk L, Duleba AJ, Kelley ST, et al. Gut Microbial Diversity in Women with Polycystic Ovary Syndrome Correlates with Hyperandrogenism. J Clin Endocrinol Metab. 2018;
77. Lach G, Schellekens H, Dinan TG, Cryan JF. Anxiety, Depression, and the Microbiome: A Role for Gut Peptides. Neurotherapeutics. 2018.

78. Kadosh E, Snir-Alkalay I, Venkatachalam A, May S, Lasry A, Elyada E, et al. The gut microbiome switches mutant p53 from tumour-suppressive to oncogenic. Nature [Internet]. 2020 Jul 29; Available from: http://www.nature.com/articles/s41586-020-2541-0
79. Nunn KL, Forney LJ. Unraveling the dynamics of the human vaginal microbiome. Yale Journal of Biology and Medicine. 2016.
80. Dréno B, Araviiskaia E, Berardesca E, Gontijo G, Sanchez Viera M, Xiang LF, et al. Microbiome in healthy skin, update for dermatologists. Journal of the European Academy of Dermatology and Venereology. 2016.
81. Müller-Wieland D, Gallwitz B, Haak T. Deutschland = Diabetesland: Deutscher Gesundheitsbericht Diabetes 2008. Diabetologie und Stoffwechsel. 2008.
82. Johansen MY, Macdonald CS, Hansen KB, Karstoft K, Christensen R, Pedersen M, et al. Effect of an intensive lifestyle intervention on glycemic control in patients with type 2 diabetes: A randomized clinical trial. JAMA - J Am Med Assoc. 2017 Aug 15;318(7):637–46.
83. Simões FR, Xavier MG. Electrochemical Sensors [Internet]. Nanoscience and its Applications. Elsevier Inc.; 2017. 155–178 p. Available from: http://dx.doi.org/10.1016/B978-0-323-49780-0/00006-5
84. Islam SK, Haider MR. Sensors and low power signal processing. Sensors and Low Power Signal Processing. 2010.
85. Hayes DF. Biomarker validation and testing. Molecular Oncology. 2015.
86. Baron RJ, Berinsky AJ. Mistrust in Science — A Threat to the Patient–Physician Relationship. N Engl J Med. 2019;
87. Kumar S, Mohan A, Guleria R. Biomarkers in cancer screening, research and detection: present and future: a review. Biomarkers [Internet]. 2006 Jan 8 [cited 2019 Feb 4];11(5):385–405. Available from: http://www.ncbi.nlm.nih.gov/pubmed/16966157
88. Sidransky D. Emerging molecular markers of cancer. Nat Rev Cancer [Internet]. 2002 Mar [cited 2019 Feb 4];2(3):210–9. Available from: http://www.ncbi.nlm.nih.gov/pubmed/11990857
89. Jazayeri MH, Amani H, Pourfatollah AA, Pazoki-Toroudi H, Sedighimoghaddam B. Various methods of gold nanoparticles (GNPs) conjugation to antibodies. Sens Bio-Sensing Res [Internet]. 2016 Jul 1 [cited 2019 Jan 18];9:17–22. Available from: https://www.sciencedirect.com/science/article/pii/S2214180416300344

90. Gillman MW. Primordial prevention of cardiovascular disease. Circulation. 2015.
91. Wall HK, Hannan JA, Wright JS. Patients with undiagnosed hypertension hiding in plain sight. JAMA - Journal of the American Medical Association. 2014.
92. Gyberg V, Bacquer D, Backer G, Jennings C, Kotseva K, Mellbin L, et al. Patients with coronary artery disease and diabetes need improved management: A report from the EUROASPIRE IV survey: A registry from the EuroObservational Research Programme of the European Society of Cardiology. Cardiovasc Diabetol. 2015;
93. Benjamin EJ, Muntner P, Alonso A, Bittencourt MS, Callaway CW, Carson AP, et al. Heart Disease and Stroke Statistics-2019 Update: A Report From the American Heart Association. Circulation. 2019;
94. Roger VL. Epidemiology of heart failure. Circ Res. 2013;
95. Newman JD, Vani AK, Aleman JO, Weintraub HS, Berger JS, Schwartzbard AZ. The Changing Landscape of Diabetes Therapy for Cardiovascular Risk Reduction: JACC State-of-the-Art Review. Journal of the American College of Cardiology. 2018.
96. Shah S. Prevention of Cardiovascular Disease: Guideline for assessment and management of cardiovascular risk. World Health Organization. 2007.
97. Chu W, Han Q, Xu J, Wang J, Sun Y, Li W, et al. Metagenomic analysis identified microbiome alterations and pathological association between intestinal microbiota and polycystic ovary syndrome. Fertil Steril. 2020;
98. Rowland I, Gibson G, Heinken A, Scott K, Swann J, Thiele I, et al. Gut microbiota functions: metabolism of nutrients and other food components. European Journal of Nutrition. 2018.
99. Tilg H, Kaser A. Gut microbiome, obesity, and metabolic dysfunction. Journal of Clinical Investigation. 2011.
100. Guo Y, Qi Y, Yang X, Zhao L, Wen S, Liu Y, et al. Association between polycystic ovary syndrome and gut microbiota. PLoS One. 2016;
101. Setchell KDR, Cole SJ. Method of Defining Equol-Producer Status and Its Frequency among Vegetarians. J Nutr. 2006;
102. Markowiak P, Ślizewska K. Effects of probiotics, prebiotics, and synbiotics on human health. Nutrients. 2017.
103. Lindheim L, Bashir M, Münzker J, Trummer C, Zachhuber V, Leber B, et al. Alterations in gut microbiome composition and barrier function are associated with reproductive and metabolic defects in women with polycystic ovary syndrome (PCOS): A pilot study. Yu

Y, editor. PLoS One. 2017 Jan;12(1):e0168390.

104. Elorinne AL, Alfthan G, Erlund I, Kivimäki H, Paju A, Salminen I, et al. Food and nutrient intake and nutritional status of Finnish vegans and non-vegetarians. PLoS One. 2016;
105. Atkinson C, Newton KM, Stanczyk FZ, Westerlind KC, Li L, Lampe JW. Daidzein-metabolizing phenotypes in relation to serum hormones and sex hormone binding globulin, and urinary estrogen metabolites in premenopausal women in the United States. Cancer Causes Control. 2008;19(10):1085–93.
106. Romualdi D, Costantini B, Campagna G, Lanzone A, Guido M. Is there a role for soy isoflavones in the therapeutic approach to polycystic ovary syndrome? Results from a pilot study. Fertil Steril. 2008;90(5):1826–33.
107. Khani B, Mehrabian F, Khalesi E, Eshraghi A. Effect of soy phytoestrogen on metabolic and hormonal disturbance of women with polycystic ovary syndrome. J Res Med Sci. 2011;16(3):297–302.
108. Usui T, Tochiya M, Sasaki Y, Muranaka K, Yamakage H, Himeno A, et al. Effects of natural S-equol supplements on overweight or obesity and metabolic syndrome in the Japanese, based on sex and equol status. Clin Endocrinol (Oxf). 2013;
109. Utian WH, Jones M, Setchell KDR. S-equol: A Potential Nonhormonal Agent for Menopause-Related Symptom Relief. J Women's Heal. 2015;
110. Messina M, Nagata C, Wu AH. Estimated Asian adult soy protein and isoflavone intakes. Nutrition and Cancer. 2006.
111. Messina M. Soy and health update: Evaluation of the clinical and epidemiologic literature. Nutrients. 2016.
112. Yamagata K. Soy Isoflavones Inhibit Endothelial Cell Dysfunction and Prevent Cardiovascular Disease. J Cardiovasc Pharmacol. 2019;
113. Křížová L, Dadáková K, Kašparovská J, Kašparovský T. Isoflavones. Molecules. 2019.
114. Esch HL, Kleider C, Scheffler A, Lehmann L. Isoflavones: Toxicological Aspects and Efficacy. In: Nutraceuticals: Efficacy, Safety and Toxicity. 2016.
115. Yanaka K, Higuchi M, Ishimi Y. Anti-osteoporotic effect of soy Isoflavones intake on low bone mineral density caused by voluntary exercise and food restriction in mature female rats. J Nutr Sci Vitaminol (Tokyo). 2019;
116. Moradi M, Daneshzad E, Azadbakht L. The effects of isolated soy protein, isolated soy isoflavones and soy protein containing isoflavones on serum lipids in postmenopausal

women: A systematic review and meta-analysis. Critical Reviews in Food Science and Nutrition. 2019.

117. Hilakivi-Clarke L, de Assis S. Fetal origins of breast cancer. Trends Endocrinol Metab. 2006;
118. Franke AA, Lai JF, Halm BM. Absorption, distribution, metabolism, and excretion of isoflavonoids after soy intake. Archives of Biochemistry and Biophysics. 2014.
119. Cani PD, Delzenne NM, Amar J, Burcelin R. Role of gut microflora in the development of obesity and insulin resistance following high-fat diet feeding. Pathol Biol. 2008;
120. Zhao X, Jiang Y, Xi H, Chen L, Feng X. Exploration of the Relationship between Gut Microbiota and Polycystic Ovary Syndrome (PCOS): A Review. Geburtshilfe und Frauenheilkunde. 2020.
121. Yuan JP, Wang JH, Liu X. Metabolism of dietary soy isoflavones to equol by human intestinal microflora - Implications for health. Vol. 51, Molecular Nutrition and Food Research. Food Engineering Research Center of State Education Ministry, College of Life Sciences, Sun Yat-Sen University, Guangzhou, People's Republic of China. yuanjp@mail.sysu.edu.cn; 2007. p. 765–81.
122. Zubik L, Meydani M. Bioavailability of soybean isoflavones from aglycone and glucoside forms in American women. Am J Clin Nutr. 2003;
123. Rowlands DJ, Chapple S, Siow RCM, Mann GE. Equol-stimulated mitochondrial reactive oxygen species activate endothelial nitric oxide synthase and redox signaling in endothelial cells: Roles for F-actin and GPR30. Hypertension. 2011;
124. Harada K, Sada S, Sakaguchi H, Takizawa M, Ishida R, Tsuboi T. Bacterial metabolite S-equol modulates glucagon-like peptide-1 secretion from enteroendocrine L cell line GLUTag cells via actin polymerization. Biochem Biophys Res Commun. 2018;
125. Iino C, Shimoyama T, Iino K, Yokoyama Y, Chinda D, Sakuraba H, et al. Daidzein intake is associated with equol producing status through an increase in the intestinal bacteria responsible for equol production. Nutrients. 2019;
126. Hafaiedh I, Chammem H, Abdelghani A, Ait E, Feldman L, Meilhac O, et al. Supported protein G on gold electrode: Characterization and immunosensor application. Talanta. 2013;
127. Khashayar P, Amoabediny G, Larijani B, Hosseini M, Verplancke R, De Keersmaecker M, et al. A highly sensitive electrochemical biosensor based on AuNP-modified gold electrodes for selective determination of serum levels of crosslaps. 3 Biotech [Internet].

2017 Oct [cited 2019 Jan 15];7(5):312. Available from: http://www.ncbi.nlm.nih.gov/pubmed/28955609

128. Lerga TM, Skouridou V, Bermudo MC, Bashammakh AS, El-Shahawi MS, Alyoubi AO, et al. Gold nanoparticle aptamer assay for the determination of histamine in foodstuffs. Microchim Acta. 2020;
129. Jauset-Rubio M, Sabaté del Río J, Mairal T, Svobodová M, El-Shahawi MS, Bashammakh AS, et al. Ultrasensitive and rapid detection of B-conglutin combining aptamers and isothermal recombinase polymerase amplification. Anal Bioanal Chem. 2017;
130. Weston PD, Devries JA, Wrigglesworth R. Conjugation of enzymes to immunoglobulins using dimaleimides. BBA - Enzymol. 1980;
131. Te Piao King, Loucia Kochoumian. A comparison of different enzyme-antibody conjugates for enzyme-linked immunosorbent assay. J Immunol Methods. 1979;
132. Karyakin AA, Presnova G V., Rubtsova MY, Egorov AM. Oriented immobilization of antibodies onto the gold surfaces via their native thiol groups. Anal Chem. 2000;
133. Kausaite-Minkstimiene A, Ramanaviciene A, Kirlyte J, Ramanavicius A. Comparative study of random and oriented antibody immobilization techniques on the binding capacity of immunosensor. In: Analytical Chemistry. 2010.
134. Jarocka U, Sawicka R, Góra-Sochacka A, Sirko A, Zagórski-Ostoja W, Radecki J, et al. An immunosensor based on antibody binding fragments attached to gold nanoparticles for the detection of peptides derived from avian influenza hemagglutinin H5. Sensors (Switzerland). 2014;
135. Wasowicz M, Milner M, Radecka D, Grzelak K, Radecka H. Immunosensor incorporating Anti-His (C-term) IgG F(ab') fragments attached to gold nanorods for detection of His-tagged proteins in culture medium. Sensors. 2010;
136. Fischer LM, Tenje M, Heiskanen AR, Masuda N, Castillo J, Bentien A, et al. Gold cleaning methods for electrochemical detection applications. Microelectron Eng. 2009;
137. Libansky M, Zima J, Barek J, Reznickova A, Svorcik V, Dejmkova H. Basic electrochemical properties of sputtered gold film electrodes. Electrochim Acta. 2017;
138. Piepoli MF, Hoes AW, Agewall S, Albus C, Brotons C, Catapano AL, et al. 2016 European guidelines on cardiovascular disease prevention in clinical practice. The Sixth Joint Task Force of the European Society of Cardiology and Other Societies on Cardiovascular Disease Prevention in Clinical Practice (constituted by representati. G

Ital Cardiol (Rome). 2017;

139. Rstudio Team. RStudio: Integrated development for R. RStudio, Inc., Boston MA. RStudio. 2019.

140. Purdie AW. Association of Oligomenorrhoea, Hirsuties, and Infertility. Br Med J [Internet]. 1965 Jul 10 [cited 2020 Sep 9];2(5453):69–72. Available from: https://www.ncbi.nlm.nih.gov/pmc/articles/PMC1845336/

141. Azziz R, Carmina E, Sawaya ME. Idiopathic Hirsutism [1]. Endocr Rev [Internet]. 2000;21(4):347–62. Available from: https://academic.oup.com/edrv/article-lookup/doi/10.1210/edrv.21.4.0401

142. Lindheim L, Bashir M, Münzker J, Trummer C, Zachhuber V, Pieber TR, et al. The salivary microbiome in polycystic ovary syndrome (PCOS) and its association with disease-related parameters: A pilot study. Front Microbiol. 2016;7(AUG).

143. Grace PB, Mistry NS, Carter MH, Leathem AJ, Teale P. High throughput quantification of phytoestrogens in human urine and serum using liquid chromatography/tandem mass spectrometry (LC-MS/MS). J Chromatogr. 2007 Jun;853(1–2):138–46.

144. Kozich JJ, Westcott SL, Baxter NT, Highlander SK, Schloss PD. Development of a Dual-Index Sequencing Strategy and Curation Pipeline for Analyzing Amplicon Sequence Data on the MiSeq Illumina Sequencing Platform. Appl Environ Microbiol. 2013;

145. Edgar RC, Haas BJ, Clemente JC, Quince C, Knight R. UCHIME improves sensitivity and speed of chimera detection. Bioinformatics. 2011;

146. DeSantis TZ, Hugenholtz P, Larsen N, Rojas M, Brodie EL, Keller K, et al. Greengenes, a chimera-checked 16S rRNA gene database and workbench compatible with ARB. Appl Environ Microbiol. 2006;

147. Afgan E, Baker D, Batut B, Van Den Beek M, Bouvier D, Ech M, et al. The Galaxy platform for accessible, reproducible and collaborative biomedical analyses: 2018 update. Nucleic Acids Res. 2018;46(W1):W537–44.

148. Caporaso JG, Kuczynski J, Stombaugh J, Bittinger K, Bushman FD, Costello EK, et al. QIIME allows analysis of high-throughput community sequencing data. Nature Methods. 2010.

149. Agarwala R, Barrett T, Beck J, Benson DA, Bollin C, Bolton E, et al. Database resources of the National Center for Biotechnology Information. Nucleic Acids Res. 2018;

150. Edgar RC. Search and clustering orders of magnitude faster than BLAST. Bioinformatics. 2010;

151. Zakrzewski M, Proietti C, Ellis JJ, Hasan S, Brion MJ, Berger B, et al. Calypso: A user-friendly web-server for mining and visualizing microbiome-environment interactions. Bioinformatics. 2017;
152. Segata N, Izard J, Waldron L, Gevers D, Miropolsky L, Garrett WS, et al. Metagenomic biomarker discovery and explanation. Genome Biol [Internet]. 2011;12(6):R60. Available from: http://genomebiology.com/2011/11/6/R60
153. Langille MGI, Zaneveld J, Caporaso JG, McDonald D, Knights D, Reyes JA, et al. Predictive functional profiling of microbial communities using 16S rRNA marker gene sequences. Nat Biotechnol. 2013;
154. Ogata H, Goto S, Sato K, Fujibuchi W, Bono H, Kanehisa M. KEGG: Kyoto encyclopedia of genes and genomes. Nucleic Acids Research. 1999.
155. FISHER RA. the Use of Multiple Measurements in Taxonomic Problems. Ann Eugen [Internet]. 1936;7(2):179–88. Available from: http://doi.wiley.com/10.1111/j.1469-1809.1936.tb02137.x
156. Martinez AM, Kak AC. PCA versus LDA. IEEE Trans Pattern Anal Mach Intell. 2001;
157. Wooldridge JM. Introductory Econometrics: A Modern Approach. Econ Anal. 2003;
158. Rao Yarlagadda RK. Analog and digital signals and systems. Analog and Digital Signals and Systems. 2010.
159. Lin A V. Indirect ELISA. Methods Mol Biol. 2015;
160. Wang J. Analytical Electrochemistry, Third Edition. Analytical Electrochemistry, Third Edition. 2006.
161. Müllner D. Fastcluster: Fast hierarchical, agglomerative clustering routines for R and Python. J Stat Softw. 2013;
162. Shortt C, Hasselwander O, Meynier A, Nauta A, Fernández EN, Putz P, et al. Systematic review of the effects of the intestinal microbiota on selected nutrients and non-nutrients. European Journal of Nutrition. 2018.
163. Haudum C, Lindheim L, Ascani A, Trummer C, Horvath A, Münzker J, et al. Impact of short-term isoflavone intervention in polycystic ovary syndrome (PCOS) patients on microbiota composition and metagenomics. Nutrients. 2020;
164. Pyrczak F, Oh DM, Pyrczak F, Oh DM. z Score. In: Making Sense of Statistics. 2019.
165. Salkind N. z Score. In: Encyclopedia of Research Design [Internet]. 2455 Teller Road, Thousand Oaks California 91320 United States: SAGE Publications, Inc.; 2011. Available from: http://methods.sagepub.com/reference/encyc-of-research-

design/n509.xml
166. Jarczewska M, Rębiś J, Górski Ł, Malinowska E. Development of DNA aptamer-based sensor for electrochemical detection of C-reactive protein. Talanta. 2018;
167. Ali MH, Elsherbiny ME, Emara M. Updates on aptamer research. International Journal of Molecular Sciences. 2019.
168. Bruno JG. Long Shelf Life of a Lyophilized DNA Aptamer Beacon Assay. J Fluoresc. 2017;
169. Horiuchi H, Usami A, Shirai R, Harada N, Ikushiro S, Sakaki T, et al. S -Equol Activates cAMP Signaling at the Plasma Membrane of INS-1 Pancreatic β-Cells and Protects against Streptozotocin-Induced Hyperglycemia by Increasing β-Cell Function in Male Mice . J Nutr. 2017;
170. Hooper L, Ryder JJ, Kurzer MS, Lampe JW, Messina MJ, Phipps WR, et al. Effects of soy protein and isoflavones on circulating hormone concentrations in pre- and post-menopausal women: A systematic review and meta-analysis. Vol. 15, Human Reproduction Update. 2009. p. 423–40.
171. Jamilian M, Asemi Z. The effects of soy isoflavones on metabolic status of patients with polycystic ovary syndrome. J Clin Endocrinol Metab. 2016 Aug;101(9):3386–94.
172. Rajaei S, Alihemmati A, Abedelahi A. Antioxidant effect of genistein on ovarian tissue morphology, oxidant and antioxidant activity in rats with induced polycystic ovary syndrome. Int J Reprod Biomed. 2019;
173. Alivandi Farkhad S, Khazali H. Therapeutic effects of isoflavone-aglycone fraction from soybean (Glycine max L. Merrill) in rats with estradiol valerate-induced polycystic ovary syndrome as an inflammatory state. Gynecol Endocrinol. 2019;
174. Zhang T, Chi XX. Estrogenic properties of genistein acting on FSHR and LHR in rats with PCOS. Pol J Vet Sci. 2019;
175. Chi XX, Zhang T, Chu XL, Zhen JL, Zhang DJ. The regulatory effect of genistein on granulosa cell in ovary of rat with PCOS through BCL-2 and BAX signaling pathways. J Vet Med Sci. 2018;
176. Ko TF, Tsai HS, Lin SM, Liu CD, Learn SP, Chiou RY. GC-MS Determined Distribution of Urinary Equol Producers as Affected by Age, Gender, and Repeated Ingestions of Soymilk. J Food Sci. 2010;
177. Franke AA, Lai JF, Pagano I, Morimoto Y, Maskarinec G. Equol production changes over time in pre-menopausal women. Br J Nutr. 2012;

178. Nakatsu CH, Armstrong A, Clavijo AP, Martin BR, Barnes S, Weaver CM. Fecal bacterial community changes associated with isoflavone metabolites in postmenopausal women after soy bar consumption. PLoS One. 2014;
179. Rajan RK, Kumar M. SS, Balaji B. Soy isoflavones exert beneficial effects on letrozole-induced rat polycystic ovary syndrome (PCOS) model through anti-androgenic mechanism. Pharm Biol. 2017 Jan;55(1):242–51.
180. Atkinson C, Frankenfeld CL, Lampe JW. Gut bacterial metabolism of the soy isoflavone daidzein: Exploring the relevance to human health. Vol. 230, Experimental Biology and Medicine. 2005. p. 155–70.
181. Torres PJ, Siakowska M, Banaszewska B, Pawelczyk L, Duleba AJ, Kelley ST, et al. Gut Microbial Diversity in Women with Polycystic Ovary Syndrome Correlates with Hyperandrogenism. J Clin Endocrinol Metab. 2018;103(4):1502–11.
182. David LA, Maurice CF, Carmody RN, Gootenberg DB, Button JE, Wolfe BE, et al. Diet rapidly and reproducibly alters the human gut microbiome. Nature. 2014;
183. Kashyap PC, Marcobal A, Ursell LK, Larauche M, Duboc H, Earle KA, et al. Complex interactions among diet, gastrointestinal transit, and gut microbiota in humanized mice. Gastroenterology. 2013;
184. Tilocca B, Burbach K, Heyer CME, Hoelzle LE, Mosenthin R, Stefanski V, et al. Dietary changes in nutritional studies shape the structural and functional composition of the pigs' fecal microbiome-from days to weeks. Microbiome. 2017;
185. Bonder MJ, Tigchelaar EF, Cai X, Trynka G, Cenit MC, Hrdlickova B, et al. The influence of a short-term gluten-free diet on the human gut microbiome. Genome Med. 2016;
186. Ze X, Duncan SH, Louis P, Flint HJ. Ruminococcus bromii is a keystone species for the degradation of resistant starch in the human colon. ISME J. 2012;6(8):1535–43.
187. Wang K, Liao M, Zhou N, Bao L, Ma K, Zheng Z, et al. Parabacteroides distasonis Alleviates Obesity and Metabolic Dysfunctions via Production of Succinate and Secondary Bile Acids. Cell Rep. 2019;
188. Nallabelli N, Patil PP, Pal VK, Singh N, Jain A, Patil PB, et al. Biochemical and genome sequence analyses of Megasphaera sp. strain DISK18 from dental plaque of a healthy individual reveals commensal lifestyle. Sci Rep [Internet]. 2016;6(September):1–13. Available from: http://dx.doi.org/10.1038/srep33665
189. Shetty SA, Marathe NP, Lanjekar V, Ranade D, Shouche YS. Comparative genome

analysis of Megasphaera sp. reveals niche specialization and its potential role in the human gut. PLoS One. 2013;

190. Flint HJ, Scott KP, Duncan SH, Louis P, Forano E. Microbial degradation of complex carbohydrates in the gut. Vol. 3, Gut Microbes. 2012.
191. Harvey L, Arnold B, S Lawrence Z, Pau 1M, David B, James D. Molecular Cell Biology. 4th edition. Journal of the American Society for Mass Spectrometry. 2000.
192. Wright EM, Martín MG, Turk E. Intestinal absorption in health and disease - Sugars. Bailliere's Best Pract Res Clin Gastroenterol. 2003;
193. Seelinger G, Merfort I, Wölfle U, Schempp CM. Anti-carcinogenic effects of the flavonoid luteolin. Vol. 13, Molecules. 2008. p. 2628–51.
194. Ramos S. Cancer chemoprevention and chemotherapy: Dietary polyphenols and signalling pathways. Vol. 52, Molecular Nutrition and Food Research. 2008. p. 507–26.
195. Ingram D, Sanders K, Kolybaba M, Lopez D. Case-control study of phyto-oestrogens and breast cancer. Lancet. 1997;350(9083):990–4.
196. Zern TL, Fernandez ML. Cardioprotective effects of dietary polyphenols. J Nutr [Internet]. 2005;135(10):2291–4. Available from: http://www.ncbi.nlm.nih.gov/pubmed/16177184
197. Szczuko M, Skowronek M, Zapałowska-Chwyć M, Starczewski A. Quantitative Assessment of Nutrition in Patients With the Polycystic Ovary Syndrome (Pcos ). Rocz Panstw Zakl Hig [Internet]. 2016;67(4):419–26. Available from: http://wydawnictwa.pzh.gov.pl/roczniki_pzh/
198. Eslamian G, Hekmatdoost A. Nutrient Patterns and Risk of Polycystic Ovary Syndrome. J Reprod Infertil. 2019;20(3):161–8.
199. Miret S, Simpson RJ, McKie AT. P Hysiology and M Olecular B Iology of D Ietary I Ron a Bsorption . Annu Rev Nutr [Internet]. 2003;23(1):283–301. Available from: http://www.annualreviews.org/doi/10.1146/annurev.nutr.23.011702.073139
200. Fleet JC, Schoch RD. Molecular mechanisms for regulation of intestinal calcium absorption by vitamin D and other factors. Vol. 47, Critical Reviews in Clinical Laboratory Sciences. 2010. p. 181–95.
201. Tremellen K, Pearce K. Dysbiosis of Gut Microbiota (DOGMA) - A novel theory for the development of Polycystic Ovarian Syndrome. Med Hypotheses. 2012;79(1):104–12.
202. Viollet B, Guigas B, Sanz Garcia N, Leclerc J, Foretz M, Andreelli F. Cellular and molecular mechanisms of metformin: An overview. Clinical Science. 2012.